ABSTRACT

BLACKWELL, CHARLES EDWARD. Effect of Lignocellulosic Derivatives on the Structure and Properties of Gel-Spun Polyacrylonitrile Fibers. (Under the direction of Dr. Ericka Ford).

Gel-spinning techniques were used in the fabrication of bio-sourced carbon fiber precursors. Lignin, although being an amorphous material after recovery, is the structural component to plant cell walls and provides a rigid structure. Lignin/polyacrylonitrile (PAN) nanocomposite fibers were gel-spun with up to 50 % (weight to weight, wt/wt) lignin content with only nano-scale phase separation within the fiber structure, mimicking the well-integrated lignin in plants and enhancing toughness and modulus of the fibers. Alternative coagulation baths with reduced methanol (MeOH) concentration were developed utilizing Hansen Solubility Parameters (HSPs) and corresponding Teas Ratios. These alternative coagulation baths generally increased fiber processibility and mechanical properties as well as reduced lignin migration. The alternatives also lowered the flammability threat and toxicity of the system through the means of more environmentally friendly solvents, improving the feasibility of use in industrial settings. The alternative baths had flash points at ~65 °C higher than traditionally used MeOH. The overall highest mechanical properties were observed in the fibers spun in the 50 % MeOH bath with neat PAN modulus at 50.9 cN/dtex and tenacity at 3.0 cN/dtex and 50 % Lignin/PAN modulus at 85.3 cN/dtex and tenacity at 2.4 cN/dtex. To summarize, bio-sourced/acrylic nanocomposite fibers were successfully gel-spun in environmentally friendlier, industrially safer, engineered coagulation baths and resulted in fibers with higher overall performance.

Gel-spinning techniques were used to spin carbon fiber (CF) precursors utilizing a cellulosic derivative additive. Polyacrylonitrile (PAN) is often plasticized through excessive amounts of additives or copolymerized such that the comonomer can take up to 15 % of the chain. Glucaric Acid (GA) is a natural, acidic small molecule that has been used as an

antiplasticizer for solution spun polymeric fibers. A key characteristic of antiplasticizers can be to lower elasticity during processing yet mechanically reinforce the polymer system after drawing. Antiplasticized PAN fibers were gel-spun containing up to 5 % (wt/wt) of the ammonium salt form of GA incorporated at the dope level. With as little as 1 % GA content, the additive improved the overall ease of handling of the fiber during processing, changed crystallinity, increased mechanical performance, and raised thermal stability of the PAN. The overall highest mechanical properties were seen in the 3.5 % GA fibers with Young's modulus and toughness of 193.5 cN/dtex and 20.7 J/g respectively. Essentially, the GA works effectively as an antiplasticizer at low concentration.

The gel-spinning technique was used to fabricate lignin/polyacrylonitrile (PAN) fibers. Lignin-co-PAN (MODL) polymer of 1:4 lignin to PAN ratio was employed as a compatibilizer for the spinning of lignin/PAN fibers with up to 10 % (wt/wt) lignin to PAN. The compatibilizer did not hinder the dissolution of the lignin/PAN in the dope, but the overall drawability of spun fibers was reduced, as well as the fibers' mechanical performance. Lignin/PAN fiber not having the compatibilizer had a Young's modulus of 53.8 cN/dtex and toughness of 16.0 J/g. On the other hand, the best performance when using PAN-modified lignin had a modulus of 35.2 cN/dtex and toughness of 2.2 J/g.

Effect of Lignocellulosic Derivatives on the Structure and Properties of Gel-Spun Polyacrylonitrile Fibers

by
Charles Edward Blackwell

A thesis submitted to the Graduate Faculty of
North Carolina State University
in partial fulfillment of the
requirements for the degree of
Doctorate of Philosophy

Fiber & Polymer Science

Raleigh, North Carolina

2019

APPROVED BY:

_____	_____
Ericka Ford Committee Chair	Philip Bradford
_____	_____
Lucian Lucia	Richard Spontak

DEDICATION

I dedicate this document in its entirety first for the works of the LORD, Jesus Christ, and second, for my grandparents who always encouraged me to obtain as much education as possible.

Proverbs 16:3 "Commit your works to the LORD and your plans will be established."

BIOGRAPHY

Charles Edward Blackwell of Dothan, AL. He began his academic career at Auburn University in the Samuel Ginn College of Engineering in the Department of Polymer & Fiber Engineering in August 2007. There, he joined Lambda Chapter of the Phi Psi Honorary Textile Fraternity in September 2008 and has been an active member since. Charles was the student chapter president when Lambda Chapter hosted the annual convention in 2010. He graduated with his BS and MS in Polymer & Fiber Engineering in 2011 and 2012, and then took a job as a Quality Engineer at CSP Technologies in Auburn, AL. After working in industry for a few years, he returned to graduate school in August 2014 for a PhD in Fiber & Polymer Science at NC State University where he became an active member of Eta Chapter of Phi Psi. Charles has participated in each convention since 2009 and has assumed the Junior and Senior Warden positions on the Grand Council when requested. In February 2019, Charles was elected as Grand President of Phi Psi. In his free time, Charles enjoys archery and marksmanship, camping, reading, watching football, and cooking Southern BBQ.

ACKNOWLEDGEMENTS

I'd like to start with a praise for answered prayers. God has blessed me with the incredible opportunity to come so far. He has given me all the tools, knowledge, and wisdom required to complete the task at hand. He has granted me wonderful family, friends, colleagues, and mentors. Through Christ's blessings, I have done what I once believed was impossible.

To my family, I love y'all. Your constant encouragement and support (and sometimes frank rebuttals) were invaluable to this endeavor. I would've likely driven myself nuts and pulled my hair out without you. Mom, you always pushed me to my limits, asking where the last 4 points went. While I may've been stubborn and frustrated with that at times (fine, a lot of the time), I look back and see that you weren't pushing me past the limits, but rather expanding them. Dad, you were the constant voice of "stop worrying and take it one task at a time." Without that mindset, there's no way the following document would be anything more than a jumbled mess of ideas, scribbles, and disconnected papers in a pile behind the bookshelf.

To my friends, thank you. There are many of you whom I haven't spoken to in… well, forever, but y'all know that I can pick up exactly where I left off. The PFEN crew and the Mad Hatters helped me keep my sanity in undergrad. From the crazy firefights, hordes, and wing nights, to keeping me safe (and putting up with me) during games at Jordan-Hare, y'all have always had my back. Even after graduation, you put me up between moves, prayed with me, and celebrated with me. Specifically to my brothers in Phi Psi, y'all have a special place in my heart. Lambda and Eta both are my family away from southern Alabama. I've met so many great people with diverse ways of thinking that have helped me along this journey.

To my old guard colleagues, thank you. Chunhong, you were my first lab partner at NC State; we suffered the gauntlet in the dungeon together and came out on top! Preeti, you were

the voice of calm most days, easily taking the edge off of a rough patch in my research. Yaewon, you challenged me and kept me on my toes, broadening my thought processes. Y'all were invaluable to my thinking and learning.

To my mentors, thank you. Throughout my life, I've been guided by amazing people. At Auburn: Mrs. Julia Freeman, Dr. Peter Schwartz, Dr. Maria Auad, Dr. Sabit Adanur, Dr. Yasser Gowayed, and Dr. Gwynedd Webster. At NC State: Mr. Kent Hester, Ms. Judy Elson, Ms. Barbara White, Ms. Teresa White, Dr. Behnam Pourdeyhimi, Dr. Sam Hudson, and Dr. Stephen Michielsen. Without all of you, there is no way I would be as successful as I am today. You gave me a chance to learn, to work, and to create.

To my industry support, thank you. I'm amazed that my research would interest so many and garner such support from the textile industry and beyond: Mr. Ben Delgado and Mr. Tracy McGee, Cutty International; Mr. Darcy Prather, Kalion Incorporated; Mr. Tom Janicki, Fortified Textiles; and Dr. Sean Su, Tyton BioEnergy Systems.

To my committee, thank you. I am humbled by the people who accepted me as their student to shape into a peer. I've received wonderful advice, perspectives, and guidance from each of you, even when I felt it challenged my whole enrollment. It is to you who I am happy to give gratitude: Dr. Philip Bradford, Dr. Lucian Lucia, and Dr. Richard Spontak.

Last, to Dr. Ford, thank you so much. You believed in me. You challenged me. You taught me. You took a respectfully snarky process engineer and turned him into a polymer physicist, a writer, a planner, and (begrudgingly) a chemist. You gave me the opportunity to move forward in my career and my life. Without you, **none** of this would be possible. I will praise the LORD daily for that simple phone call that moved me into the next phase of my life God had prepared.

Thank you all for this work and for being in my life.

TABLE OF CONTENTS

LIST OF TABLES

LIST OF FIGURES

LIST OF SYMBOLS

°	Degrees
°C	Degrees centigrade
'	Feet
"	Inches
%	Percent
% wt	Percent weight
% v	Percent volume
2θ	Diffractometer angle
A_{CS}	Cross sectional area
cal	Calories
cN	Centinewtons
cN/dtex	Centinewtons per decitex
cm	Centimeters
cSt	Centistokes
Da	Daltons
dtex	Decitex; grams per 10000 meters
den	Denier; grams per 9000 meters
dL	Deciliters
DR	Draw ratio
f	Teas Plot Coordinate
f_D	Dispersive Teas Plot Coordinate
f_P	Polar Teas Plot Coordinate

f_H ..... Hydrogen Bonding Teas Plot Coordinate

g ..... Grams

g/den ..... Grams per denier

g/dL ..... Grams per deciliter

g/mL ..... Grams per milliliter

ga ..... Gauge

GPa ..... Gigapascals

h ..... Hours

J ..... Joules

J/g ..... Joules Per Gram

kcal ..... Kilocalories

kcal/mol ..... Kilocalories Per Mole

kDa ..... Kilodaltons

L ..... Liters

m ..... Meters

m/min ..... Meters Per Minute

mm ..... Millimeters

min ..... Minutes

mm/min ..... Millimeters Per Minute

MPa ..... Megapascals

mol ..... Moles

N ..... Newtons

P_{amb} ..... Ambient pressure

P^{sat}	Vapor pressure at flash point
Pa	Pascals
Pa·s	Pascal·Seconds
Ra	Hansen Solubility Parameter Distance
s	Seconds
St	Stokes
tanδ	Dynamic Loss; Phase Angle Tangent
v	Volume Fraction
V	Volume
v/v	Volume to volume
V_F	Feed Speed
V_T	Take-up Speed
w_f	Weight Fraction
wt/wt	Weight to weight
γ	Activity coefficient
δ	Hildebrand Solubility Parameter
δ_D	Dispersive Hansen Solubility Parameter
δ_H	Hydrogen Bonding Hansen Solubility Parameter
δ_P	Polar Hansen Solubility Parameter
η	Viscosity
η^*	Dynamic Viscosity
θ	Orientation Angle
μm	Micrometers

ρ ..... Density

ρ_{fiber} ..... Composite Fiber Density

ρ_{lignin} ..... Lignin Density

ρ_{PAN} ..... Polyacrylonitrile Density

ω ..... Angular Speed

Л ..... Linear Density

LIST OF ABBREVIATIONS

ASTM	American Society for Testing and Materials
BDU	Battle Dress Uniform
CNT	Carbon Nanotube
DMAc	Dimethyl Acetamide
DMF	Dimethyl Formamide
DMSO	Dimethyl Sulfoxide
DTGA	Differential Thermogravimetric Analysis
DSC	Dynamic Scanning Calorimeter
FTIR	Fourier Transform Infrared
GA	Glucaric Acid
HCl	Hydrochloric Acid
HSP	Hansen Solubility Parameter
IPA	Isopropanol
IR	Infrared
MODL	Polyacrylonitrile Grafted Lignin
PAN	Polyacrylonitrile
PE	Polyethylene
PEO	Polyethylene Oxide
PP	Polypropylene
PS	Polystyrene
PTFE	Polytetrafluoroethylene
PVA	Polyvinyl alcohol

$scCO_2$	Supercritical Carbon Dioxide
SEM	Scanning Electron Microscope
Temp	Temperature
TGA	Thermogravimetric Analysis
UHMWPE	Ultra High Molecular Weight Polyethylene
UV	Ultraviolet
WAXD	Wide Angle X-ray Diffraction

1. INTRODUCTION & MOTIVATION

1.1. High-Performance Fibers

High-performance fibers are used in a multitude of applications where strength, durability, and often the weight of materials is a limiting factor. Some fibers are engineered to match or even exceed the mechanical properties of metals. The term "high-performance fiber" can refer to aspects of exceptional thermal, chemical, conductive, and mechanical performance as belonging to the fibrous materials. For instance, a high-performance fiber can have a storage modulus on the order of hundreds of gigapascals. Commodity fibers, in comparison, are not engineered to perform on the same level of exceptionalism; a simple t-shirt is not designed for the same level of tear resistance as a soldier's battle dress uniform (BDU). Commodity fibers are typically used in clothing, apparel, and home furnishing industries, and are found in general everyday use items such as umbrellas, suitcases, and bags. Use of protective materials can overlap between high-performance and commodity applications, but the performance requirements are extreme for high-performance applications. Leather boots, for example, are worn to protect feet from the elements while maintaining comfort, but specialized carbon fiber composite toe boots can absorb impact without damaging appendages at greater capacity-without the added weight of steel plating.

DuPont's Kevlar® and Nomex®, Toyobo's Zylon®, and Honeywell's Spectra® are all well-known high-performance fibers that are utilized across several fields of interest: from law enforcement, space travel and aeronautics, and even military applications. These materials replace denser metal wires and glass fibers without compromising mechanical performance, as seen in **Table 1.1**. For example, steel wire is strong, but polymeric materials such as Spectra® are 8× less dense and are mechanically stronger[1-3].

Table 1.1. Values of Strength Parameters of Some Specialty Fibers[1-3].

Fiber Type	Density (g/mL)	Tenacity (cN/dtex)	Initial Modulus (cN/dtex)	Breaking Elongation (%)
Kevlar® 29	1.44	20.30	490	3.6
Kevlar® 49	1.44	20.80	780	2.4
Kevlar® 149	1.44	16.80	1150	1.3
Twaron®	1.44	21.00	600	3.6
Nomex®	1.46	04.85	75	35
HPPE (Dyneema® SK60)–1 dpf	0.97	28.00	910	3.5
HPPE (Dyneema® SK65)–1 dpf	0.97	31.00	970	3.6
HPPE (Dyneema® SK71)–1 dpf	0.97	35.00	1220	3.7
Spectra 900–10 dpf	0.97	26.00	750	3.6
Spectra 2000–3.5 dpf	0.97	34.00	1200	2.9
Polyvinyl Alcohol	1.31	—	0.6	15.0
Polyacrylonitrile	1.18	0.08	1.4	6.4
PBO poly(p–phenylene benzobisoxazole)	1.56	25.40	1770	—
Carbon fiber–PAN® (Toray)	1.80	20–60	1800–4500	0.7–2.0
E–Glass	2.55	15–25	540	1.8–3.2
S–Glass	2.50	20–30	620	4.0
Steel Wire	7.85	1.80	260	1.5

The most notable high-performance fibers are synthetically produced from hazardous or toxic precursors, petroleum derivatives, or nonrenewable resources. Most naturally occurring fibers do not have equivalent degrees of order and molecular orientation among their microstructures to give them the same strength as synthetic high-performance fibers. Through engineered man-made materials and processing techniques, high-performance fibers can be fabricated.

1.1.1. Common High-Performance Microstructures

High-performance fibers typically are manufactured with high degrees of molecular orientation, crystalline order among their microstructures, and in some cases strong forms of secondary bonding between polymer chains. Structurally rigid macromolecules can engage in several types of secondary bonding between the polymer chains. Lining the molecular backbone with aromatic rings causes strong secondary bonding such as "plate stacking," hydrogen bonding with proton donating groups, or charge transfer with electron donating or withdrawing groups. Para-aramids, benzobisazoles, and carbon fiber are among the most notable of high-performance fibers from rigid rod-like polymers. These fibers are used extensively in advanced military and aeronautics applications; where ballistic armor, lightweight, and fire resistance are desired.

1.1.1.1. Para-aramids

Kevlar® fiber was developed by DuPont in the 1960's from poly(p-phenylene terephthalamide) (PPTA) a para-aramid polymer. To synthesize Kevlar® polymer, para-phenylenediamine and terephthaloyl chloride are reacted by step-growth polymerization; this reaction also releases hydrochloric acid (HCl) as a by-product[4]. The polymer is liquid-crystalline in nature and has a high degree of molecular orientation in the direction of axial fiber

drawing. The para-aramid structure allows plate stacking to occur, as well as intermolecular hydrogen bonding between the backbone amide groups, as seen in **Figure 1.1**.

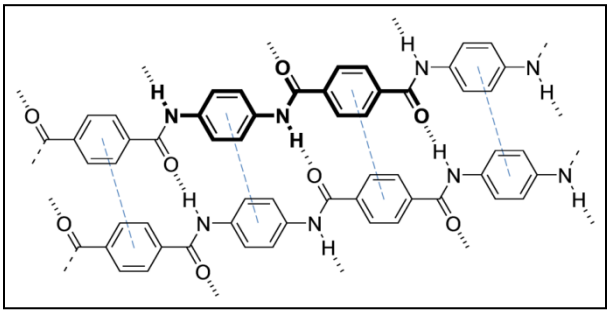

Figure 1.1: Plate stacking and hydrogen bonding between para-aramid chains[5].

During dry-jet wet spinning of para-aramids fibers, the liquid-crystalline polymer assumes a rod-like conformation with a high degree of molecular orientation along the fiber axis. Upon impact, structurally ordered polymer chain results in the micro-fibrillation of fibers. Kevlar® is a well-known and widely-used high-performance material; however, its production requires the use of highly corrosive materials, such as sulfuric acid and hydrogen chloride (HCl)-chemicals that are costly to handle and difficult to dispose of safely. Para-aramids are ultraviolet (UV) and visible light sensitive polymers, whose service life is adversely affected by prolonged exposure to sunlight or UV radiation. Both forms of electromagnetic radiation can hydrolyze polymer chains, which in turn drastically reduces fiber strength. As a result, para-aramid fibers often require coating or containment within a structure in order to protect their structural and mechanical integrity.

1.1.1.2. Benzobisazoles

Benzobisazoles are aromatic polymers; the most renown of its class is polybenzobisoxazole, also known simply as "PBO" or "Zylon®," as seen in **Figure 1.2**.

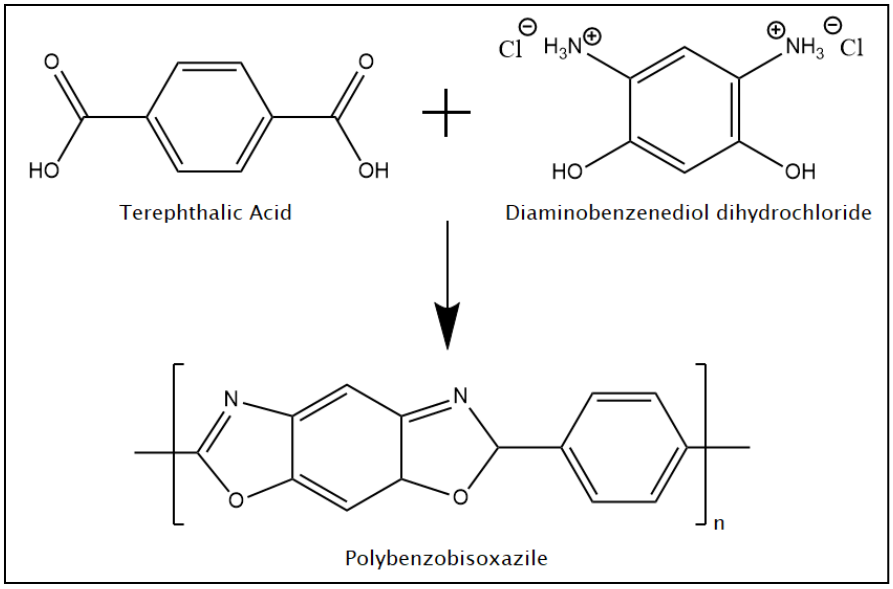

Figure 1.2: Synthesis of PBO.

PBO is synthesized from terephthalic acid and diaminobenzenediol dihydrochloride in polyphosphoric acid. Terephthalic acid particles exceeding 10 μm in size are difficult to fully dissolve in phosphoric acid for polymerization. Like the para-aramid polymer class, the synthesis and fiber spinning of PBO is often expensive and yields environmentally hazardous or toxic waste by-products.

The service life of PBO is shortened by exposure to normal atmospheric conditions of air and UV light due to rapid degradation. PBO will degrade and suffer strength losses more rapidly under those conditions in comparison to para-aramids. First Choice Armor & Equipment, the Plaintiff in a case against Toyobo America, Inc., reported that the vests made with PBO fibers were failing upon exposure to light, moisture, heat, and general manufacture. Further, PBO fiber was banned from use in bullet-resistant vests by the National Institute of Justice in August 2005[6]. Exposure to 85 % relative humidity and ~70 °C for 11 weeks can cause the loss of 20 % of its initial fiber strength, and UV exposure for 100 h can cause the loss of 30 % of its initial strength[7]. To circumvent the degradation of PBO and para-aramid fibers under environmental

conditions, these fibers are often post-processed with sealed vinyl coatings, braided with UV resistant fiber sheaths, or encased within shielded environments.

1.1.1.3. Carbon Fiber

Carbon fiber is industrially used to manufacture extraordinarily high strength composite materials at relatively lower densities than metal parts. While carbon fiber (at 1.8 g/mL) does in fact have a higher density than Kevlar® (at 1.44 g/mL) or Zylon® (at 1.56 g/mL), its initial modulus of 4500 cN/dtex far exceeds the initial modulus of Kevlar® at 1150 cN/dtex or Zylon® at 1770 cN/tex, as shown in **Table 1.1**. Carbon fibers are also more resistant to UV radiation and moisture than para-aramids or benzobisazoles, which depolymerize by hydrolysis upon exposure to environmental conditions.

Like other structurally rigid high-performance fibers, carbon fiber is strong due to its anisotropic microstructure of highly aligned molecules along its fiber axis and plate stacking between chains. In the case of carbon fiber, Van der Waals forces are responsible for interlayer adhesion, but it also allows layers to slip past one another under shear.

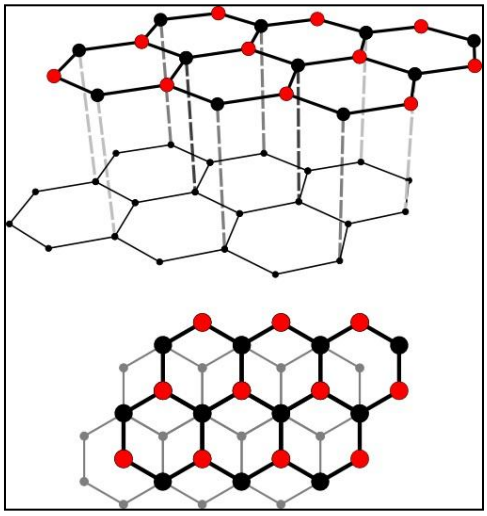

Figure 1.3: Structure of graphitic carbon[8].

Typically, high-performance fibers are melt extruded from resin (i.e. Zylon®) or spun from dopes of dissolved polymer (Kevlar®). In contrast, carbon fiber is derived from a variety of previously spun organic fibers, also known as "precursor fibers." The process to fabricate carbon fiber essentially involves the heating of a precursor fiber above 1000 °C until cyclization reorganizes the backbone chain into a series of aromatic rings. Further, graphitization removes non-carbon elements from the precursors, but this process requires extreme temperatures in excess of 2500 °C.

1.2. Carbon Fiber Precursors

Commercially, carbon fiber is derived from a variety of sources, but pitch, cellulose, and polyacrylonitrile (PAN) are primarily utilized. "Pitch" is a term used for aromatic oligomers of hydrocarbon. These often comprised of naphthalene or other multi-ring compounds. Cellulosic precursors for carbon fiber are typically from the regenerated cellulose class of fibers or "viscose rayon" in particularly. Industry is selective about their use of carbon fiber precursor. The decision depends upon production costs in lieu of post-production yardage and weight. Typically, carbon yield, the efficiency of pyrolysis, is a metric to help discern how much carbon fiber can be produced. Carbon yield, char yield, or carbon content is the ratio of the mass of charcoal to the initial mass of the substance. As a result, a low carbon yield effectively means the manufacturers would spend more capital on feedstock and time relative to carbon fiber production, thus decreasing plant efficiency[8]. Precursor materials also affect the final properties of the resulting carbon fiber. Carbon fibers made from synthetic precursors often have higher carbon yield and stronger tensile properties than that of natural precursors. **Table 1.2** shows the mechanical properties and carbon yield based upon the precursor.

Table 1.2. Mechanical Properties of Carbon Fibers from Different Precursors.

Precursor	Tensile Strength (GPa)	Modulus (GPa)	Carbon Yield (%)	Reference
Rayon	2.50	520	20-25	10
PAN	2.40	490	55-60	10
Anisotropic Pitch	2.20	830	80-85	10
Isotropic Pitch	0.70	33	80-85	10
Lignin	0.42	40	46	9

1.2.1. Bio-based Precursors

Natural, cellulosic fibers as found in cotton are too short in length for conversion into continuous carbon fiber. Due to their staple fiber length, cellulose requires reprocessing into continuous filament before conversion into carbon fiber[11]. Regenerated cellulosic fibers are typically derived from wood pulp, a renewable resource. Cellulose dissolves in sodium hydroxide, a caustic hazard, and carbon disulfide, a highly toxic and carcinogenic material, to create cellulose xanthate, a highly viscous solution that has been coined "viscose." The viscose is filtered, extruded through the spinneret into the mineral acid bath, and finally hydrolyzed to re-form cellulose again (as shown in **Figure 1.4**).

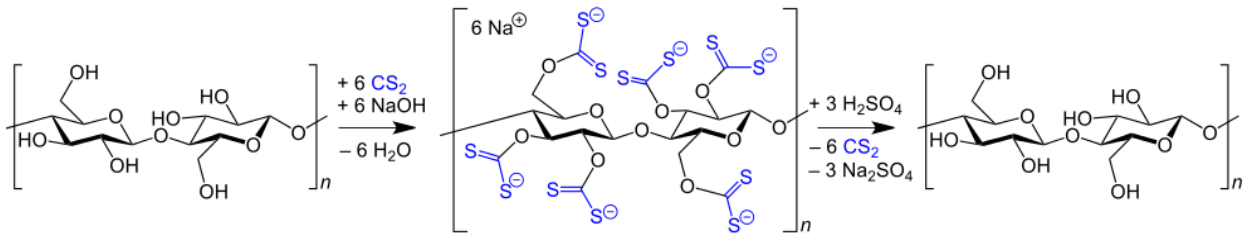

Figure 1.4: Regeneration of cellulose[12,13].

Lignocellulosics are from renewable biopolymers; the most abundant resources on Earth is plant matter. This group of biopolymers comprises cellulose, hemicellulose, and lignin. Lignin is a prime candidate for carbon fiber production due to its aromatic structure, high char yield,

global abundance, and low cost due to its production as a waste by-product of the paper pulping industry. Paper mills often burn lignin for energy to fuel reactors; however facilities are moving toward petroleum-based fuels as demand rises[14,15]. However, the mechanical performance of lignin-based carbon fiber is often lower than synthetically derived carbon fiber, only suitable for "general purpose grade" or aesthetic use[9], as shown in **Table 1.2**. Kadla et al. utilized melt extrusion to spin neat lignin and lignin/polyethylene oxide (PEO) blended fibers, which were later stabilized and carbonized. The resulting fibers from lignin/PEO blends showed commercially available lignin's potential as a processible source for carbon fiber with no molecular modification. It was also noted by Kadla et al. that extensive pre-processing, such as washing, and use of hardwood lignin was preferred for the spinning of lignin/PEO blends that were suitable for carbonization[9].

1.2.2. Synthetic Precursors

1.2.2.1. Pitch Precursor

Pitch is classified as isotropic or anisotropic, based on its molecular structure. Typically, pitch is an amalgamation of aromatic hydrocarbons that lack order and are isotropic in nature or pre-treated into anisotropic pitch. Isotropic pitch contains a wide range of molecular weights between 180-600 kDa[16] that makes spinning difficult and resulting carbon fiber properties low, as shown in **Table 1.2**. Isotropic pitch based carbon fiber can be used for superficial and moderate-performance applications, but mesophase pitch is required for high-performance properties to occur in pitch based carbon fiber. Using hazardous solvents such as hexane, toluene, and quinoline, pitch is pre-treated to remove low molecular weight molecules like aromatic naphthalenes and volatile compounds that hinder anisotropic formation. Polymerization occurs simultaneously, increasing molecular weights to ~1200 kDa in multi-ring

macromolecules. The residue leftover is then heated between 300-500 °C where the anisotropic pitch forms and is extruded into fiber form[16,17]. **Table 1.2** shows carbonized anisotropic pitch has far greater tensile strength and modulus than isotropic pitch as a result of the extra processing.

1.2.2.2. Polyacrylonitrile Precursor

In contrast to pitch, PAN is an aliphatic macromolecule. Carbon fiber cross sections from pitch and PAN precursors were illustrated by Dumanlı and Windle (**Figure 1.5**).

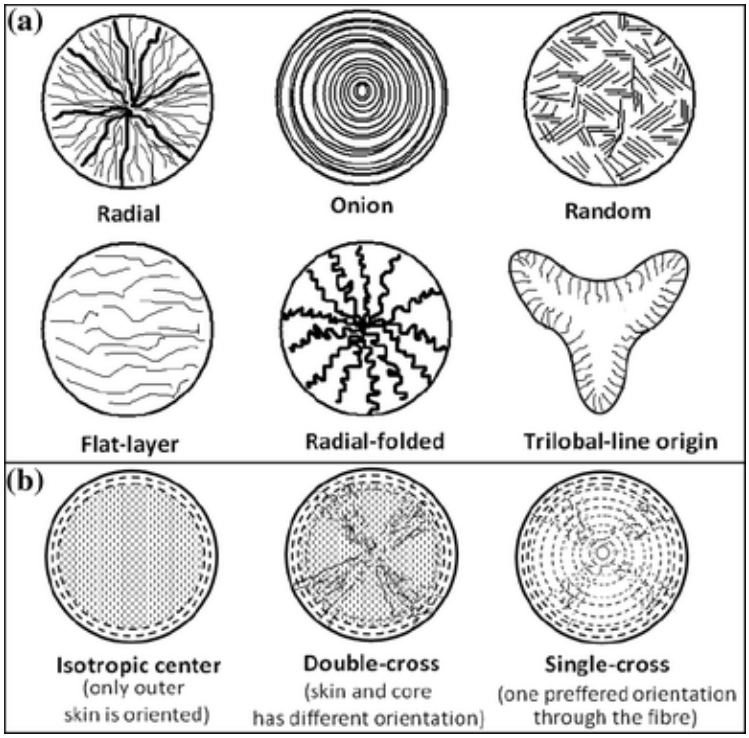

Figure 1.5: Cross sections of carbon fiber from (a) pitch and (b) PAN based precursors[18].

PAN precursor fiber is readily carbonized into fiber immediately after spinning and drawing; unlike pitch, PAN does not need to be subjected to chemical pre-treatments. Instead, it is oxidized–or stabilized–and carbonized through stages of thermal processing under tension in order to form carbon fibers. Carbonized PAN fibers have a moderately high carbon yield; upwards of 60 % of their original mass is retained post-carbonization[10,19]. Wet spun PAN

fibers are the primary source for high strength carbon fibers due to their high strength and low processing cost relative to pitch. PAN based carbon fibers have been reported to have higher compressive strength (0.7 to 5.6 GPa) than pitch based carbon fibers (0.45 to 1.15 GPa), making them ideal for structural composites[20,21].

1.3. Physical Properties of Polyacrylonitrile

While PAN is often used as a precursor to carbon fiber, they can also be independently strong and utilized in the non-carbonized form. PAN fibers are spun for use in specialty applications as textiles, yarns and staple fiber filler material in composites. The chemical resistance of PAN makes it is able to withstand most acids and bases without much loss in mechanical performance. PAN is used where chemical, thermal, and UV resistance are important; in such applications as fiber reinforced concrete (FRC)[22,23]. The mechanical properties of industrial PAN fiber can vary depending on its processing and molecular composition, as determined by the comonomers used during polymerization. High-performance PAN has shown tensile strength as high as 8.14 cN/dtex and elastic modulus as high as 178 cN/dtex once fibers were highly drawn up to 90×[24,25]. In comparison, textile grade PAN has been reported to have tensile strength as low as 2.14 cN/dtex[26].

1.3.1. Molecular Structure

1.3.1.1. Chemistry

PAN is a linear polymer, typically comprised of a repeating pendant group of the carbon atom triple bonded to a nitrogen atom (i.e. the cyano group in **Figure 1.6**). This cyano pendant group gives PAN the potential to form strong intermolecular bonds resulting from dipole-dipole interaction. Typically, PAN for apparel and general grade carbon fiber has molecular weight as low as 78 kDa[24,27], whereas high-performance carbon fiber precursor can have molecular

weight upwards of 250 to 500 kDa[25,27,28]. PAN homopolymer is more difficult to process than PAN copolymers, so often PAN is polymerized with comonomers; however, it must contain 85 % acrylonitrile monomers to be labeled as an acrylic polymer[22,29]. Itaconic acid [24,30], methacrylate, and vinyl chloride[29] (**Figure 1.7**) are copolymerized with vinyl acrylonitrile monomers to improve processibility and carbonization[31,32]. The comonomers disrupt the strong intermolecular dipole-dipole bonding between to allow molecular movement between PAN chains. Polymers are engineered having the end use of PAN fibers in mind. For instance, itaconic acid comonomers can improve the efficiency of thermal oxidation among PAN. This enhances the efficiency of carbonization by maximizing oxidized sites along the chain. Zhidkova et al. observed that the thermal energy required for stabilization dropped as a result of copolymerizing PAN with 1.2 - 6.4 % itaconic acid monomer[30].

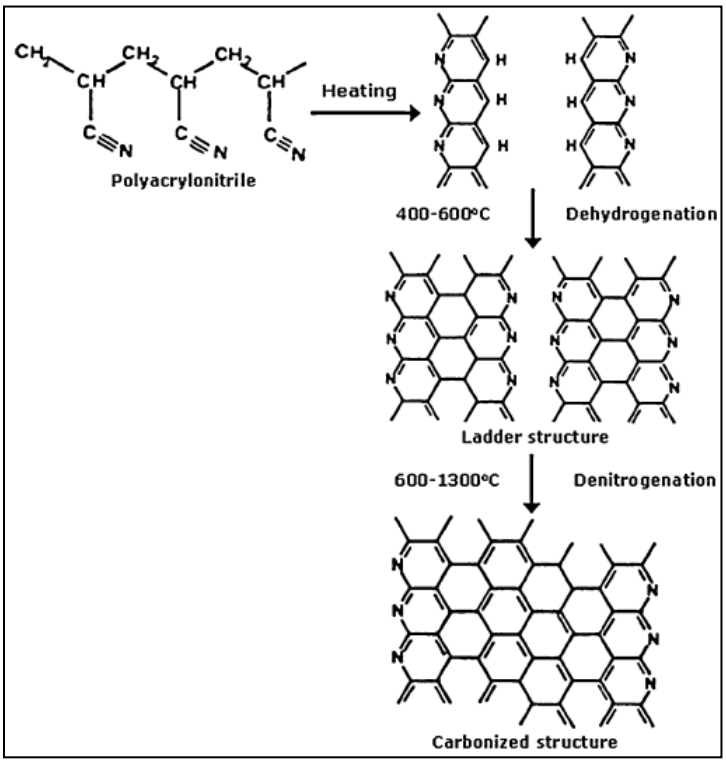

Figure 1.6: Molecular structures of PAN and its conversion to carbon fiber[19].

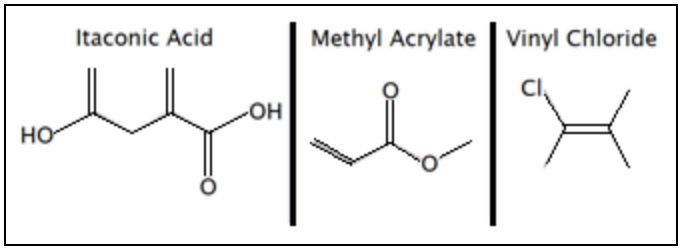

Figure 1.7: Common PAN comonomers.

Linear PAN is typically synthesized from acrylonitrile monomers by free radical polymerization utilizing suspension and solution techniques. Solution polymerization leaves some content of unreacted acrylonitrile monomers, which are known carcinogens, as well as utilizes solvents such as dimethyl acetamide (DMAc), dimethyl formamide (DMF), and dimethyl sulfoxide (DMSO) which have high transfer coefficients through human skin, posing a significant health risk during disposal. Suspension polymerization is more environmentally controllable, avoids the use of such solvents, and the resulting PAN is recovered easily by filtration[21]. PAN is also synthesized using supercritical carbon dioxide ($scCO_2$), which avoids solvent handling altogether[33-35].

1.3.1.2. Microstructure

The crystalline microstructure of PAN is not entirely defined[36-43]. Bashir and Bohn et al. both refer to wide-angle x-ray diffraction (WAXD) to determine the crystalline structure, but note that the common PAN diffraction patterns actually show limited information[36,39,44]. These diffraction patterns show intense equatorial arcs that are indicative of crystalline polymer, but the lack of meridional or off-axis peaks implies an unordered structure. Both Bohn et al. and Bashir show how oriented PAN fibers exhibit lateral regularity but axial irregularity, as seen in **Figure 1.8**.

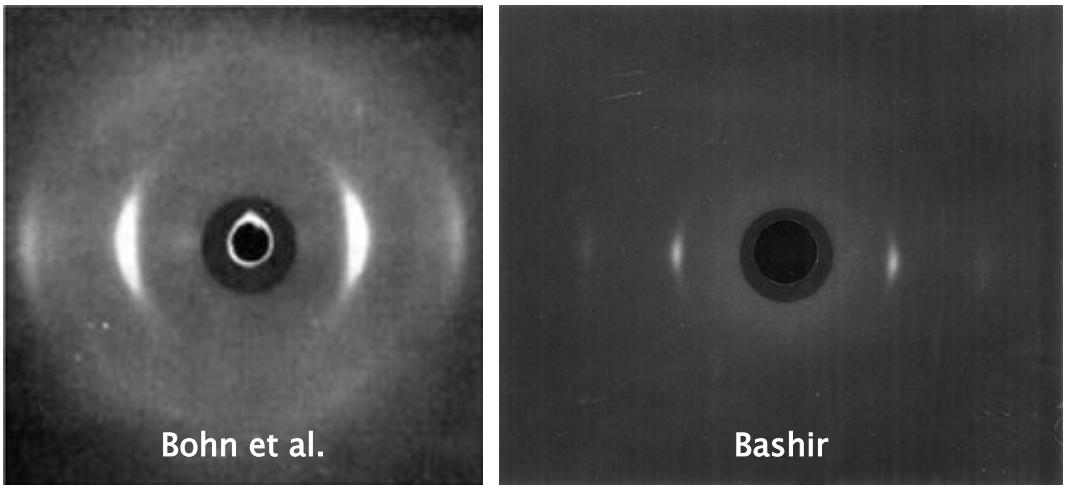

Figure 1.8: X-ray diffraction patterns of PAN[36,44].

Colvin and Storr also utilized WAXD to analyze the crystalline structure of PAN fibers, but unlike other literature, found some meridional markings in the diffraction pattern when measured at 16.5° off axis. These diffraction patterns implied an orthorhombic crystalline cell, which fits the hexagonal models suggested by Bashir and Bohn et al., but Klement and Geil argue hexagonal models are not appropriate since the longitudinal measurement of the cell is undefined and report unit cells with a/b ratios other than $\sqrt{3}$ characteristic of hexagonal forms, as seen in **Figure 1.9**[36,38,39,44]. Bashir notes that literature often describes this phenomenon with various terms including "condis-crystal" coined by Wunderlich and Grebowicz, "orthorhombic polymorph," "irregular helix," and "hexagonal mesophase," but ultimately describes the same behavior[36,45]. The hexagonal mesophase refers to PAN's atypical crystalline formation where the cross-axial directions are regular and the axial direction is random. This is a result of the conformational disorder and simultaneous orientational and positional order caused by the strong polar cyano groups[36]. In other words, if chains crystallize from helix structures, the diameter is constant, but the handedness and pitch are random. The tacticity of PAN is typically atactic in part due to the strong polar interactions between cyano pendant groups. The lack of

stereoregularity is not entirely random but instead a distribution of isotactic and syndiotactic regions.

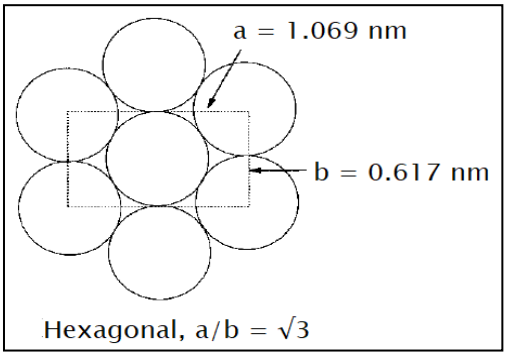

Figure 1.9: Diagram of the hexagonal structure of a PAN crystal[36].

The crystallinity of PAN can be further characterized with Raman and Infrared (IR) spectroscopy; both techniques work in conjunction with each other to define PAN's tacticity. Raman and IR have been used to identify the crystalline structure of vinyl polymers based upon their reactive modes[41,46]. According to Koenig, combinations of polarized and depolarized Raman spectra and dichroic IR spectra are characteristic of specific crystalline structures and molecular conformations for vinyl polymers, as shown in **Figure 1.10**[46],

STRUCTURE		SYMMETRY	OPTICAL ACTIVITY			EXAMPLE
		R IR	p p d d π σ π σ	p d 0 0	0 0 π σ	
CENTER OF SYMMETRY		D_{2h} C_{2h}		✓ ✓	✓ ✓	PE, PES
ATACTIC			✓ ✓ ✓ ✓			PVF
SYNDIOTACTIC	HELIX >3_1	D_n	✓	✓ ✓	✓	PEO
	HELIX 3_1	D_3	✓	✓	✓	
	HELIX 2_1	D_2	✓ ✓	✓		
	PLANAR	C_{2v}	✓ ✓ ✓	✓		PVC
ISOTACTIC	HELIX>3_1	C_n	✓ ✓	✓		POLYBUTENE
	HELIX 3_1	C_3	✓ ✓			PP
	PLANAR	C_s	✓ ✓			

Figure 1.10: Selection rules for monosubstituted polyvinyl polymers[46].

Huang and Koenig commented on how limitations in the sensitivity of their Raman and IR did not permit the identification of "nonreactive" modes, which constrained designations to a few atactic, syndiotactic, and isotactic models. Using these characteristic selection rules, Huang and Koenig were able to describe potential models for PAN crystal structures and corresponding molecular conformations[41,46].

1.3.2. Processing Polyacrylonitrile Fibers

1.3.2.1. Wet Spinning

Unlike melt spinning–wherein polymer is melted and then extruded through spinnerets–wet spinning transforms dope (of dissolved polymer) into fiber. Polymers whose degradation temperature is lower than their melting temperature are solution spun. The wet spinning process, as shown in **Figure 1.11**, is primarily used for textile grade applications, where molecular weights of PAN range from 70 to 200 kDa[47].

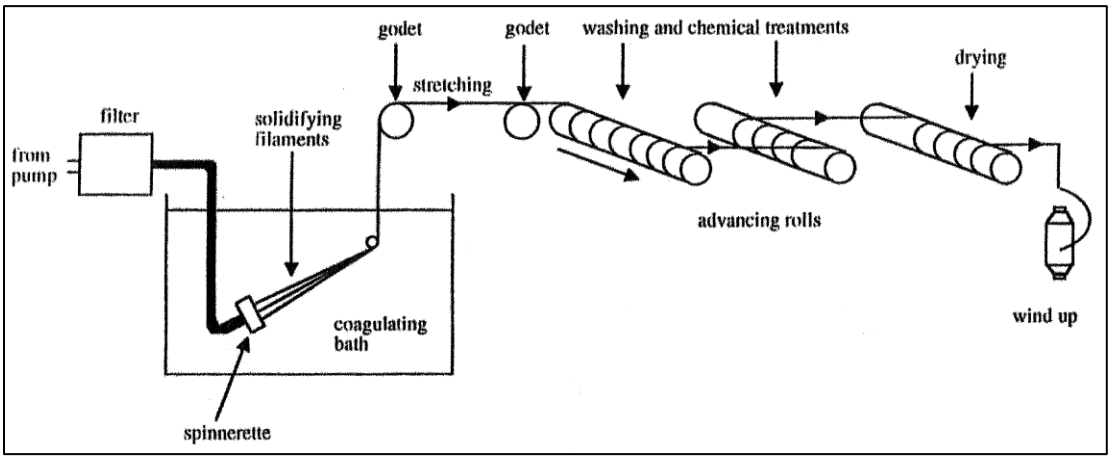

Figure 1.11: Wet spinning diagram[29].

Wet spinning exhibits its complexity through solvent diffusion within a heated coagulation bath to solidify the as-spun fiber. Bath formulation, polymer concentration in the spinning dope, and temperature can greatly impact the product, increasing in-line defects and the general shape of fibers. PAN is sensitive to these parameters, so in order to obtain high-

performance product, there must be a high degree of control[48,49]. Frank et al. reported that the spinning parameters of solvent concentration and temperature can alter cross sections as a result of diffusion rates. Low temperatures and high solvent content decreases the rates of diffusion, thereby lowering coagulation rate. Kidney bean cross sections are the result of fast coagulation as opposed to circular ones as shown by Frank et al. (see **Figure 1.12**)[48].

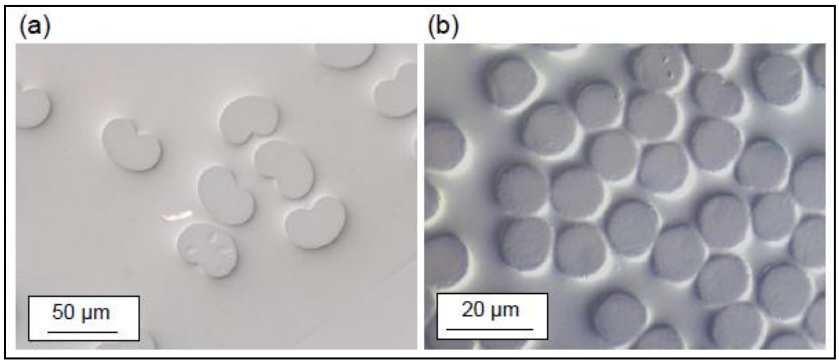

Figure 1.12: Effect of (a) high and (b) low coagulation rate on PAN fiber cross section by wet spinning[48].

1.3.2.2. Gel-Spinning

Gel-spinning is a type of dry jet solution spinning and significantly modified version of wet spinning. This technique differentiates from wet spinning based on its dope properties, coagulation step, and mechanical performance of fully drawn fiber. Molecular weight of the polymer plays a role in determining the overall strength of gel-spun fiber[50,51]. Smith et al. found that the ratio of the weight average and number average molecular weight (i.e. polydispersity index or "PDI") was indicative of fiber strength during their investigation of ultra high molecular weight polyethylene (UHMWPE)[51]. In **Figure 1.13**, Liu et al. showed a clear increase in the breaking strength when the weight average molecular weight is increased with constant number average molecular weight[51].

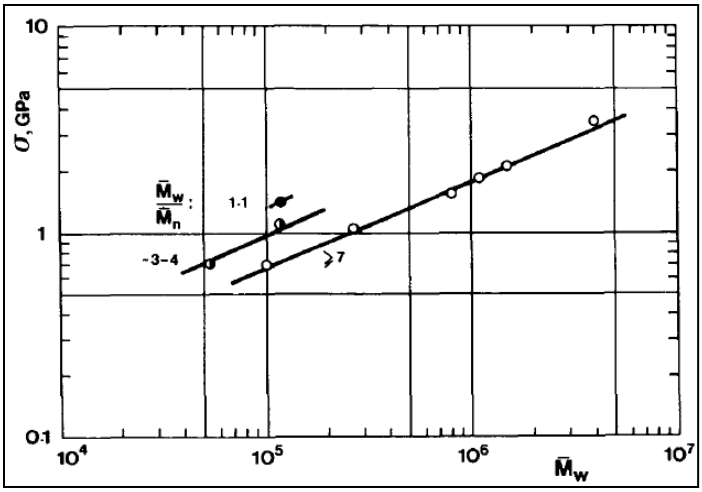

Figure 1.13: Tensile strength of highly oriented polyethylene[51].

Some gel-spinning processes can utilize molecular weights in excess of 1000 kDa[52], however, it is not molecular weight alone that determines strength, but rather its application. These high molecular weight polymers, in excess of 250 kDa for PAN[25,28], require narrow molecular weight distributions. Both properties of molecular weight and PDI are designed to optimize the density of chain entanglements in the dope while promoting high draw ratios from the as-spun fibers. The resulting fiber then possesses long chain polymers that are highly aligned. Chain alignment is also promoted within the long air gap between the spinneret and coagulation bath; this pre-alignment also lends to the bulk of the strength of the fully-drawn gel-fiber[50]. The microstructure of gel-spun fibers is comprised of extended chain crystals, as seen in **Figure 1.14**. These crystals provide greater strength and rigidity to drawn fiber than the folded chain crystals, which are structural characteristics of commercial apparel textile fibers[23,24,29,50,53,54].

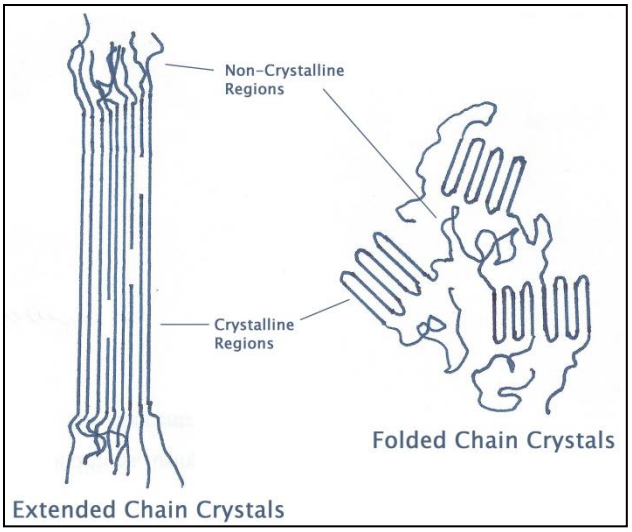

Figure 1.14: Extended chain crystals and folded chain crystals as found in fiber microstructures. In-line tension assists in the formation and alignment of extended chain crystals as opposed to folded chain crystals that occur naturally without any outside forces. Extended chain crystals have fibrillar structures, as observed by TEM imaging from Wunderlich in **Figure 1.15**.

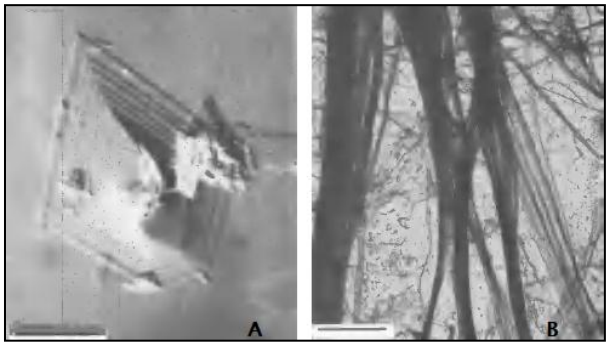

Figure 1.15: TEM of (a) polyethylene growth spiral and (b) fibrillar polytetrafluoroethylene[55]. Wunderlich also noted that extended chain crystals manifest "equilibrium properties," where their measured properties are close to or have exceeded theoretical values[55]. According to Beloshenko et al., Li et al., and Wunderlich, evidence for extended chain crystals comprise density values indicative of wholly crystalline structures, positive shifts in melting temperature, and fibrillar macrostructures[55-57]. Extended chain crystals can potentially reach 30° above the

melting point in some polymers[55]. These crystalline structures also provide more graphiticizable sites in the PAN fiber for stronger, more homogeneous carbon fiber[18].

During gel-spinning, gel-fiber is thermally induced with cooling and one-way diffusion occurs with solvent extraction[27] to ultimately form the gel-fiber. Liu et al. reported fibers are often more uniform and circular than wet-spun that result from dynamic solvent exchange (see **Figure 1.16**). Because methanol is miscible with DMSO, but not a good solvent for PAN, the diffusion of solvent into the coagulation bath is essentially a uniform extraction of the solvent, which leaves the gel-fiber behind. The lack of interaction between the methanol and the PAN implies the gelation is thermally induced[27].

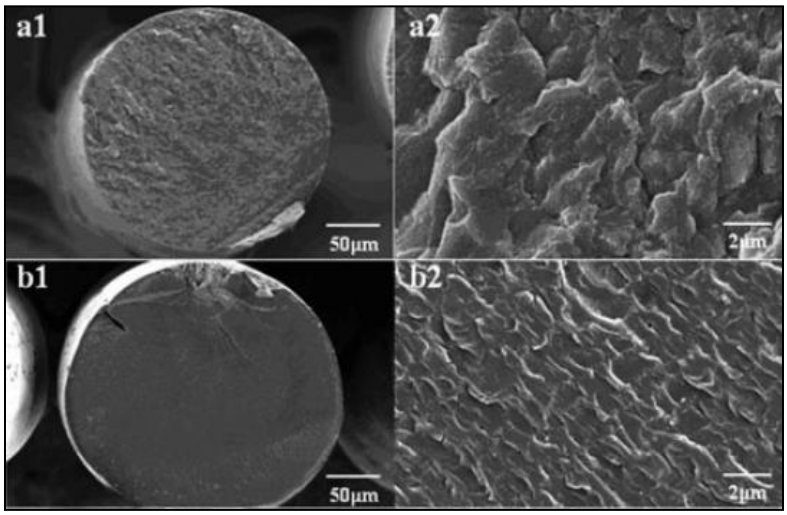

Figure 1.16: Morphology for (a) dry-jet wet-spun and (b) gel-spun polyacrylonitrile fibers[27].

1.3.3. Effect of Processing on Mechanical Properties

PAN fibers have a wide range of mechanical properties, depending on its structure and processing. A clear difference is seen between gel-spun and wet spun fibers, as reported in **Table 1.3**. Fiber formation by gel-spinning produces fibers with superior mechanical properties. This is likely due to the formation of extended chain crystals, which are highly aligned along the axis of gel-spun fibers.

Table 1.3. Effect of Solution Spinning Technique on the Mechanical Properties of PAN Fibers[†].

Gel-Spun		Wet Spun	
Modulus (cN/dtex)	**Tenacity (cN/dtex)**	**Modulus (cN/dtex)**	**Tenacity (cN/dtex)**
140	6.8	57	4.2
133	8.1	66	1.9
178	7.2	103	5.6
186	7.6	104	6.1

[†]Data were obtained from[24,27,28,54-59]

1.3.4. Processing Innovations

Modifications to gel-spinning have been researched to improve fiber properties and improve the drawability of as-spun fiber. To minimize the cost of new spinning lines investments, process optimization is achieved through modular assemblies of existing equipment.

1.3.4.1. Spinning Dopes

1.3.4.1.1. Solvents

PAN is difficult to process due to the strong attractive forces between cyano side groups. The strength of secondary bonding is influenced by PAN polymerization and its dryness after synthesis. PAN is soluble at ~20 °C when dried between 70-80 °C, but higher dissolution temperatures of 60-85 °C are required when PAN is dried above room temperature or homopolymer is used. Inter and intramolecular bonding within PAN lend to higher values of cohesive energy, which in turn affects dissolution [60,61]. Polar aprotic solvents such as DMAc, DMF, and DMSO are used to dissolve PAN[22,61,62], but DMSO is preferred for the dissolution of PAN spinning dopes. Eom and Kim observed that even though DMF dissolved PAN at a faster rate, the DMSO dissolved PAN was more homogenous[63]. DMF constricts the

free volume between PAN chains more than DMSO; these solvent complexes are shown in **Figure 1.17**.

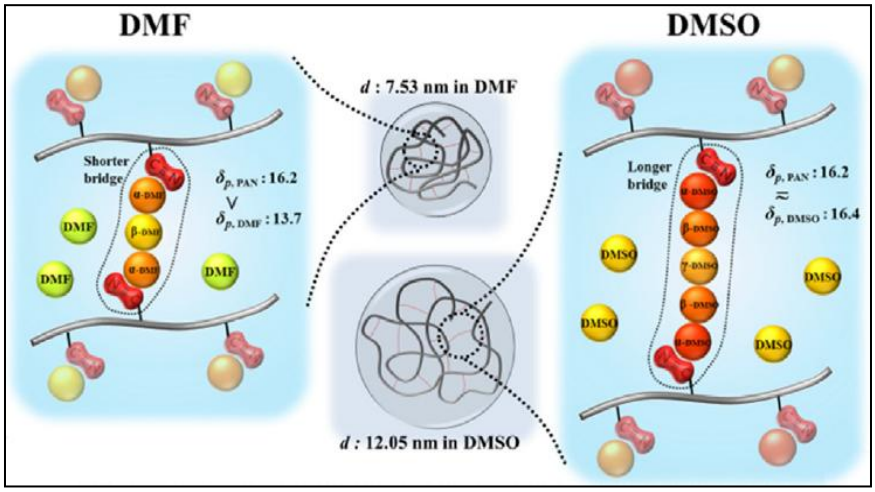

Figure 1.17: Schematic representation of PAN coil dimensions in DMF and DMSO[63].

DMF will form smaller solvent bridges than DMSO due to the increased inter-chain spacing, according to Eom and Kim[63]. DMF forms a dense solvent cage around PAN, which in turn localizes PAN microheterogeneities. Evidence for these heterogeneities are determined from rheological measurements of dope viscosity at elevated temperatures (**Figure 1.18**)[63].

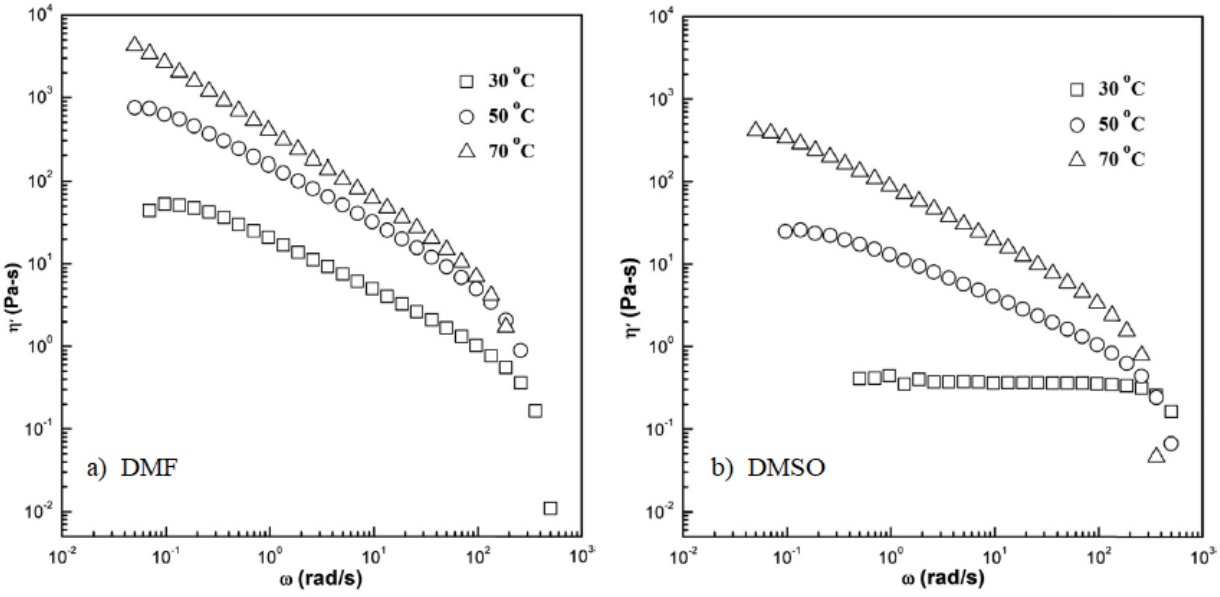

Figure 1.18: Complex viscosity of PAN in (a) DMF and (b) DMSO at 30, 50, and 70 °C[63].

1.3.4.1.2. Aging

The structure of spinning dopes are also engineered by the aging technique. Aging was employed to form "gel-like" networks within dopes of medium molecular weight PAN (less than 100 kDa)[24,27,64]. Liu et al. showed take-up speeds increased by 150 %, as seen in **Figure 1.19**, yielding faster processing speeds.

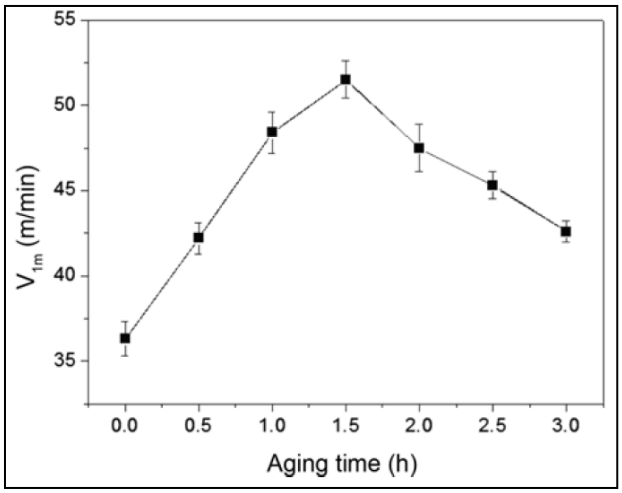

Figure 1.19: Relationship between takeup speed and aging time[64].

Liu et al. found aging dopes at room temperatures for 1.5 to 2.0 h resulted in the best "pre-gelled" network for gel-spinning the fiber[24,27]. Microheterogeneities within pre-gelled dopes mimicked entanglements within dopes of ultra-high molecular weight polymer. This enabled PAN having molecular weight as low as 78 kDa[24,27] to render fibers properties similar to fibers spun from PAN having almost four times its molecular weight!

1.3.4.2. Coagulation Baths

Wet spun PAN is coagulated in a bath comprising DMSO/water. These bath systems are maintained at much warmer temperatures than those used in gel-spinning. By comparison, methanol coagulation baths are used for gel-spinning due to an extraction interaction that occurs with the spinning dope solvent[27,54]. The below freezing temperature typically run with

methanol aids thermally-induced gelation[25,27,49,65]. Recently, the cold methanol coagulation baths have been studied for alteration to accommodate the strong diffusion and loss of solids that some composite fibers may have to endure.

1.3.5. Filler Reinforced Polyacrylonitrile

Properties of PAN fibers can be improved by incorporating filler materials such as nanoparticles to fabricate high strength, high modulus composite fibers. Research into these PAN-based composite fibers was for enhancing the mechanical strength of carbon fiber precursors. Filler like nanocrystalline cellulose[47] and carbon allotropes[58,59,66] have been employed by researchers. Alternatively, fillers were investigated to reduce the cost of carbon fiber. Among these fillers, renewable biomaterials are the most attractive candidates. Thus, CNTs and lignin from biomass are among the most commonly used PAN additives. Both have been shown to improve oxidation, carbon yield, and mechanical properties[28,59].

CNTs are inorganic fillers and renowned for their high-performance properties. The nanotube is a sheet of graphene rolled into a seamless tube. Their "honeycomb" lattice structure is classified as armchair, zigzag, or chiral, which are all based on the angle of hexagonal carbons to the transverse axis of unwrapped tubes (see **Figure 1.20**). If the longitudinal direction of the tube is considered the vertical axis, and the transverse axis is considered the horizontal axis, then as the angle of orientation, θ, can be used to describe configurations. As θ approaches 0° at the meta-position of the honeycomb, the tube is considered in a zigzag configuration. Similarly, as θ approaches 30° at the para-position of the honeycomb, then it is considered in an armchair configuration. If θ is between 0° and 30°, then the nanotube is simply known as "chiral." While these configurations are different, they have minimal statistical effect on the mechanical

properties of the tubes, but can affect the optical properties given the diameters are large enough[68-70].

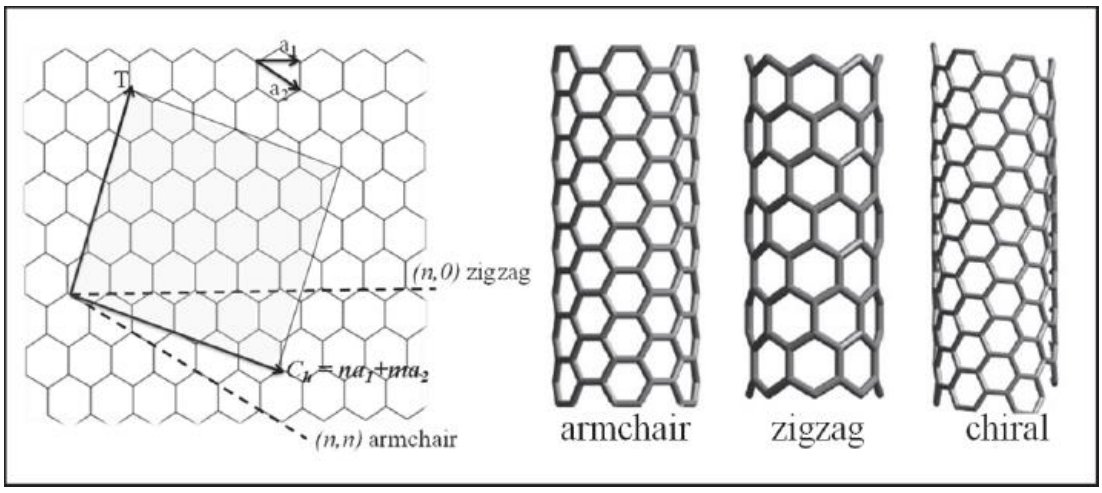

Figure 1.20: Chirality of CNT structures[68].

1.4. Lignin Precursors for Low Cost Carbon Fiber

Lignin is a by-product of the pulp and paper process and sometimes considered either furnace fuel or waste material from the paper industry. Roughly 2 % is actually recovered from liquors, while the remainder is burned by mills for energy. Advancements in lignin recovery incentivizes the paper industry to seek alternate, value-added uses for lignin, a sustainable bioresource[14,71-74].

1.4.1. Physical Properties of Lignin

Lignin is somewhat an enigma as its properties are not well known aside from the lignin recovered from pulping[14,75-77]. Each plant species typically differs in terms of its ratio of three monolignols. That is why the protolignin structure differs for every plant. Its supramolecular structure is believed by some to be random and distributed unevenly throughout the plant. What is known is that plants integrate lignin as a structural component within their cell walls[98]. Lignin is crosslinks with hemicellulose, which in turn enables it to bond with other

polysaccharides. The structural rigidity that lignin provides holds up the plant while also acting as a transporter for water[77]. Lignin is also a natural deterrent against insects that might harm the plant.

1.4.2. Molecular Structure

Lignin is widely available, inexpensive, and renewable. As a result, lignin has been tapped as popular low cost filler for PAN composite fibers. Lignin is a naturally occurring biopolymer in plants, its abundance is second only to cellulose[9,14,78]. It is an aromatic, non-crystalline, cross-linked polymer that is formed from three types of phenylpropane monolignols (shown in **Figure 1.21**).

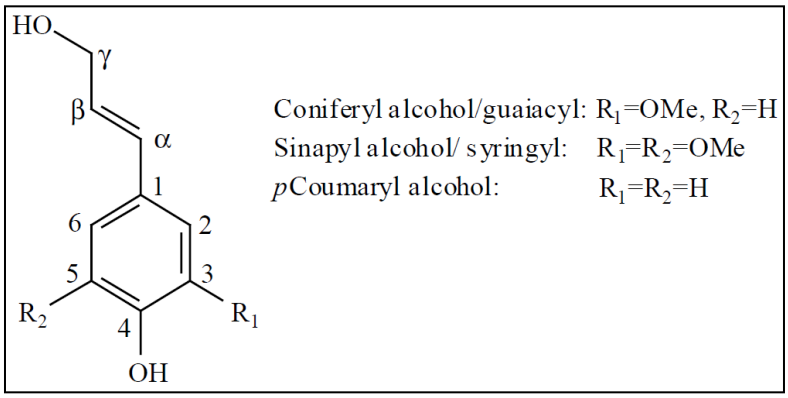

Figure 1.21: The three building blocks of lignin[76].

Lignin polymers' molecular weight and total content within the plant can range depending on its source, specifically between species of plant[14]. Typically, softwoods and eucalypts contain the highest percentages of lignin, as seen in **Table 1.4**. In its natural state, lignin is referred to as "protolignin," which is still relatively unknown in terms of supramolecular structure[76]. Source-specific types of lignin, specifically between species, differ greatly in terms of their chemistry, so ultimately the heterogeneity of protolignin is a wide range. Cell type and genetics heavily influences the locale and development of biopolymers within plant cell walls, which suggests an endless variety of protolignin networks exist in nature[14,75,79]. Softwood lignin is known to be

composed mostly of coniferyl alcohol with trace coumaryl alcohol, but no sinapyl alcohol. Hardwood and grass grades of lignin feature all three monolignols[14]. These realities affect the type of lignin produced by pulping mills[15]. A mill producing soft paper products–such as tissue paper–primarily uses hardwoods[29], so the lignin by-product will reflect the hardwood source.

Table 1.4. Cellulose, Hemicellulose, and Lignin Content of Different Types of Wood[14].

Wood Type	Cellulose (%)	Hemicellulose (%)	Lignin (%)
Temperate Hardwood	40-45	25-30	25-30
Temperate Softwood	40-45	30-35	20-25
Eucalypt	40	20	30

1.4.3. Extraction Techniques for Lignin

With improved black liquor recovery methods and greater demand for pulp and paper products, lignin can be easily recovered and utilized as an inexpensive raw material. For over a century, the pulp and paper industry has used the same approach to black liquor recovery and runoff for fuel. As value-added applications for lignin are developed, demand for solid lignin increases, and lignin recovery techniques become more advanced, lignin will be all the more readily available at low cost.

1.4.3.1. Kraft

Most commercial operations for paper pulping are conducted with Kraft processing, a chemical pulping technique method that loads the pulp with sulfur to remove lignin[82]. Kraft pulping is known to produce quality pulp having high strength, simple black liquor recovery, and offer a versatile approach for handling pulp from different plant sources (such as softwood vs hardwood)[14,80]. Sodium hydroxide and sodium sulfide separates lignin from pulp by breaking

lignin macromolecules into smaller water and alkaline soluble chemistries[75]. Through experience, industry has streamlined the process to have the highest yield of paper cellulose and most efficient pulping processing times. Kraft processing temperatures are maintained between 150 - 165 °C. Wood pulp is pressurized within vessels to improve the efficiency and consistency delignified pulp. Homogenous delignification of pulp is not currently possible. "Black liquor" contains remnants of degraded cellulose, hemicellulose, lignin, inorganics, and other waste materials. The waste products are recoverable and concentrated into solids for use as fuel. Black liquor is the primary source for recovered lignin, where it is in a digested state and has a wide range of molecular weights[80,81]. Bajpai reports the process yields lignin having molecular weights ranging between 2 to 3 kDa[75]. The Kraft process also yields DMSO, a widely used solvent, in significant quantities[82]. Processing the black liquor for lignin has become even more efficient, since paper mills run at the rate of biofuel recovery[73-75].

1.4.3.2. Steam Explosion

Steam explosion is a cleaner alternative to Kraft pulping. Wood chips are processed at temperatures around 285 °C at 3.5 MPa of pressured, before rapidly increasing pressure to 7 MPa. Afterwards, chips are depressurized to atmospheric pressure, which in turn defibrillates cellulose portions and promotes hydrolysis in cellulose and hemicellulose zones[83]. Acids catalyze the hydrolysis rate of hemicellulose; nevertheless, only water is needed for lignin extraction by steam explosion. This method is environmentally friendly due to the lack of corrosive chemicals that can degrade equipment and pose a threat to the health of workers. However, the lignin recovered by this method is significantly more degraded in size than for other extraction techniques[75]. The molecular weight of lignin obtained by steam explosion ranges between 0.8 - 2.0 kDa[84].

1.4.3.3. Organosolv

Lignin is considered a waste by-product Kraft pulp and paper processing; by which lignin and hemicellulose are separated from cellulosic pulp. However, the organosolv process was specifically designed to separate those distinct fractions of lignocellulosic material from each other. Organic solvents such as acetone, ethanol, methanol, and organic acids are used to extract lignin and to depolymerize hemicellulose crosslinks. As a result, organosolv lignin is much higher in purity than lignin from either Kraft or steam explosion methods. Further, organosolv yields a lignin having a relatively narrow molecular weight distribution, and low sulfur content. Cellulose is separated in the solid phase as organic solvent (heated to 130 - 200 °C) is added to the feedstock. Black liquor, containing lignin and hemicellulose, separates into the liquid phase. Afterwards, black liquor is separated into aqueous and organic phases. The organic phase is comprised mainly of lignin, which is recovered through distillation[75]. While volatile organic solvents are indeed used, these are easily distilled off for reuse and to extract lignin. The cons of organosolv processing include the use of relatively expensive organic solvents, which are sensitive to temperature and atmospheric pressure. Its narrow processing window generally incurs higher operating expenses and initial capital investment.

1.4.4. Melt-spun Lignin Fibers

Differences between plant and environmentally dependent properties of lignin make melt spinning lignin challenging [14,85]. It was reported by Smith that lignin has a glass transition temperature as low as 60 °C in the presence of water[86]. This low value is likely due to the moisture retention, which in turn disrupts hydrogen bonding between lignin molecules and plasticizing lignin by way of water bridges[87].

The structure of lignin depends upon its source and the technique use to separate lignin from cellulosic polymers; this in turn greatly affects the thermal properties of the lignin. Hardwood lignin comprises more structurally linear lignin due, which is due to its high content of synapyl alcohols. Softwood lignin is primarily comprised of coniferyl alcohols that are connected through crosslinks. Subsequently, softwood lignin is more difficult to melt extrude than hardwood lignin. Nordström et al. successfully melt spun lignin using a twin-screw extruder[85] at temperatures ranging from 140 - 200 °C. Twin screw extrusion is less commonly used than a single-screw for melt spinning, because these are generally used to compound polymer melts[27]. Impurities found within the blends of softwood and hardwood lignin were noted to plasticize their melt viscosities. The mechanical properties of those melt spun blends of lignin were not reported by Nordström et al.[85].

1.4.5. Lignin as Composite Filler

Instead of compounding lignin with plasticizers using an extruder with excessive shear and temperature, gel-spinning can provide another avenue to incorporate lignin with a polymer without the harsh conditions, for example PAN. Among gel-spun fibers, lignin has been shown to decrease the mechanical properties PAN-based precursor fibers at high percentages of lignin; nevertheless, Liu et al observed some positive improvements for carbon fiber production [71]. In **Figure 1.22**, Liu et al. showed a downward shift and broadening of the tanδ peak for molecular mobility among PAN/lignin fibers in comparison to neat PAN and PAN/lignin/CNT fibers. The shift was evidence that the glass transition temperature had decreased.

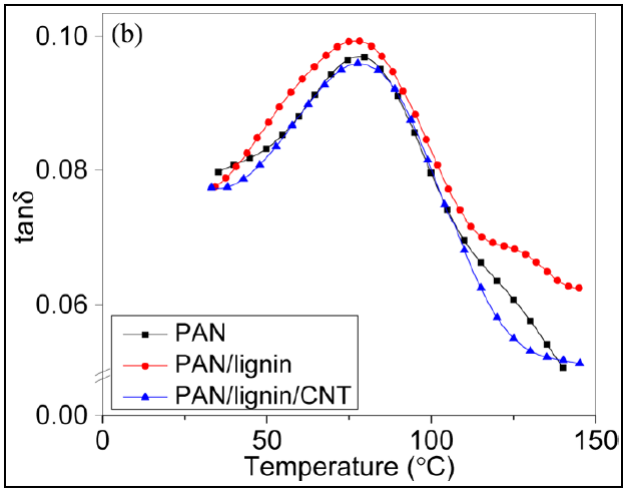

Figure 1.22: Tanδ plot vs temperature of precursor fibers[71].

In terms of carbonization, lignin behaves like PAN comonomers, which are known to catalyze stabilization[71,88]. Fitzer and Müller observed a decrease in the activation energy that was required for the stabilization of polyvinylacrylonitrile-*co*-methacrylate by 4.6 kcal/mol in nitrogen and 12.2 kcal/mol in air[88].

1.5. References

[1] El Mogahzy, Y. E. *Engineering Textiles: Integrating the Design and Manufacture of Textile Products;* Woodhead Publishing Limited: Cambridge, England, 2009;.

[2] Kwon, Y. D.; Kavesh, S.; Prevorsek, D. C. United States of America Patent US4883628, 1989.

[3] Spitalsky, Z.; Tasis, M.; Papagelis, K.; Galiotis, C. Carbon nanotube–polymer composites: Chemistry, processing, mechanical, and electrical properties. *Progress in Polymer Science* **2009**, *35*, 357.

[4] Kwolek, S.; Morgan, P. United States of America Patent US3287323, 1966.

[5] Anonymous. Kevlar chemical structure H-bonds. *https://upload.wikimedia.org/wikipedia/commons/b/b7/Kevlar_chemical_structure_H-bonds.png* (accessed June 12, 2017).

[6] Cohen, D. M.; Carr, W. P.; Palmer, E.; Appel, M. S. First Choice Armor & Equipment v Toyobo America. **2010**, *717*, 156.

[7] Cunniff, P. M.; Auerbach, M. A. High performance "M5" fiber for ballistics/structural composites. *23rd Army Science Conference* **2002**.

[8] Anonymous. Macromolecules. *https://www.minichemistry.com/wp-content/uploads/2015/02/graphite.jpg* (accessed 12/12, 2017).

[9] Kadla, J. F.; Kubo, S.; Venditti, R. A.; Gilbert, R. D.; Compere, A. L.; Griffith, W. Lignin-based carbon fibers for composite fiber applications. *Carbon* **2002**, *40*, 2913.

[10] Matsumoto, T. Mesophase pitch and its carbon fibers. *Pure and Applied Chemistry* **1985**, *57*, 1553.

[11] Karacan, I.; Gül, A. Carbonization behavior of oxidized viscose rayon fibers in the presence of boric acid–phosphoric acid impregnation. *Journal of Material Science* **2014**, *49*, 7462.

[12] Anonymous. Xanthogenate Ceullolose Structural Formula. *https://upload.wikimedia.org/wikipedia/commons/e/e8/Xanthogenate_Cellulose_Structural_Formula_V1.svg* (accessed December 12, 2017).

[13] Anonymous. Xanthogenate Cellulose Acid Hydrolysis. *https://upload.wikimedia.org/wikipedia/commons/c/c2/Xanthogenate_Cellulose_Acid_Hydrolysis_V1.svg* (accessed December 12, 2017).

[14] Norberg, I. Carbon fibres from kraft lignin, KTH Royal Institute of Technology, Stockholm, Sweden, 2012.

[15] Brodin, I.; Sjöholm, E.; Gellerstedt, G. Kraft lignin as feedstock for chemical products: the effects of membrane filtration. *Holzforschung* **2008**, *63*, 290.

[16] Özel, M. Z.; Bartle, K. D. Production of mesophase pitch from coal tar and petroleum pitches using supercritical fluid extraction. *Turkish Journal of Chemistry* **2002**, *26*, 417.

[17] Uemura, S.; Yamamoto, S.; Hirose, T.; Takashima, H.; Kato, O. United States of America Patent , 1986.

[18] Dumanlı, A. G.; Windle, A. H. Carbon fibres from cellulosic precursors: a review. *Journal of Material Science* **2012**, *47*, 4236.

[19] Nataraj, S. K.; Yang, K. S.; Aminabhavi, T. M. Polyacrylonitrile-based nanofibers—a state-of-the-art review. *Progress in Polymer Science* **2012**, *32*, 487.

[20] Chae, H. G.; Choi, Y. H.; Minus, M. L.; Kumar, S. Carbon nanotube reinforced small diameter polyacrylonitrile based carbon fiber. *Composites Science and Technology* **2009**, *69*, 406.

[21] Kozey, V. V.; Jiang, H.; Mehta, V. R.; Kumar, S. Compressive behavior of materials: Part II. High Performance Fibers. *Journal of Materials Research* **1994**, *10*, 1044.

[22] Zheng, Z.; Feldman, D. Synthetic fibre-reinforced concrete. *Program of Polymer Science* **1995**, *20*, 185.

[23] Afroughsabet, V.; Biolzi, L.; Ozbakkaloglu, T. High-performance fiber-reinforced concrete: a review. *Journal of Material Science* **2016**, *51*, 6517.

[24] Tan, L.; Liu, S.; Song, K.; Chen, H.; Pan, D. Gel-Spun Polyacrylonitrile Fiber From Pregelled Spinning Solution. *Polymer Engineering and Science* **2010**, *50*, 1290.

[25] Chae, H. G.; Minus, M. L.; Rasheed, A.; Kumar, S. Stabilization and carbonization of gel spun polyacrylonitrile/single wall carbon nanotube composite fibers. *Polymer* **2007**, *48*, 3781.

[26] Sedghi, A.; Farsani, R. E.; Shokuhfar, A. The effect of commercial polyacrylonitrile fibers characterizations on the produced carbon fibers properties. *Journal of Materials Processing Technology* **2008**, *198*, 60.

[27] Liu, S.; Tan, L.; Pan, D.; Chen, Y. Gel spinning of polyacrylonitrile fibers with medium molecular weight. *Polymer International* **2011**, *60*, 453.

[28] Liu, Y.; Chae, H. G.; Kumar, S. Gel-spun carbon nanotubes/polyacrylonitrile composite fibers. Part I: Effect of carbon nanotubes on stabilization. *Carbon* **2011**, *49*, 4466.

[29] Adanur, S. *Wellington Sears Handbook of Industrial Textiles;* Technomic Publishing Company, Inc.: Lancaster, PA, 1995;.

[30] Zhidkova, O. V.; Andreeva, I. N.; Radishevskii, M. B.; Serkov, A. T.; Kalashnik, A. T.; Chichinova, N. V. Thermal properties of polyacrylonitrile copolymers having various chemical compositions. *Fibre Chemistry* **1994**, *25*, 368.

[31] Bajaj, P.; Sreekumar, T. V.; Sen, K. Effect of Reaction Medium on Radical Copolymerization of Acrylonitrile with Vinyl Acids. *Journal of Applied Polymer Science* **2000**, *73*, 1640.

[32] Gupta, A. K.; Paliwal, D. K.; Bajaj, P. Acrylic Precursors for Carbon Fibers. *Journal of Macromolecular Science* **1991**, *31*, 1.

[33] Shiho, H.; DeSimone, J. M. Dispersion Polymerization of Acrylonitrile in Supercritical Carbon Dioxide. *Macromolecules* **2000**, *33*, 1565.

[34] Shlyahtin, A. V.; Nifant'ev, I. E.; Bagrov, V. V.; Lemenovskii, D. A.; Tavtorkin, A. N.; Timashev, P. S. Synthesis of polyacrylonitrile copolymers as potential carbon fiber precursors in CO_2. *Green Chemistry* **2014**, *16*, 1344.

[35] Okubo, M.; Fujii, S.; Maenaka, H.; Minami, H. Production of polyacrylonitrile particles by precipitation polymerization in supercritical carbon dioxide. *Colloidal Polymer Science* **2003**, *281*, 964.

[36] Bashir, Z. The hexagonal mesophase in atactic polyacrylonitrile: a new interpretation of the phase transitions in the polymer. *Journal of Macromolecular Science Part B* **2001**, *B40*, 41.

[37] Olabisi, O.; Adewale, K., Eds.; In *Handbook of Thermoplastics;* CRC Press: Boca Raton, FL, 2016;.

[38] Colvin, B. G.; Storr, P. The Crystal Structure of Polyacrylonitrile. *European Polymer Journal* **1974**, *10*, 337.

[39] Bohn, C. R.; Schaefgen, J. R.; Statton, W. O. Laterally ordered polymers: polyacrylonitrile and polyvinyl trifluoroacetate. *Journal of Polymer Science* **1961**, *55*, 531.

[40] Hu, X. The Molecular Structure of Polyacrylonitrile Fibers. *Journal of Applied Polymer Science* **1996**, *62*, 1925.

[41] Huang, Y. S.; Koenig, J. L. Raman Spectra of Polyacrylonitrile. *Applied Spectroscopy* **1971**, *25*, 620.

[42] Dong, L.; Liu, X.; Zhao, X.; Dong, Y.; Cheng, B.; Zhuang, X.; Meng, D. Study on raman spectra of the polyacrylonitrile iron complex nanofibers. *Applied Mechanics and Materials* **2014**, *513-517*, 273.

[43] Yamadera, R.; Tadokoro, H.; Murahashi, S. Normal Vibrations of Polyacrylonitrile and Deuterated Polyacrylonitriles. *The Journal of Chemical Physics* **1964**, *41*, 1233.

[44] Klement, J. J.; Geil, P. H. Growth and drawing of polyacrylonitrile crystals grown from solution. *Journal of Polymer Science* **1968**, *6*, 1381.

[45] Wunderlich, B.; Grebowicz, J. Thermotropic mesophases and mesophase transitions of linear, flexible macromolecules. *Advances in Polymer Science* **1984**, *60/61*, 1.

[46] Koenig, J. L. Raman scattering of synthetic polymers-a review. *Applied Spectroscopy Reviews* **1971**, *4*, 233.

[47] Kaur, J.; Millington, K.; Smith, S. Producing high-quality precursor polymer and fibers to achieve theoretical strength in carbon fibers: A review. *Journal of Applied Polymer Science* **2016**.

[48] Frank, E.; Ingildeev, D.; Buchmeiser, M. R. High-performance PAN-based carbon fibers and their performance requirements. **2017**, 7.

[49] Dong, X.; Wang, C.; Bai, Y.; Cao, W. Effect of DMSO/H2O Coagulation Bath on the Strucutre and Property of Polyacrylonitrile Fibers During Wet-Spinning. *Journal of Applied Polymer Science* **2007**, *105*, 1221.

[50] Ford, E. Carbon nanotubes as structural templates within poly(vinyl alcohol) composite fibers, 2012.

[51] Smith, P.; Lemstra, P. J.; Pijpers, J. P. L. Tensile strength of highly oriented polyethylene. II. Effect of molecular weight distribution. *Journal of Polymer Science, Polymer Physics Edition* **1982**, *20*, 2229.

[52] ISO 11542-2:1998 Ultra-high-molecular-weight polyethylene (PE-UHMW) moulding and extrusion materials. International Organization for Standardization. **2013**.

[53] Meng, J.; Zhang, Y.; Song, K.; Minus, M. L. Forming Crystalline Polymer-Nano Interphase Structures for High-Modulus and High-Tensile/Strength Composite Fibers. *Macromolecular Materials and Engineering* **2014**, *299*, 144.

[54] Hao, J.; An, F.; Yu, Y.; Zhou, P.; Liu, Y.; Lu, C. Effect of coagulation conditions on solvent diffusions and the structures and tensile properties of solution spun polyacrylonitrile fibers. *Journal of Applied Polymer Science* **2016**, 44390.

[55] Wunderlich, B. Extended chain crystals of linear high polymers. *Pure and Applied Chemistry* **1972**, *31*, 49.

[56] Beloshenko, V. A.; Askadskii, A. A.; Varyukhin, V. N. Promising aspects of the structural modifications of polymers and polymer composites with the aid of high pressures. *Russian Chemical Reviews* **1998**, *67*, 951.

[57] Li, Y.; Tang, S.; Pan, M.; Zhu, L.; Zhong, G.; Li, Z. Polymorphic extended-chain and folded-chain crystals in polyvinylidene fluoride achieved by combination of high pressure and ion-dipole interaction. *Macromolecules* **2015**, *48*, 8565.

[58] Sreekumar, T. V.; Liu, T.; Min, B. G.; Guo, H.; Kumar, S.; Hauge, R. H.; Smalley, R. E. Polyacrylonitrile Single-Walled Carbon Nanotube Composite Fibers. *Advanced Materials* **2004**, *16*, 58.

[59] Chae, H. G.; Minus, M. L.; Kumar, S. Oriented and exfoliated single wall carbon nanotubes in polyacrylonitrile. *Polymer* **2006**, *47*, 3494.

[60] Feldman, D. *Polymeric Building Materials;* Elsevier Applied Science: London, 1989;.

[61] McNaught, A. D.; Wilkinson, A. In *Compendium of Chemical Terminology;* IUPAC Gold Book; Blackwell Scientific Publications: Oxford, 1997;.

[62] Iovleva, M. M.; Smirnova, V. N.; Budnitskii, G. A. The Solubility of Polyacrylonitrile. *Fibre Chemistry* **2001**, *33*, 262.

[63] Eom, Y.; Kim, B. C. Solubility parameter-based analysis of polyacrylonitrile solutions in N,N-dimethyl formamide and dimethyl sulfoxide. *Polymer* **2014**, *55*, 2570.

[64] Liu, S.; Jiang, H.; Du, W.; Pan, D. Spinnability in pre-gelled gel spinning of polyacrylonitrile precursor fibers. *Fibers and Polymers* **2012**, *13*, 846.

[65] Tan, L.; Wan, A.; Pan, D. Pregelled gel spinning of polyacrylonitrile precursor fiber. *Materials Letters* **2011**, *65*, 887.

[66] Chien, A.; Liu, H. C.; Newcomb, B. A.; Xiang, C.; Tour, J. M.; Kumar, S. Polyacrylonitrile fibers containing graphene oxide nanoribbons. *ACS Applied Materials & Interfaces* **2015**, *7*, 5281.

[67] Lu, C.; Blackwell, C.; Ren, Q.; Ford, E. Effect of Coagulation Bath on the Structure and Mechanical Properties of Gel Spun Lignin/Polyvinyl Alcohol Fibers. *ACS Sustainable Chemistry & Engineering* **2017**.

[68] Choudhary, V.; Gupta, A. In *Polymer/Carbon Nanotube Nanocomposites;* Yellampalli, S., Ed.; Carbon Nanotubes – Polymer Nanocomposites; Intech: 2011; pp 65.

[69] Popov, V. N. Carbon nanotubes: properties and application. *Materials Science and Engineering* **2003**, *43*, 61.

[70] Yakobson, B. I.; Avouris, P. Mechanical Properties of Carbon Nanotubes. *Carbon Nanotubes* **2001**, *80*, 287.

[71] Liu, H. C.; Chien, A.; Newcomb, B. A.; Liu, Y.; Kumar, S. Processing, Structure, and Properties of Lignin- and CNT- Incorporated Polyacrylonitrile-Based Carbon Fibers. *ACS Sustainable Chemistry & Engineering* **2015**, *3*, 1943.

[72] Boeriu, C. G.; Fitigau, F. I.; Gosselink, R. J. A.; Frissen, A. E.; Stoutjesdijk, J.; Peter, F. Fractionation of five technical lignins by selective extraction in green solvents and characterisation of isolated fractions. *Industrial Crops and Products* **2014**, *62*, 481.

[73] Öhman, F.; Wallmo, H.; Theliander, H. Precipitation and filtration of lignin from black liquor of different origin. *Nordic Pulp and Paper Research Journal* **2007**, *22*, 188.

[74] Öhman, F.; Wallmo, H.; Theliander, H.; Axegârd, P. United States of America Patent US20150119559, 2013.

[75] Bajpai, P. *Carbon fibre from lignin;* Springer Nature: Kanpur, India, 2017;.

[76] Chakar, F. S.; Ragauskas, A., J. Review of current and future softwood kraft lignin process chemistry. *Industrial Crops and Products* **2004**, *20*, 131.

[77] Fengel, D.; Wegner, G.; Eds. *Wood Chemistry, Ultrastructure, and Reactions,* Walter de Gruyter: Berlin, Germany 1989;.

[78] Guerra, A.; Filpponen, I.; Lucia, L. A.; Saquing, C.; Baumberger, S.; Argyropoulos, D. S. Toward a Better Understanding of the Lignin Isolation Process from Wood. *Journal of Agriculturual and Food Chemistry* **2006**, *54*, 5939.

[79] Chabannes, M.; Ruel, K.; Yoshinaga, A.; Chabbert, B.; Jauneau, A.; Joseleau, J.; Boudet, A. *In situ* analysis of lignins in transgenic tobacco reveals a differential impact

[80] Wang, K.; Xu, F.; Sun, R. Molecular Characteristics of Kraft-AQ Pulping Lignin Fractionated by Sequential Organic Solvent Extraction. *International Journal of Molecular Sciences* **2010**, *11*, 2988.

[81] Sixta, H. *Handbook of Pulp;* Wiley-VCH: 2006;.

[82] Lora, J. In *Industrial commercial lignins: Sources, properties and applications;* Belgacem, M. N., Gandini, A., Eds.; Monomers, Polymers and Composites from Renewable Resources; Elsevier Science: 2008; pp 225.

[83] Mason, W. H. United States of America Patent US1578609, 1926.

[84] Li, J.; Gellerstedt, G.; Toven, K. Steam explosion lignins; their extraction, structure and potential as feedstock for biodiesel and chemicals. *Bioresource Technology* **2009**, *100*, 2556.

[85] Nordström, Y.; Norberg, I.; Sjöholm, E.; Drougge, R. A New Softening Agent for Melt Spinning of Softwood Kraft Lignin. *Journal of Applied Polymer Science* **2012**, 1274.

[86] Irvine, G. M. The significance of the glass transition of lignin in thermomechanical pulping. *Wood Science and Technology* **1985**, *19*, 139.

[87] Aklonis, J. J.; MacKnight, W. J.; Shen, M. *Introduction to polymer viscoelasticity;* Wiley-Interscience: New York, 1972;.

[88] Fitzer, E.; Müller, D. J. The influence of oxygen on the chemical reactions during stabilization of PAN as carbon fiber precursor. *Carbon* **1975**, *13*, 63.

[89] Husman, G. Development and commercialization of a novel low-cost carbon fiber. **2014**.

[90] Burke, J. Solubility Parameters: Theory and Application. http://www.cool.conservation-us.org/coolaic/sg/bpg/annual/v03/bp03-04.html.

[91] Grulke, E. A. Solubility Parameter Values. In The Wiley Database of Polymer Properties. **2003**.

[92] Hansen, C. M. The Three Dimensional Solubility Parameter and Solvent Diffusion Coefficient. **1967**.

[93] Yamamoto, H. Hansen Solubility Parameters (HSP) Application Notes. https://pirika.com/ENG/HSP/index.html.

[94] Gårdebjer, S.; Andersson, M.; Engström, J.; Restorp, P.; Persson, M.; Larsson, A. Using Hansen solubility parameters to predict the disperson of nano-particles in polymer films. *Polymer Chemistry* **2016**, *7*, 1756.

1.6. Thesis Objectives

Industry is investing in research involving environmentally sound chemistries that can compete with products from 100 % synthetic, raw materials. Low cost, renewable fillers are ideal raw materials, especially if they can improve processes of fiber production and lower the industry's dependency on petroleum- in consideration of how resin prices fluctuate with the cost of oil. Lignin is abundant, biorenewable resource in the USA and globally. This biomaterial has been investigated as a green source of carbon fiber production with some success; nevertheless the strength of lignin-based fibers is often lacking. Gel-spinning PAN composite fibers with fillers like CNTs is promising for the development of high-performance PAN precursor fibers, but CNT addition would inflate raw material costs. The gel-spinning technique was employed by Liu et al. to obtain composite fibers of PAN and lignin having high-performance and low cost [70]. But their use of methanol poses a problem for maintaining the integrity of composite fibers by limiting lignin migration from as-spun fiber and into the coagulation bath. The loss of lignin to coagulation baths for solution spinning was left unaddressed until recently, when Lu et al. mixed solvents to reduce lignin migration[66]. The need for alternative coagulation baths permits an opportunity to use less volatile, inexpensive, and more environmentally friendly solvent mixtures for the coagulation bath. The research goals of this study were to:

- Understand the role of alternative coagulation baths on the gel-spinning, properties, and structure of lignin/PAN fibers comprised of more than 10% lignin to matrix polymer. The goal is to retain lignin in the fiber structure at high concentrations.
- Employ glucaric acid (a green, biomass derivative) to improve the gel-spinning of PAN fibers and identify characteristics of antiplasticization among spun fibers.

- Examine the role of lignin grafted with PAN as compatibilizers between PAN and lignin within gel-spun fibers.

2. TEAS MAPPING OF REDUCED-METHANOL COAGULATION BATHS FOR LIGNIN/POLYACRYLONITRILE GEL-FIBER SPINNING

2.1. Introduction

Global demands for carbon fiber (CF) are largely met by the stabilization, carbonization, and graphitization of polyacrylonitrile (PAN). PAN precursor fibers produce the strongest grades of high-performing CF. The raw material cost for PAN resin constitutes the bulk cost of CF manufacturing. As industry contends for sustainable CF, research has emerged around lignin- an aromatic, biomass derivative as a CF precursor. Lignin is the most globally, abundant phenolic resin from nature. The only biopolymer more naturally abundant than lignin is cellulose[1,2]. During the pulp and paper process, lignin and hemicellulose waste byproducts are extracted from cellulose pulp and are often repurposed as fuel for plant operations[3]. Woody plants and grasses are reinforced by lignin biomacromolecules, but each will differ in their composition of phenolic p-coumaryl, coniferyl, and sinapyl monomers[1,2]. In consequence, plant source has shown to greatly influence carbon yield for each type of thermally treated lignin. Lignin has 45.7 % carbon yield when it is sourced from hardwood Kraft lignin, which is more than tar pitch having a carbon yield of 33.4 % according to Kalda et al.[4]. Thus, lignin's high carbon yield and natural abundance makes it an attractive precursor for CF.

The thermoplastic behavior of lignin has led to research on the melt extrusion of lignin. Lignin has a detectable glass transition temperature (T_g), which allows it to soften and flow. Its T_g depends upon its source-dependent chemistry and approach used for chemical extraction. Softwood lignin has a T_g between 132 – 148 °C; whereas, hardwood lignin has a T_g between 102 and 119 °C[1]. The feasibility of melt extrusion has been explored for lignin fiber spinning; however, the mechanical performance of CF derived from those lignin fibers is significantly

lower than CF derived from solution spun PAN. Kadla et al. carbonized hardwood Kraft lignin fiber that were melt spun at 195 to 228 °C[4]. Lignin-derived CFs had a breaking strength of 420 MPa and Young's modulus of 40 GPa. In contrast, Bahl et al. fabricated CFs-derived from PAN with breaking strength of 7100 MPa and Young's modulus of 590 GPa[5].

Lignin and PAN have properties that are valuable for CF production; namely lignin's low cost and the high strength and modulus afforded by PAN. Several researchers have carbonized lignin/PAN CF precursors by solution spinning[6-8]. Seydibeyoğlu blended PAN with up to 30 % lignin in DMAc to produce films having similar strength to neat PAN[9]. The lignin/PAN film having 30 % lignin had a storage modulus of 1.7 GPa; whereas, the neat PAN film had a storage modulus of 0.9 GPa[9]. The implications of that work suggest similar properties are achievable between PAN and lignin/PAN fibers. Liu et al. gel-spun lignin/PAN fibers with up to 30% lignin to polymer in the dope using dimethylacetamide (DMAc) as the dissolving solvent and methanol (MeOH) as the coagulating solvent. The Young's modulus of lignin/PAN fiber (17.2 GPa) was weaker than that of neat PAN fiber (19.9 GPa). Post-carbonization at 1100 °C, CF from neat PAN fiber had a modulus of 223 GPa; whereas, CF from lignin/PAN fiber had a higher modulus of 230 GPa[6].

In literature, it is known that lignin dissolves in MeOH and other organic solvents[5,8,10,11]. Dissolution studies performed by Cybulska et al. had shown organosolv lignin was less soluble in dimethyl sulfoxide (DMSO) than in MeOH [10]. The solubility of raw lignin from prairie cord grass was 33 % (wt/wt) in DMSO and 77 % (wt/wt) in MeOH[10]. Sameni et al. observed Kraft and soda lignin were soluble in both DMSO and MeOH; however, their solubility in DMSO was higher than in MeOH[11]. From these sources, we observe the important role of lignin's source on its solubility in DMSO relative to MeOH.

Polar aprotic solvents (such as DMAc, DMSO, and dimethylforamide, DMF) are commonly used to dissolve lignin/PAN spinning dopes[12-17]. DMSO/water is common for the coagulation of wet-spun PAN fibers [14,18], and MeOH is often used to coagulate gel-spun PAN fibers[5,6,9,16,17]. Thus, lignin is expected to dissolve in PAN spinning dopes that use an aprotic solvent, but lignin can also migrate from the as-spun fiber and into the coagulation bath. Lignin migration into the coagulation bath was reported in the 2014 Husman report to the Department of Energy on solution spun lignin/PAN fiber[8]. Challenges emerged from the production of as-spun fiber at pilot-scales. Voids among off-quality fiber resulted from lignin migration from as-spun fiber and into the coagulation bath, however the solvents for coagulation were not specified[7,8].

In 2017, Lu et al. pioneered research on the use of solvent mixtures to deter lignin migration from lignin/poly(vinyl alcohol) (PVA) as-spun fibers and into coagulation baths for gel-fiber spinning[19]. In that work, lignin/PVA dopes were gel-spun using solvent mixtures of acetone/MeOH[19]. At more than 20 % lignin to polymer, lignin readily migrated into the MeOH coagulation bath along with DMSO/water, which resulted in the loss of lignin solids from fiber and voids. Both acetone and methanol are good coagulants for removing DMSO and water from dissolved PVA. Acetone soluble fractions of softwood pine lignin was removed from lignin, but all lignin fractions remained soluble in methanol. As a result, 15/85 MeOH/acetone mixtures successfully maintained the bulk of lignin within the PVA gel-fiber during coagulation. MeOH/acetone coagulation also yielded mechanically stronger lignin/PVA fibers than by MeOH coagulation. Lu et al. noted how the saturation of polymer-rich domains likely caused lignin to reside within the solvent-rich domains of PVA gel-fibers[19].

Therefore, using solvent mixtures to tune the coagulation of lignin/PAN is a promising technique for deterring lignin migration into the coagulation bath and the spinning of stronger lignin/PAN fibers. The solution spinning of lignin-based fibers by alternate solvent systems would benefit from the mapping of promising coagulants. That predictive capability requires an understanding of how solubility parameters affect the dissolution of lignin, matrix polymer, and solvent mixtures. Hansen solubility parameters (HSPs) are quantifiable terms that aid the prediction of dissolution by molecular affinity. This technique for low molar mass molecules aids an understanding of how polymers dissolve without considering molecular weight effects.

HSPs classify molecular interactions for dissolution in terms of their dispersive (δ_D), polar (δ_P), and hydrogen (δ_H) bonding behaviors[20-23]. Hansen and Yamamoto have plotted HSP values to represent three-dimensional domains of solubility in "Hansen Space"[21,23]. Spatial proximity in Hansen Space is a useful tool to predict miscibility and dissolution between molecules [21,23]. HSP values for solvent mixtures are expressed by **Equation 2.1**:

$$\delta_i{}' = \frac{v_1\delta_{1i} + v_2\delta_{2i}}{V} \qquad (2.1)$$

where, δ_i' is the HSP for the mixture in terms of δ_D, δ_P, or δ_H; v is the volume fraction of each solvent in a binary system; δ_i is the HSP value for each solvent; and V is the total volume of the solvent mixture[21,23]. Calculated values for δ_D', δ_P', and δ_H' are then plotted in three-dimensional Hansen Space, but Burke has suggested an alternative two-dimensional plot called the Teas Plot[24]. Teas Plots instead graphically show the dispersive (f_D), polar (f_P), and hydrogen (f_H) bonding fractions of the solvent system based on individual HSP values (δ_i) on a 2-D ternary plot. **Equation 2.2** shows how f_i values are determined:

$$f_i = 100 \times \frac{\delta_i}{\delta_D + \delta_P + \delta_H} \qquad (2.2)$$

Since each HSP value is based on volume fraction, the Teas plot could easily extend to the mapping of ternary solvent systems.

Teas plots are typically used to understand the driving forces for solubility; nevertheless, we propose the use of these plots to map lignin/PAN coagulation by a system involving non-solvents. To map coagulation systems using the Teas plot, it was necessary to define the desired properties of gel-fiber upon coagulation. The criteria defined in this study were for flexible, as-spun lignin/PAN fiber in the form of a drawable physical gel. Further, Teas plots of the engineered solvent mixtures should minimize lignin migration during coagulation with less dependency on trial and error when it comes to the determination of new bath compositions. Solvent mixtures of acetone, isopropanol (IPA), MeOH, and water were test baths for PAN gelation and averting lignin migration during the spinning of as-spun gel-fiber.

2.2. Experimental

2.2.1. Materials

PAN powder having a molecular weight of 150 kDa was procured from Scientific Polymer. Powdered Kraft lignin from Domtar was used as-received. Solvents included water, DMSO from Sigma Aldrich, acetone, ethyl acetate (EA), IPA, and MeOH from BDH Chemicals.

2.2.2. Spinning Dope Preparation

Spinning dopes of PAN and lignin/PAN (containing up to 50 % lignin, or 2:1 PAN:lignin, by solids) were prepared. Because Lu et al. observed lignin migration at 20 % lignin [19], lignin to PAN was exaggerated at 50 % lignin in this study. 10 g of PAN was dissolved in 50 mL of DMSO under constant stirring at 85 °C for approximately 10 h before spinning. Lignin was sonicated in 50 mL DMSO for up to 18 h prior to its addition to dissolved PAN. Sonicated lignin was combined with PAN dissolved in DMSO for lignin/PAN dopes. Dopes were heated at

85 °C and stirred for approximately 10 h. The final concentration of PAN in the spinning dope was 20 g/dL.

2.2.3. Gel-Spinning

The gel-spinning process in **Figure 2.1** is labeled according to three important steps: dope feed, coagulation, and thermal drawing.

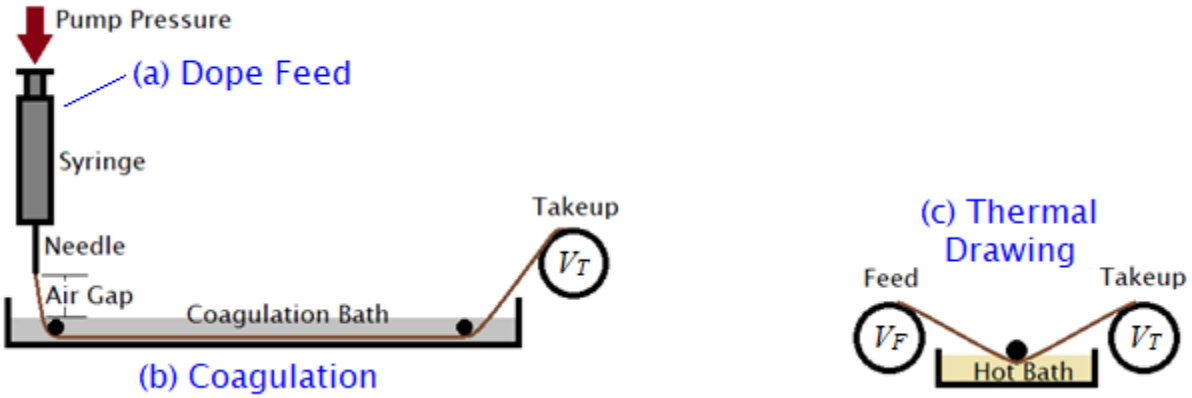

Figure 2.1. Schematic of gel-spinning labels the process as (a) Dope Feed, (b) Coagulation, and (c) Thermal Drawing.

Dope Feed: Spinning dopes were dispensed using a high pressure, stainless steel syringe that was equipped with a 19-gauge needle (0.69 mm inner diameter and 50.8 mm in length). In **Figure 2.1a**, the dope was loaded into the syringe and allowed to settle (or age) for at least 2 h at ~21 °C. This process of PAN dope aging is known as "pre-gelation" or the equilibration of dope at room temperature. According to literature, pre-gelation results in a gel-like network; wherein the dope phase separates into domains of polymer-rich PAN and solvent[12,16,17,25]. Tan et al. aged PAN dope (of 78 kDa polymer) for up to 10 h. Aging significantly increased the shear modulus (i.e. elasticity) of the dope, while decreasing the number of breaks during fiber spinning[16]. Liu et al. aged 78 kDa PAN dopes for up to 3 h, but dope aged for 1.5 h spun at the highest draw ratio and were the strongest[17].

Coagulation: As seen in **Figure 2.1b**, the dope was fed into the coagulation bath with a vertical dry jet of ~3 cm from the tip of the needle to solvent surface. The coagulation bath comprised of solvent mixtures described in **Table 2.1**. Afterwards, as-spun gel-fibers were wound onto a spool at linear velocities greater than their feed speeds.

Table 2.1. Coagulation Bath Formulations for Spun Lignin/PAN Fibers.

Mixture	Acetone % v/v	IPA % v/v	MeOH % v/v	Water % v/v
1			100	
2	15	85		
3	85	15		
4	15		85	
5	85		15	
6		85	15	
7		15	85	
8		15		85
9		25	50	25
10	25	25		50

Thermal Drawing: As shown in **Figure 2.1c**, as-spun gel-fibers were thermally drawn through glycerol in two stages at temperatures ranging from 130 to 170 °C. Fiber draw ratios (*DR*) were calculated according to **Equation 2.3** the ratio of fiber take-up speed (V_T) to feed speed (V_F):

$$DR = \frac{V_T}{V_F} \qquad (2.3)$$

2.2.4. Testing Lignin/PAN Coagulation

Qualitative droplet testing was used to visually compare the coagulation of lignin/PAN dopes and lignin migration into coagulation solvents (see **Table 2.1**). Spinning dope (less than 1 mL) was dispensed into scintillation vials containing 10 mL of solvent.

Cybulska et al. described a test method to quantify the solubility of lignin in a solvent[10]. A modification to this approach was used to quantify the solubility of lignin

dissolved in DMSO with potential coagulation baths (see **Table 2.1**). Lignin was sonicated in DMSO for a final concentration of 10 g/dL. 0.5 mL of sonicated lignin/DMSO was then added to 10 mL of each coagulation bath, shaken, and then allowed to stand for 5 minutes. Lignin precipitant was collected on Whatman 42 filter paper, dried under a fume hood, and weighed. The mass of insoluble lignin mass (m_{lignin}) was then calculated from **Equation 2.4**,

$$m_f - m_0 = m_{lignin} \tag{2.4}$$

where m_f is the mass of the filter paper after filtration and drying and m_0 is the original mass of the filter paper.

2.2.5. Flammability of Solvent Mixtures for Coagulation

The Lower Flammability Limit (LFL) is the lower end of a range of volumetric percent of flammable vapors in air that can be ignited at a given temperature and pressure. The LFL determines the least volumetric percent of a flammable vapor and can be a predictor of when vapors can ignite given an ignition source. Utilizing LeChatelier's Rule, **Equation 2.5**, the lower flammability limit (LFL) could be calculated for a mixture:

$$MLFL = \frac{1}{\sum \frac{x_i}{LFL_i}} \tag{2.5}$$

where *MLFL* is the mixture lower flammability limit, x_i is the molar fraction of the solvent *i*, and LFL_i is the lower flammability limit of solvent *i*. Individual LFLs are calculated theough **Equation 2.6**:

$$LFL_i = \frac{P_i^{sat}}{P_{amb}} \tag{2.6}$$

where P_i^{sat} is the vapor pressure at the flash point of solvent *i* and P_{amb} is the ambient pressure. The flash point, T_F, is the lowest temperature at which the flammable vapors will ignite at a given an ignition source. The flash point of the solvent mixture can be estimated by **Equation 2.7**:

$$1 = \sum \frac{x_i \gamma_i P_i^{sat}}{P_i^{sat}} \quad (2.7)$$

where γ_i is the activity coefficient of solvent *i* and P_i^{sat} is the partial vapor pressure of solvent *i* at temperature *T*. The temperature that satisfies **Equation 2.7** is the mixture's flash point[26-29]. To simplify the equation for estimation at ideal conditions, the activity coefficient γ_i can be set to 1. Using Antoine's Equation, **Equation 2.8** can directly relate to the flash point of the mixture[26-29]:

$$1 = \sum x_i \frac{10^{A_i - \frac{B_i}{T_{MFP} - C_i}}}{10^{A_i - \frac{B_i}{T_{iFP} - C_i}}} \quad (2.8)$$

where A_i, B_i, and C_i are Antoine Coefficients of solvent *i*, T_{iFP} is the flash point of solvent *i*, and T_{MFP} is the flash point of the mixture.

2.2.6. Mechanical Testing

The mechanical properties of lignin/PAN fibers were tested using the MTS-Q testing system according to ASTM D3379. Parameters were set to 15 mm/min strain rate, 25.4 mm gauge length, and up to 20 specimen sample sizes. Lignin/PAN fiber density was calculated according to the inverse rule of mixtures (**Equation 2.9**):

$$\rho_{fiber} = \left(\frac{1-w}{\rho_{PAN}} + \frac{w}{\rho_{lignin}}\right)^{-1} \quad (2.9)$$

where *w* is weight fraction, ρ_{fiber} is the density of the lignin/PAN fiber, ρ_{PAN} is the density of PAN at 1.184 g/mL[30], and ρ_{lignin} is the density of lignin at 1.3 g/mL[31].

2.2.7. Imaging

Linear density, $\mathcal{J}$, reported in dtex, was calculated from measurements of cross-sectional area (*Acs*), which were determined by IMAGEJ analysis. Confocal micrographs were taken on

the LEXT OSL4000. With A_{CS} and ρ_{fiber} available, the linear density was calculated according to **Equation 2.10**:

$$\mathcal{J}I = A_{CS} \times \rho_{fiber} \quad (2.10)$$

Fiber fracture tips from mechanical testing were imaged by FEI Verios 460L Scanning Electron Microscope (SEM) at 2kV. Prior to imaging, samples were sputter-coated with a 60/40 gold/palladium mixture.

2.2.8. Thermal Characterization

Thermal analysis was conducted through the means of Dynamic Scanning Calorimetry (DSC) and Thermogravimetric Analysis (TGA). The DSC data were retrieved from the DSC Q2000 V24.11 on a range of -20 to 400 °C at a ramp rate of 5 °C/min, with nitrogen carrier gas, and modulating ±5 °C/min. The TGA data were taken with the TGA Q500 V6.7 on a range of 30 to 600 °C at a ramp rate of 10 °C/min with nitrogen carrier gas.

2.2.9. Structural Characterization

Using a Nicolet 510P IR spectrometer, IR spectra between 400 to 4000 cm^{-1} were recorded at a resolution of 4 cm^{-1} and over 64 scans per spectrum. 1-D equatorial X-Ray Diffraction (WAXD) was also conducted for crystallinity and crystal size, using the Empyrean diffractometer system. The crystal size for each of the samples was calculated through the Scherrer Equation, **Equation 2.11**:

$$\tau = \frac{K\lambda}{\beta\cos(\theta)} \quad (2.11)$$

where τ is the crystal size in Å, K is a shape factor of 0.9, λ is the wavelength for the copper source of 1.54 Å, β is the full width at half max of the crystalline peak in radians, and θ is the Bragg Angle in radians of the crystalline peak.

2.3. Results & Discussion

2.3.1. Effect of Solvent Mixtures on Dope Coagulation and Lignin Migration

Micrographs of lignin/PAN spinning dopes reveal their homogeneity prior to coagulation in solvent. Unlike the homogeneous solutions observed for neat PAN/DMSO and lignin/DMSO after sonication, lignin/PAN dopes show evidence of phase separation that was likely due to lignin-rich domains (**Figure 2.2**).

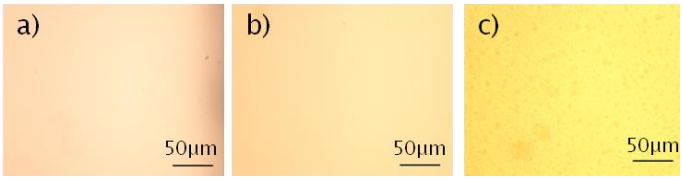

Figure 2.2. Optical micrographs of (a) Neat PAN in DMSO, (b) sonicated lignin in DMSO, and (c) lignin/PAN in DMSO.

Coagulants in **Table 2.1** were evaluated based on the ductile nature of lignin/PAN droplets (at 50 % lignin) in those solvent mixtures and retention of lignin within the as-dropped dope (**Figure 2.3**). 'Good' coagulants for lignin/PAN droplets should yield drawable, soft solids. When lignin/PAN was added to mixtures 2, 3, 5, and 7, soft droplets formed, but these lacked cohesion for hand-drawing. In direct contrast, mixtures 4, 6, and 8 rapidly coagulated lignin/PAN droplets and the resulting droplets were too hard to draw by hand. Mixtures 1, 9, and 10 resulted in "semi-soft" gel-phases that were cohesive and drawable.

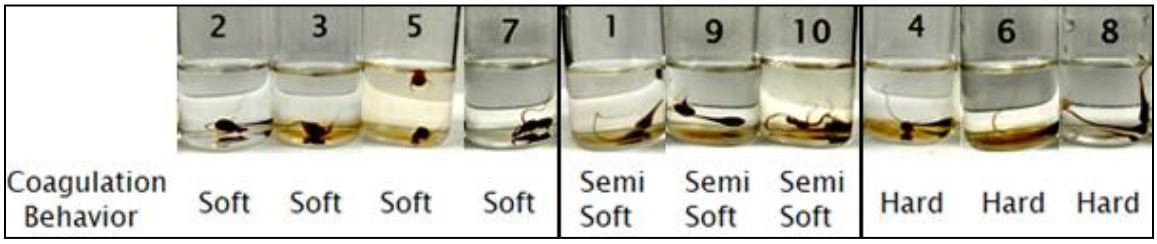

Figure 2.3. Droplet testing of the lignin/PAN dope at 50 % lignin in solvent mixtures 1-10 as described in **Table 2.1**.

From droplet testing, lignin leaching into the coagulation bath occurred on several instances. The rate of leaching seemed influenced by the relative hardness of coagulated lignin/PAN droplets. Supporting information shows lignin diffusion from the dope and into solvent mixture 1 occurred more rapidly than from 9 and 10 (tension was not applied to the jets of dope). Solvent mixtures 1, 9 and 10 were selected, because these would likely yield the most drawable as-spun lignin-PAN fibers.

To better understand the propensity of lignin to diffuse from as-spun fiber and into solvent mixtures for coagulation, the insoluble fractions from DMSO-dissolved lignin (**Table 2.2**) were measured after exposure to each coagulation bath in **Table 2.1**. Data on insoluble fractions were arranged according to coagulation behaviors noted by drop testing (**Figure 2.3**).

Table 2.2. Insolubility of Lignin in Solvent Mixtures with their Teas Ratios.

	Solvents/Mixtures	m_{lignin} (%)	f_D (%)	f_P (%)	f_H (%)
PAN Non-solvents	**Acetone**	21.6	15.5	10.4	7.0
	EA	33.0	15.8	5.3	7.2
	IPA	33.8	15.8	6.1	16.4
	Water	92.0	15.5	16.0	42.3
Soft	**#2**	23.4	40.7	18.8	40.5
	#3	22.0	45.8	29.0	25.2
	#5	21.0	43.6	30.2	26.2
	#7	18.0	38.1	18.3	43.6
Semi-soft	**#1 (MeOH)**	20.0	30.4	24.7	44.9
	#9	43.2	28.9	22.2	48.9
	#10	28.0	28.3	22.3	49.4
Hard	**#4**	28.2	32.1	25.5	42.4
	#6	48.8	31.6	23.8	44.7
	#8	98.8	22.7	21.3	56.1

†Based on lignin/PAN dopes at 50 % lignin to PAN.
‡Lignin solubility in PAN non-solvents (like acetone, EA, IPA, and water) was included.

Among the pure solvents, lignin was least soluble in water. For the lignin used in this study, MeOH (#1) and acetone had similar values of lignin solubility. Lignin insoluble fractions were similar for EA and IPA, but both were slightly higher than those reported for acetone and

MeOH. Based on data in **Table 2.2**, the volume fraction of pure solvents did not predict coagulation as well as f_D, f_P, and f_H values.

Hard droplets coagulated in mixtures 4, 6, and 8, wherein insoluble fractions of lignin were $m_{lignin} \geq 28$ %. Soft droplets coagulated in mixtures 2, 3, 5, and 7, where insoluble fractions of lignin were $m_{lignin} \geq 23$ %. Semi-soft droplet formation occurred among solvent mixtures 1, 9, and 10, however lignin dissolution was not deterred more or less than in the 'hard' and 'soft' coagulants of lignin/PAN.

Based on the Teas Ratios in **Table 2.2**, some trends are apparent for coagulation and lignin's solubility in solvent systems. Based on lignin insolubility in water, $f_H \geq 42$ % coagulates PAN and precipitates lignin when f_D and f_P values are also low. In comparison to MeOH, mixtures 9 and 10 have higher f_H values but lower f_D and f_P values, which could explain the slower rates of lignin diffusion (see Supporting Information). The relatively rapid diffusion of lignin from dopes coagulated in pure MeOH, makes this pure solvent less ideal for gel-spinning lignin/PAN fibers, especially at high loadings of lignin (see Supporting Information). Relative to Teas ratios for hard coagulation, mixtures 9 and 10 also offer a drawable dope perhaps due to low f_D and f_P values, which 1) permits lignin mobility at the lignin/polymer interface and 2) slows lignin diffusion from the coagulating PAN. Mixture 8 (for hard coagulation) has a high fraction of insoluble lignin due to its high f_H value of 56.1 % that is coupled with low f_D and f_P values (22.7 % and 21.3 %, respectively).

2.3.2. Mapping Lignin/PAN Coagulation on Teas Plots

The Teas plot graphs differences between the HSP character of pure solvents, solvent mixtures, lignin and PAN. By increasing f_H character, nonsolvent mixtures for PAN coagulation into hard, highly crystalline polymer or soft, gel structures are formulated, as observed

empirically by drop testing. Lignin has greater f_H character than PAN, therefore it can remain soluble in MeOH. The Teas plot effectively maps how variations in f_i can affect PAN coagulation and lignin solubility using known solvent mixtures.

Mixture 9 and 10 are encircled on **Figure 2.4** to emphasize similarities between their f_H, f_D, and f_P character. The calculated HSP values for mixtures 9 and 10 were within 0.8 % for each of their respective HSP values. Water, MeOH, and IPA are coagulating, nonsolvents for PAN, but only water is an exceptional nonsolvent for lignin. Interestingly, their spatial midpoint (in terms of f_H, f_D, and f_P character) on the Teas plot is approximate to Mixtures 9 and 10 (**Figure 2.4**). Although the 55/45 EA/water mixture would give the spatial midpoint between water, MeOH and IPA, the immiscibility of these solvents prevents testing of its coagulation ability against lignin/PAN dopes. The effects of Mixture 9 and 10 on the gel-fiber spinning, structure and mechanical properties of lignin/PAN fibers were studied for the remainder of this work.

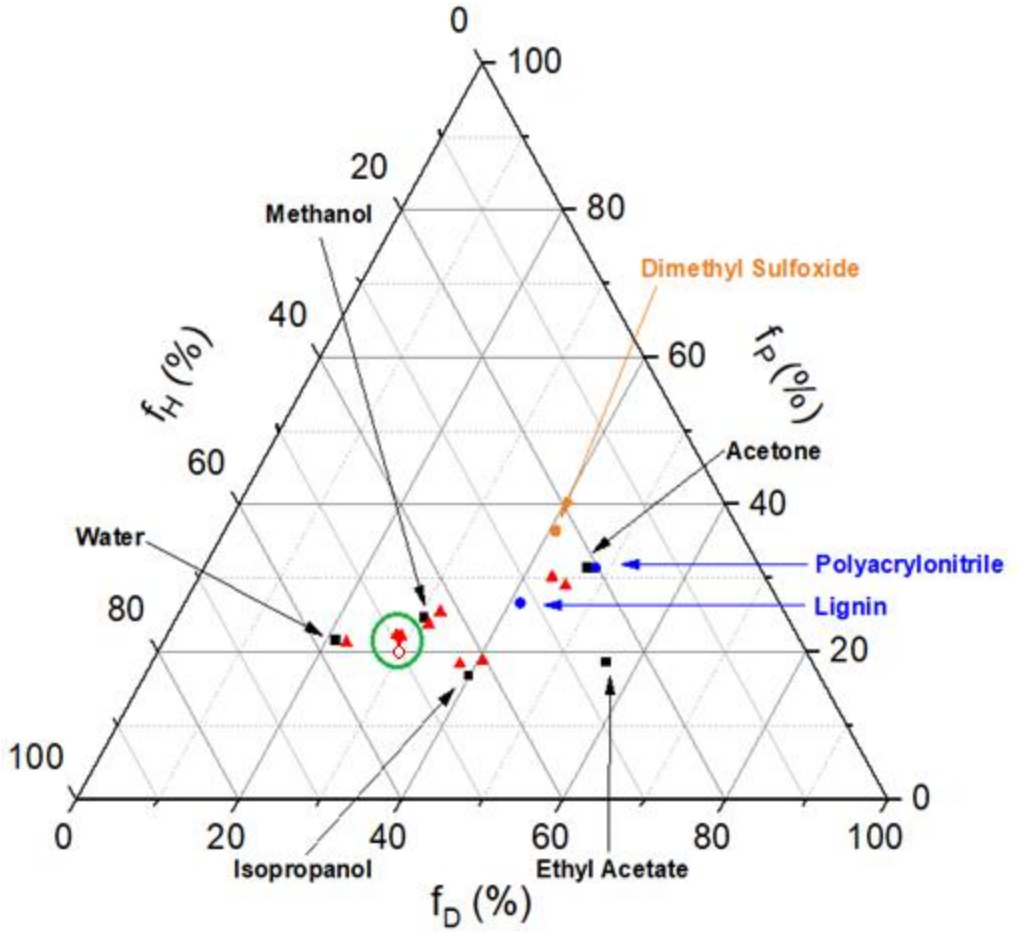

Figure 2.4. Teas plot of solvent mixtures used for lignin/PAN coagulation. "■" represents neat coagulation solvents, "●" represents neat dissolution solvents, "▲" represents mixed coagulation solvents, "●" represents solids, and "○" represents a theoretical 55/45 EA/water mixture. A green circle encloses mixtures 9 and 10 as an area of effective coagulation and lignin migration hindrance.

2.3.3. Select Coagulation Baths on Lignin Retention Among Gel-Spun Lignin/PAN Fibers

Mixtures 1, 9, and 10 were tested as coagulation baths for the spinning of lignin/PAN fibers at up to 50 % lignin to PAN. According to processing parameters for gel-spun lignin/PAN, mixtures 9 and 10 gave similar as-spun draw ratios for neat PAN and lignin/PAN fibers (**Table**

2.3) that were higher than MeOH (i.e. mixture 1). Lignin/PAN fiber spinning at 50 % lignin was attempted with neat MeOH as the coagulation bath, but the resulting as-spun fibers were non-uniform. As a result, lignin/PAN as-spun fibers were not drawable at elevated temperatures. Of those parameters, the most notable differences are in bath temperature and draw ratio. By reducing MeOH in the coagulation bath, as-spun gel-fiber was formed and drawn at higher temperatures. Further, mixture 9 yielded the highest fiber draw ratios for neat PAN fibers and those at 50 % lignin. Although the HSP values for mixture 9 and 10 are similar, both differed in terms of their ability to dissolve lignin. Nevertheless, lignin migration into the coagulation bath was unnoticeable.

Table 2.3. Processing Parameters of Lignin/PAN Fibers.

Bath ID		**#1**	**#9**		**#10**	
Sample		**Neat PAN**	**Neat PAN**	**50 % Lignin/PAN**	**Neat PAN**	**50 % Lignin/PAN**
As-spun	**DR**	6.2	7.0	7.2	7.2	7.0
	Residence Time (s)	2.4	2.1	2.1	2.0	2.1
	Temp (°C)	-20	-4	-7	3	7
Stage 1	**DR**	8.9	12.2	9.2	9.3	10.0
	Temp (°C)	130	135	133	131	140
Stage 2	**DR**	1.4	1.5	1.6	1.5	1.4
	Temp (°C)	174	168	160	173	174
Total DR		76	126	106	99	102
Linear Density (dtex)		29	13	12	18	19
Effective Diameter (µm)		56±2	37±1	35±1	44±2	44±1

Based on the confocal micrographs of lignin/PAN fibers in **Figure 2.5**, no evidence of lignin migration from PAN was observed among fibers. Aggressive voiding occurs among lignin/PAN fibers as lignin migrates in excess from coagulating fibers and into the coagulation bath. This was reported by Lu et al., when lignin/PVA fibers we spun using MeOH at 20 % lignin to matrix polymer[19]. The inclusion of an alternative solvent aided in the reduction of lignin migration. Paired with lignin non-solvents, reduced exposure time to the coagulation bath

also allowed for the gel-fiber to be drawn further. With the change in the diffusion behavior as a result of a bath mixture, lignin was given less energy and time to migrate out of the system while the PAN was coagulated, however because of the increased temperature, the DMSO solvent would require less time and energy to exit the fiber system. This would allow the gel-fiber to be "wrung out" through drawing as it was being formed in the bath, essentially mechanically aiding in the coagulation of the solids as they were drawn and oriented along the gel-fiber axis.

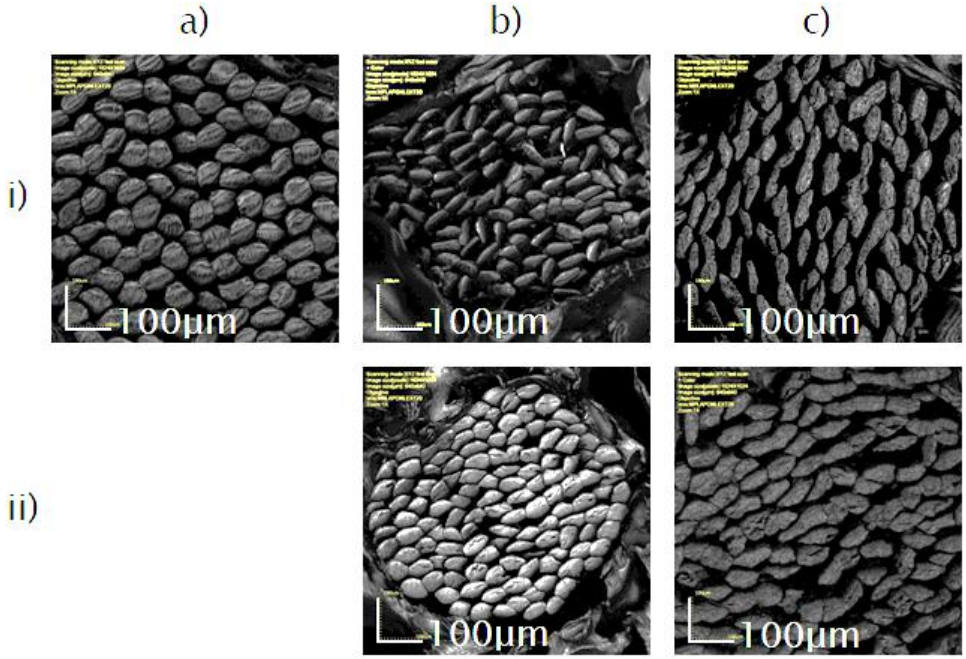

Figure 2.5. Confocal micrographs of fibers gel-spun with (a) Mixture 1, (b) Mixture 9, and (c) Mixture 10 coagulants; wherein fibers contained (i) 0 and (ii) 50 % lignin to PAN.

Further, IR spectroscopy was used to study lignin to PAN content within the final gel-spun fibers. Spectra of neat PAN and lignin/PAN fibers were normalized against the peak at 2242 cm^{-1} (**Figure 2.6**), the PAN nitrile group[6]. Strong peaks at 1261 cm^{-1} are indicative of C-O stretching in the guaiacylic rings present in lignin[32], which are derived from the coniferyl lignin monomer found in both hardwood and softwood sources[1]. Also characteristic of lignin, strong peaks between 780 cm^{-1} and 860 cm^{-1} are indicative of aromatic C-H stretching[1], and

show the same pattern in regards to coagulation bath used to spin. **Figures 2.6a** and **2.6c** show only minimal peaks while **Figures 2.6b** and **2.6d** both show sharp peaks at ~800 cm^{-1}, further supporting the reduction of lignin migration from the fiber system. These 800 cm^{-1} peaks coincide with the lack of any apparent phase separation on the micron level seen in the cross sections shown in **Figure 2.5ii**.

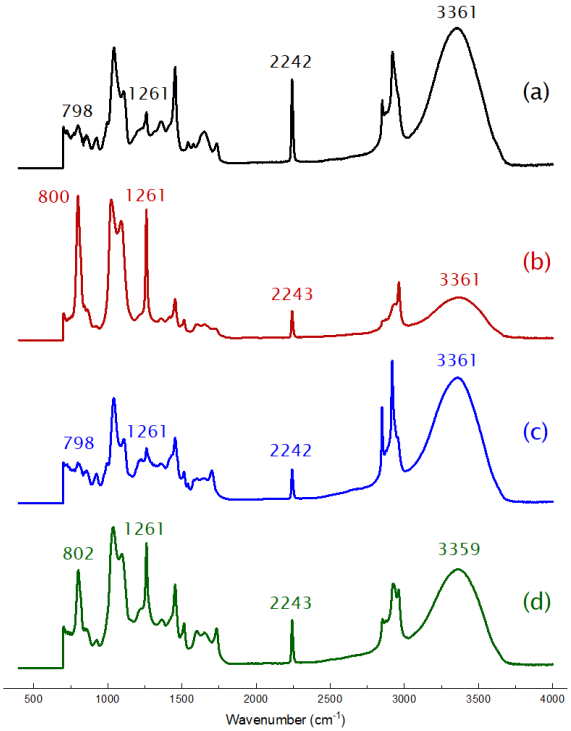

Figure 2.6. Normalized IR spectra of (a) neat PAN fibers spun in mixture 9 and lignin/PAN fibers spun in (b) mixture 9, (c) MeOH, and (d) mixture 10.

2.3.4. Select Coagulation Baths on the Mechanical Strength and Structure of Lignin/PAN Fibers

The Teas plot should enable mapping of the best solvent mixtures for gel-spinning lignin/PAN fibers with the highest mechanical properties. Interestingly, Mixture 9 yielded neat PAN and lignin/PAN having values of specific modulus 50.9 cN/dtex and 85.3 cN/dtex respectively (**Table 2.4** and **Figure 2.7**). The toughest fiber PAN-#9 had a value of 17.8 J/g;

nearly three times the toughness of PAN-#1 at 6.3 J/g in **Table 2.4**. **Table 2.3** confirms the drawability of as-spun PAN directly influenced mechanical performance, as noted by the coagulation baths used. The tenacity of gel-spun fibers dropped with the addition of lignin. Molecular weight differences between lignin and PAN can adversely affect the tenacity of the composite lignin/PAN fiber. The semi-rigid lignin molecules are at least two orders of magnitude smaller than linear PAN. Lignin/PAN samples' tenacity lowers because there are more significantly more molecular chain ends within the composite structure that may act as quasi-defect points through which breaks can propagate[33].

But, the retention of lignin within highly drawn fibers also led to higher values of specific modulus among gel-spun fibers. Lignin/PAN-#9 fiber had a modulus of 85.3 cN/dtex in contrast to 50.9 cN/dtex for PAN-#9. Lignin/PAN-#10 fiber had a modulus of 58.1 cN/dtex, which was higher than 47.6 cN/dtex for PAN-#10. According to Cousins et al., hardwood kraft lignin has a theoretical Young's modulus of 3.3 GPa[34], and Hao et al. reported Young's modulus of gel-spun PAN to be 20 GPa[14]. Based upon the rule of mixtures for composites, the modulus should decrease, however this work instead observed a reinforcing behavior which can be described as antiplasticization.

Table 2.4. Mechanical Properties of Lignin/PAN Fibers.

	Neat PAN			Lignin/PAN	
Coagulation Bath Mixture	#1	#9	#10	#9	#10
Sample Name	PAN-#1	PAN-#9	PAN-#10	Lignin/PAN-#9	Lignin/PAN-#10
Modulus (cN/dtex)	25.5±1.0	50.9±5.1	47.6±1.5	85.3±6.5	58.1±4.8
Tenacity (cN/dtex)	1.1±0.1	3.0±0.3	0.7±0.1	2.4±0.2	1.9±0.2
Toughness (J/g)	6.3±1.4	17.8±2.6	0.9±0.6	10.2±2.1	14.3±4.8
Strain at Break (%)	9.9±1.2	10.5±1.0	1.7±0.7	6.0±0.8	11.1±3.4
Linear Density (dtex)	28.8	13.0	18.4	11.5	18.6
Effective Diameter (µm)	56±2	37±1	44±2	35±1	44±1

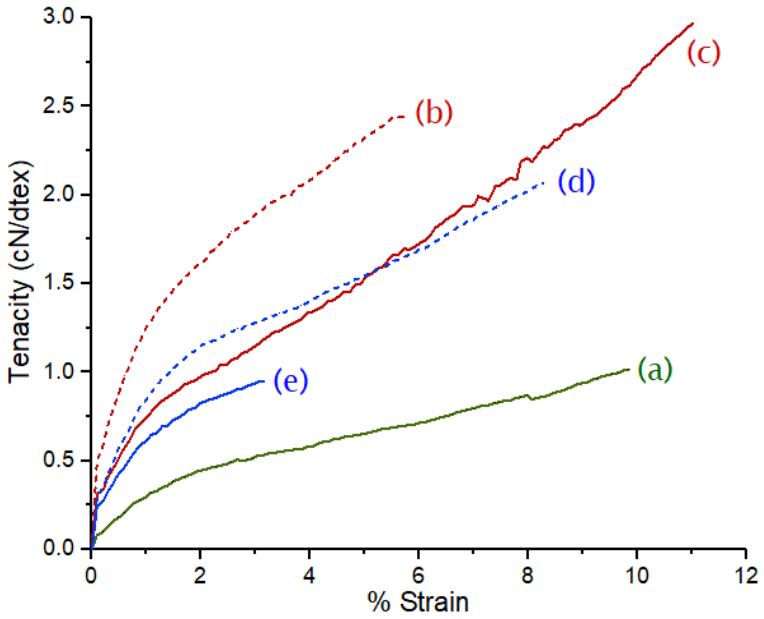

Figure 2.7. Tenacity vs strain curves of (a) PAN-#1, (b) Lignin/PAN-#9, (c) PAN-#9, (d) Lignin/PAN-#10, and (e) PAN-#10.

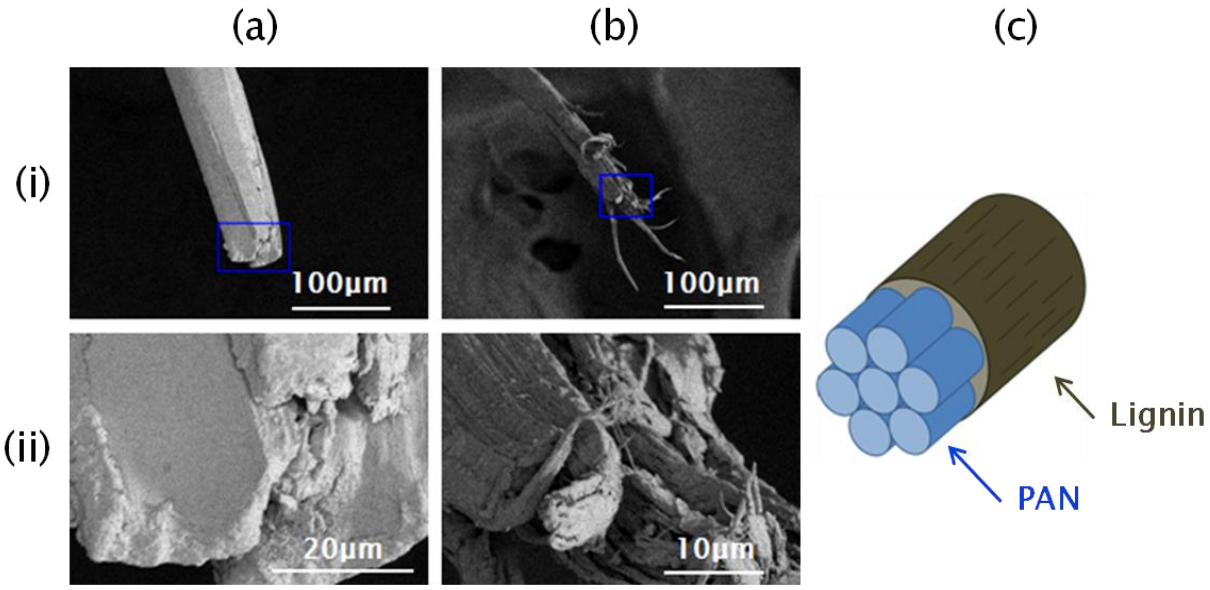

Figure 2.8. SEM micrographs of fracture tips are shown for (a) PAN-#9 and (b) Lignin/PAN-#9 at (i) low and (ii) high resolution, as well as a (c) proposed structure illustration.

SEM micrographs of lignin/PAN fracture tips reveal fibrillar morphologies of oriented, PAN crystals (**Figure 2.8**). In contrast the fibrils among PAN-#9, fibrils at the lignin/PAN-#9 fracture tip are much smaller in scale (**Figure 2.8a** and **2.8b,** respectively). Furthermore, no signs of lignin aggregation are apparent along the lignin/PAN fibrils. Thus, the observation of highly crystalline PAN fibrils suggests lignin did not hinder but rather aided PAN crystallization and orientation along the fiber axis during gel-fiber spinning. **Figure 2.8c** illustrates the proposed model for lignin and PAN integration among gel-spun lignin/PAN-#9 fibers. The lignin, being non-crystalline in nature, is proposed to behave as a matrix resin that surrounds PAN fibrils. Using the gel-spinning technique, we synthetically derived microstructures resembling natural cellulose fibrils that are reinforced with lignin[1,35].

1-D equatorial WAXD was used to compare the crystalline microstructures of PAN-#9 and Lignin/PAN-#9 fibers (**Figure 2.9**) as well as compare crystal sizes derived from the $2\theta \approx 17.0°$ peak. Both fibers feature apparent crystalline planes that are characteristic of PAN, which

are the major peaks are shown at 2θ ≈ 17.0° and 2θ ≈ 29.3°. The 17.0° peak is indicative of the (200) and (110) planes in the hexagonal form after drawing above 150 °C, and the 29.3° peak is associated with the (310) and (020) planes[6]. The crystal size calculated from the 17.0° peak is considerably larger for the lignin/PAN fiber, implying increased spacing between chains. In the Lignin/PAN-#9 sample, a small peak appears to be forming around the 2θ ≈ 11.9° mark, indicating a change in structure much like the change in crystal size.

The crystallinity, calculated with the integrated crystalline peaks, resulted in 85.9 % for Neat PAN-#9 and 86.2 % for Lignin/PAN-#9, fitting the trend in mechanical properties shown in **Table 2.4**. Though only slightly more crystalline, the lignin appeared to have a reinforcing effect in the structure, both increasing the modulus and penetrating the crystalline zones, much like what was observed by Lu et al. in PVA[19].

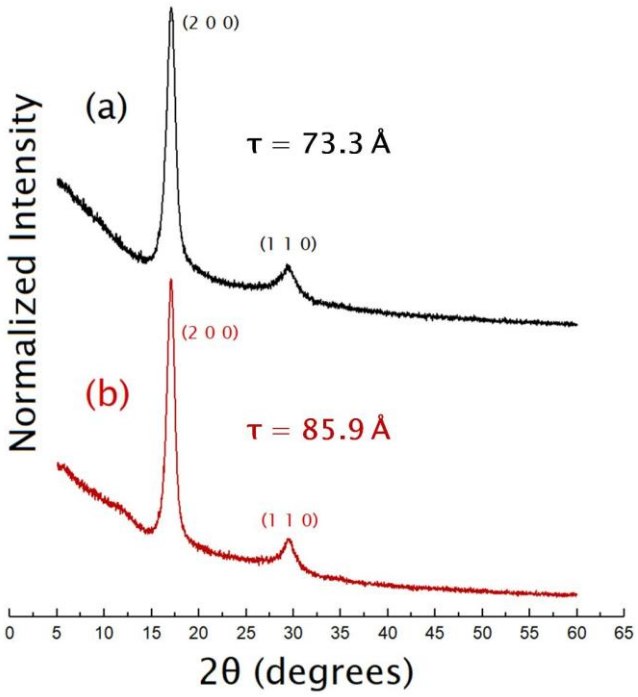

Figure 2.9. Normalized WAXD patterns of (a) PAN-#9 and (b) Lignin/PAN-#9 with Miller Indices[6] and crystal sizes.

The TGA and differential TGA (DTGA) thermograms of Lignin/PAN fibers are shown in **Figure 2.10** and the corresponding DSC thermograms are shown in **Figure 2.11**. Initial loss of mass up to ~100 °C can be attributed to the residual coagulation bath due to the low temperature required to evaporate the water and alcohols which constitute it. The mass loss between ~150 and 250 °C can possibly be attributed to residual DMSO and glycerol drawing oil. A dramatic change can be seen with the inclusion of lignin as a prominent plateau between 200 and 300 °C is shown (**Figure 2.10b**). Lignin/PAN-#9 kept ~74 % of its mass in this temperature region as opposed to the PAN-#9 which kept only ~60 %. The difference in mass retention up to 500 °C is likely due to structural changes as a result of the lignin.

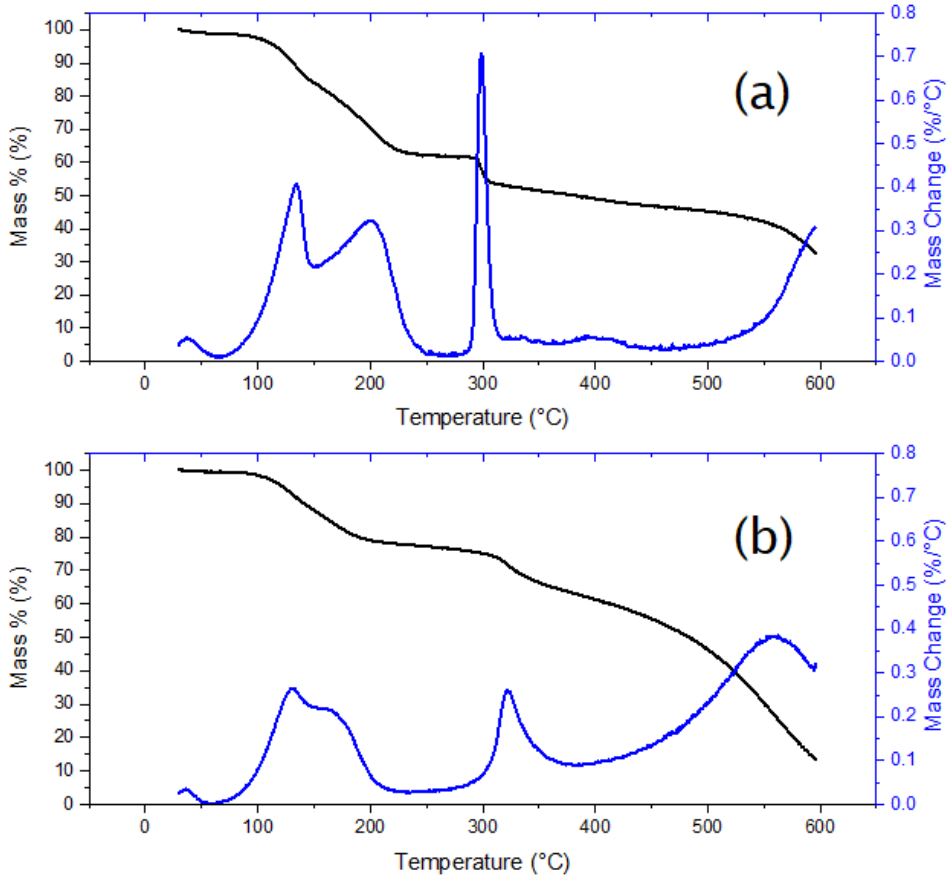

Figure 2.10. TGA and DTGA thermograms of (a) PAN-#9 and (b) Lignin/PAN-#9 fibers.

As seen in **Figure 2.11**, the addition of lignin into the sample increases the temperature required for degradation, shifting the PAN degradation peak from ~225 °C to ~305 °C. However, the degradation peak for Lignin/PAN is also tighter with 223.7 J/g of energy as opposed to the Neat PAN with 284.8 J/g, implying a more energy efficient change. As a result, in the case of stabilization for large scale carbon fiber production, the energy cost and processing time would be significantly reduced.

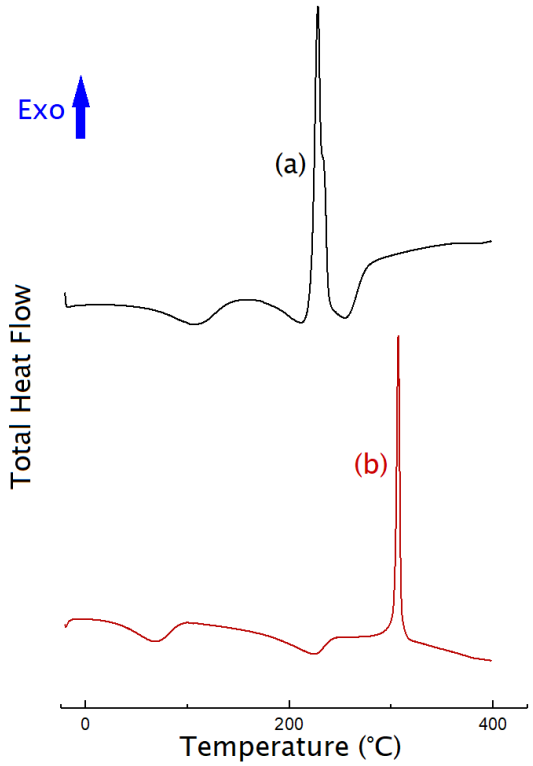

Figure 2.11. DSC thermograms of (a) PAN-#9 and (b) Lignin/PAN-#9.

2.3.5. Flammability of Reduced-MeOH and MeOH Free Coagulation Baths

Coagulation mixtures 9 and 10 showed promising results for the gel-spinning of high modulus neat PAN and lignin/PAN fibers by gel-spinning. As an added bonus to the prospects, the engineered bath mixtures also lessened the flammability of the coagulation bath for an overall safer system than pure methanol. The inclusion of water in Mixtures 9 and 10 significantly increased the LFLs of the coagulation baths while significantly increasing vapor

ignition temperatures, i.e. flash points (**Table 2.5**). A zero value for the flash point of water was used in **Equation 2.8**, because none exists for water [27]. Mixture 10 eliminates the use of methanol, a chemical irritant, while yielding the highest LFL values of 12 %. However, Mixture 9 gave the best overall performance in terms of safety and mechanical performance.

Table 2.5. Estimated Flash Points and LFLs of Engineered Coagulation Baths.

Coagulation Bath	Flash Point (°C)	LFL (%)
Neat MeOH	15	6.0
Mixture 9	81	8.2
Mixture 10	80	12.0

2.4. Conclusions

A relatively simple plot showing a region of functional, mixed coagulation baths was developed that shows promising results of coagulation and processing control of Lignin/PAN fibers. Using Hansen and Yamamoto's concepts on solution mixtures for effective solvents[21,23], mixtures of lignin non-solvents can be engineered to develop coagulation baths for lignin/PAN systems that coagulate the PAN with greatly reduced lignin migration. Because of the engineered baths, fibers at lignin content of up to 50 % (wt/wt) were shown to possess comparable mechanical performance to apparel grade acrylic fibers. Compared to neat PAN, the fibers' crystallinity, crystal size, and thermal degradation temperature also increased with the inclusion of amorphous lignin and the engineered bath designed to incorporate it.

The efficiency of processing of lignin/PAN fibers was improved. Given that the coagulation bath needs less initial cooling to reach its optimum temperature, the energy needed to cool and maintain that temperature would be noticeably less than traditional 100 % MeOH baths. Similarly, the temperature of the dopes was significantly decreased to room temperature, removing the need to maintain high spinning dope temperatures. Engineering the baths' diffusion behavior by means of the Teas plot also reduced residence time, increasing the draw ratio in the

as-spun gel-fiber, resulting in higher mechanical performance and reduced processing time for both neat PAN and lignin/PAN fibers.

More environmentally friendly coagulation baths were shown to be attainable. The use of greener solvents improves disposal cost while simultaneously lowering working hazards. Specifically using water tremendously reduced not only the cost, but the flammability of the mixtures, making it easier to handle during processing. Through the Teas plot, a series of engineered coagulation baths can be derived to further reduce the environmental impact at the cost of mechanical performance if needed, as seen with the mechanical behavior of Lignin/PAN-#9 and Lignin/PAN-#10. The engineered baths provide safer, environmentally friendlier, more energy efficient, and generally more effective coagulation baths than traditionally used neat methanol.

2.5. References

[1] Norberg, I. Carbon fibres from kraft lignin, KTH Royal Institute of Technology, Stockholm, Sweden, 2012.

[2] Bajpai, P. *Carbon fibre from lignin;* Springer Nature: Kanpur, India, 2017;.

[3] Anonymous. Gasifiers & Gasification Tech for Special Apps & Alt Feedstocks. https://www.netl.doe.gov/research/Coal/energy-systems/gasification/gasifipedia/blackliquor. (accessed 07/30, 2018).

[4] Kadla, J. F.; Kubo, S.; Venditti, R. A.; Gilbert, R. D.; Compere, A. L.; Griffith, W. Lignin-based carbon fibers for composite fiber applications. *Carbon* **2002**, *40*, 2913.

[5] Bahl, O. P.; Shen, Z.; Lavin, J. G.; Ross, R. A. In *Manufacture of Carbon Fibers;* Donnet, J. B., Rebouillat, S., Wang, T. K. and Peng, J. C. M., Eds.; Carbon Fibers; Marcel Dekker, Inc.: New York, 1998; pp 1.

[6] Liu, H. C.; Chien, A.; Newcomb, B. A.; Liu, Y.; Kumar, S. Processing, Structure, and Properties of Lignin- and CNT- Incorporated Polyacryolonitrile-Based Carbon Fibers. *ACS Sustainable Chemistry & Engineering* **2015**, *3*, 1943.

[7] Husman, G. Development and commercialization of a novel low-cost carbon fiber. **2012**.

[8] Husman, G. Development and commercialization of a novel low-cost carbon fiber. **2014**.

[9] Seydibeyoğlu, M. Ö. A Novel Partially Biobased PAN-Lignin Blend as a Potential Carbon Fiber Precursor. *Journal of Biomedicine and Biotechnology* **2012**, *2012*, 1.

[10] Cybulska, I.; Brudecki, G.; Rosentrater, K.; Julson, J. L.; Lei, H. Comparative study of organosolv lignin extracted from prairie cordgrass, switchgrass, and corn stover. *Bioresource Technology* **2012**, *118*, 30.

[11] Sameni, J.; Krigstin, S.; Sain, M. Solubility of lignin and acetylated lignin in organic solvents. *BioResources* **2017**, *12*, 1548.

[12] Liu, S.; Jiang, H.; Du, W.; Pan, D. Spinnability in pre-gelled gel spinning of polyacrylonitrile precursor fibers. *Fibers and Polymers* **2012**, *13*, 846.

[13] Tan, L.; Wan, A.; Pan, D. Pregelled gel spinning of polyacrylonitrile precursor fiber. *Materials Letters* **2011**, *65*, 887.

[14] Hao, J.; An, F.; Yu, Y.; Zhou, P.; Liu, Y.; Lu, C. Effect of coagulation conditions on solvent diffusions and the structures and tensile properties of solution spun polyacrylonitrile fibers. *Journal of Applied Polymer Science* **2016**, 44390.

[15] Iovleva, M. M.; Smirnova, V. N.; Budnitskii, G. A. The Solubility of Polyacrylonitrile. *Fibre Chemistry* **2001**, *33*, 262.

[16] Tan, L.; Liu, S.; Song, K.; Chen, H.; Pan, D. Gel-Spun Polyacrylonitrile Fiber From Pregelled Spinning Solution. *Polymer Engineering and Science* **2010**, *50*, 1290.

[17] Liu, S.; Tan, L.; Pan, D.; Chen, Y. Gel spinning of polyacrylonitrile fibers with medium molecular weight. *Polymer International* **2011**, *60*, 453.

[18] Zeng, X.; Zhang, G.; Zhang, Y.; Zhao, J.; Pan, D. Diffusion Mechanism of As-spun Polyacrylonitrile Fiber in a Dimethyl Sulfoxide-Water Coagulation Bath. *Journal of Macromolecular Science, Part A: Pure and Appied Chemistry* **2006**, *43*, 1711.

[19] Lu, C.; Blackwell, C.; Ren, Q.; Ford, E. Effect of Coagulation Bath on the Structure and Mechanical Properties of Gel Spun Lignin/Polyvinyl Alcohol Fibers. *ACS Sustainable Chemistry & Engineering* **2017**.

[20] Grulke, E. A. Solubility Parameter Values. In The Wiley Database of Polymer Properties. **2003**.

[21] Hansen, C. M. The Three Dimensional Solubility Parameter and Solvent Diffusion Coefficient. **1967**.

[22] Gårdebjer, S.; Andersson, M.; Engström, J.; Restorp, P.; Persson, M.; Larsson, A. Using Hansen solubility parameters to predict the disperson of nano-particles in polymer films. *Polymer Chemistry* **2016**, *7*, 1756.

[23] Yamamoto, H. Hansen Solubility Parameters (HSP) Application Notes. https://pirika.com/ENG/HSP/index.html.

[24] Burke, J. Solubility Parameters: Theory and Application. http://www.cool.conservation-us.org/coolaic/sg/bpg/annual/v03/bp03-04.html.

[25] Tan, L.; Pan, D.; Pan, N. Gelation behavior of polyacrylonitrile solution in relation to aging process and gel concentration. *Polymer* **2008**, *49*, 5676.

[26] Hristova, M.; Tchaoushev, S. Calculations of flash points and flammability limits of substances and mixtures. *Journal of the University of Chemical Technology and Metallurgy* **2006**, *41*, 291.

[27] Hristova, M.; Damgaliev, D.; Popova, D. Estimation of water-alcohol mixture flashpoint. *Journal of the University of Chemical Technology and Metallurgy* **2010**, *45*, 19.

[28] Janès, A.; Chaineaux, J. Experimental Determination of Flash Points of Flammable Liquid Aqueous Solutions. *Chemical Engineering Transactions* **2013**, *31*, 943.

[29] Liaw, H.; Gerbaud, V.; Chiu, C. Flash point for ternary partially miscible mixtures of flammable solvents. *Journal of Chemical Engineering Data* **2010**, *55*, 134.

[30] Polyacrylonitrile, Cat #134. *https://scientificpolymer.com/shop/polyacrylonitrile-3/*.

[31] Hu, T. Q., Ed.; In *Chemical modification, properties, and usage of lignin;* Springer: Boston, MA, 2002;.

[32] Sammons, R. J.; Harper, D. P.; Labbé, N.; Bozell, J.; Elder, T.; Rials, T. G. Characterization of Organosolv Lignins using Thermal and FT-IR Sprectroscopic Analysis. *BioResources* **2013**, *8*, 2752.

[33] Chae, H. G.; Kumar, S. Making Strong Fibers. *Science* **2008**, *319*, 908.

[34] Cousins, W. J.; Armstrong, R. W.; Robinson, W. H. Young's modulus of lignin from continuous indentation test. *Journal of Materials Science* **1975**, *10*, 1655.

[35] Raven, P. H.; Evert, R. F.; Eichhorn, S. E. *Biology of Plants;* W.H. Freeman and Company Publishers: New York, 2013;.

3. ANTIPLASTICIZATION OF GEL-SPUN POLYACRYLONITRILE FIBERS UTILIZING AMMONIUM GLUCARATE

3.1. Introduction

Acrylic fibers are the most frequented source for a majority of CF manufacturers. Processing of the precursor fibers is critical for the development of high-performance classes of CF; higher quality precursors make higher quality CF. Homopolymer PAN typically faces difficulty in processing due to the strong inter and intra molecular bonds resulting from strong dipole-dipole interactions, increasing the required amount of energy to extend molecular chains and allow flow to occur. It is often copolymerized with non-acrylic comonomers such as itaconic acid in ratios up to 15 %[1-4] in order to aid in its processing, so in this manner, PAN is most often inherently plasticized from the beginning. Itaconic acid is one of the most commonly used comonomers and is co-polymerized to disrupt PAN's inherently strong secondary bonding sites and to lower the energy required for stabilization during carbon fiber production[3,4]. Zhidkova et al. showed differential thermal analysis curves change with increasing itaconic acid content. The peaks shifted from 260 °C to 250 °C and exothermic process beginning shifted from 180 °C to 171 °C as the itaconic acid increased from 1 % to 3 %[4]. Much of the cost when processing carbon fiber comes from stabilization and carbonization furnaces where the fibers must travel slowly and with multiple passes. Additional comonomers and additives are often included with the PAN in order to reduce the residence time and save processing overhead.

A tool to consider for acrylic precursor fibers is antiplasticizers. These small molecules are similar to diluents such that they lower the glass transition temperature of the constituent polymer, however stiffen and strengthen the resulting structure[5-9]. Typically, antiplasticizers are small, rigid molecules that have polar constituent groups like halogens, nitrogen or

oxygen[5,9]. Jackson and Caldwell antiplasticized bisphenol A polycarbonate (BPA) using a series of polar antiplasticizers. Compared to the baseline breaking strength for BPA of 9.0-9.5 ksi, the highest breaking strength for BPA reported was 13.5 ksi using the antiplasticizer known as Abalyn from Hercules Powder Company[5]. However neutral alkane-based oils have also been shown to exhibit antiplasticization behavior to some extent as well. Anderson et al. utilized small quantities of mineral oil to antiplasticize polystyrene (PS) and found that molecular weight was directly tied to the effects[6]. The neat PS had a modulus of approximately 375 ksi while the PS with 6 % mineral oil had a spiked 730 ksi in comparison. On the other hand, as the concentration of mineral oil increased further, its stiffness lowered dramatically. The same effect was seen in its breaking strength of approximately 1.5 ksi for neat PS and 2.2 ksi for PS with 8 % mineral oil. Once the saturation point was reached, where the number of mineral oil molecules exceeded the PS chain ends, the mechanical properties dropped sharply to levels lower than neat PS at a modulus and breaking strength of approximately 350 ksi and 1.4 ksi respectively[6]. In a more recent study, Lu and Ford found that GA in small quantities can enhance the mechanical performance and processibility of polyvinyl alcohol (PVA) and lignin/PVA fibers[8]. The mechanical properties of the GA/PVA samples they fabricated exceeded their neat PVA with modulus of 21 GPa and breaking strength of 0.34 GPa. Their strongest fiber with 1.6 % GA concentration achieved a modulus of 49 GPa and breaking strength of 1.1 GPa[8]. Lu and Ford were also able to produce lignin/PVA composite fibers with up to 30 % lignin content and maintain mechanical properties equivalent to neat PVA fibers by means of including only 0.8 % of the antiplasticizer[8].

Utilizing the same concept of cellulosic derivative antiplasticizers, this work seeks to develop acrylic fibers with enhanced mechanical performance. This work endeavors to use

glucaric acid in the form of ammonium glucarate in an effort to enhance processibility and performance of gel-spun PAN fiber. By using GA, it is possible to increase draw ratios throughout processing, thus enhancing the mechanical properties of the resulting acrylic precursor fiber. GA/PAN samples were developed to discern an appropriate amount of GA as an anti-plasticizer additive. The GA/PAN samples were then characterized for structural changes as well as tested for mechanical and thermal performance.

3.2. Experimental

3.2.1. Materials

PAN powder having molecular weight of 150 kDa was procured from Scientific Polymer. GA in the form of ammonium salt crystals was donated by Kalion, Inc. and used as-received. Solvents included water, dimethyl sulfoxide (DMSO) from Sigma Aldrich, and isopropanol (IPA) and methanol (MeOH) from BDH Chemicals.

3.2.2. Spinning Dope Preparation

Spinning dopes of PAN and GA/PAN were prepared. 10 g of PAN was dissolved in 50 mL of DMSO under constant stirring at 85 °C for approximately 10 h. For GA/PAN dopes up to 5 % (wt/wt) GA content, the GA was sonicated in DMSO up to 18 h, and then PAN was dissolved in the GA/DMSO solution. The final PAN concentration of the spinning dopes was 20 g/dL.

3.2.3. Gel-Spinning

The spinning process can be mapped on the diagram in **Figure 3.1**, and separated into three different sections of processing: Dope, Coagulation, and Thermal Drawing.

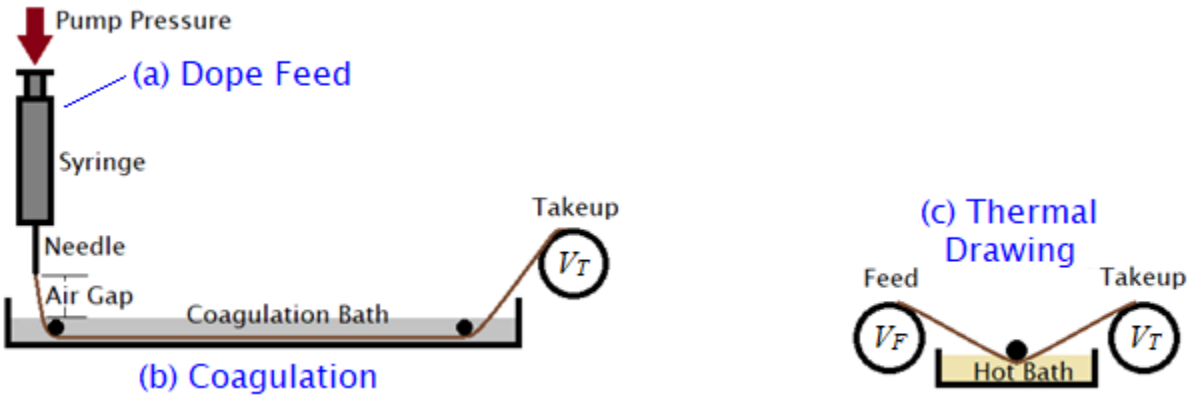

Figure 3.1. Schematic of gel-spinning labels the process as (a) Dope Feed, (b) Coagulation, and (c) Thermal Drawing.

Dope: The spinning solutions were spun using a high pressure capable stainless steel syringe equipped with a 50.8 mm (2") 19 ga needle (0.69 mm inner diameter). As depicted in **Figure 3.1a**, the dope was loaded into the syringe and aged for at least two hours at ~20 °C. Equilibration to environmental temperature allows a pre-gelation effect to occur, increasing apparent viscosity for spinning and mechanical properties, as well as preventing major temperature variations during spinning.

Coagulation: As seen in **Figure 3.1b**, the pre-gelled dope was then spun into a coagulation bath with an air gap of 3 cm from the tip of the needle. The coagulation bath consisted of a mixture of water, IPA, and MeOH. The resulting fibers were then collected onto spools.

Thermal Drawing: As shown in **Figure 3.1c**, as-spun gel fibers were thermally drawn through glycerol in two stages at temperatures ranging from 130 to 170 °C. Fiber draw ratios (*DR*) were calculated according to **Equation 3.1** the ratio of fiber take-up speed (V_T) to feed speed (V_F):

$$DR = \frac{V_T}{V_F} \qquad (3.1)$$

3.2.4. Mechanical Testing

Mechanical properties of the fibers were tested on MTS-Q testing system with ASTM D3379. Parameters were set to 15 mm/min strain rate, 25.4 mm gauge length, and up to 20 specimen sample sizes. Composite density of the fibers was calculated with the inverse rule of mixtures in **Equation 3.2**:

$$\rho_{fiber} = \left(\frac{1-w}{\rho_{PAN}} + \frac{w}{\rho_{GA}}\right)^{-1} \quad (3.2)$$

where w_f is the weight fraction, ρ_{fiber} is the density of the composite fiber, ρ_{PAN} is the density of PAN at 1.184 g/mL[10], and ρ_{GA} is the density of GA at 1.9 g/mL[11].

3.2.5. Imaging

Linear density, $\mathcal{LI}$, reported in dtex, was calculated from measurements of cross-sectional area (*Acs*), which were determined by IMAGEJ analysis. Confocal micrographs were taken on the LEXT OSL4000. With A_{CS} and ρ_{fiber} available, the linear density was calculated according to **Equation 3.3**:

$$\mathcal{LI} = A_{CS} \times \rho_{fiber} \quad (3.3)$$

Fiber fracture tips from mechanical testing were imaged by FEI Verios 460L Scanning Electron Microscope (SEM) at 2kV. Prior to imaging, samples were sputter-coated with a 60/40 gold/palladium mixture.

3.2.6. Thermal Characterization

Thermal analysis was conducted through the means of Dynamic Scanning Calorimetry (DSC) and Thermogravimetric Analysis (TGA). The DSC data were retrieved from the DSC Q2000 V24.11 on a range of -20 to 400 °C at a ramp rate of 5 °C/min, with nitrogen carrier gas, and modulating ±5 °C/min. The TGA data were taken with the TGA Q500 V6.7 on a range of 30 to 600 °C at a ramp rate of 10 °C/min with nitrogen carrier gas.

3.2.7. Structural Characterization

1-D equatorial X-Ray Diffraction (WAXD) was also conducted for crystallinity and crystal size, using the Empyrean diffractometer system. The crystal size for each of the samples was calculated through the Scherrer Equation, **Equation 3.4**:

$$\tau = \frac{K\lambda}{\beta\cos(\theta)} \qquad (3.4)$$

where τ is the crystal size in Å, K is a shape factor of 0.9, λ is the wavelength for the copper source of 1.54 Å, β is the full width at half max of the crystalline peak in radians, and θ is the Bragg Angle in radians of the crystalline peak.

3.3. Results & Discussion

3.3.1. Effect of Ammonium Glucarate on PAN Gel-Spinning

Table 3.1 displays the processing parameters of the gel-spun GA/PAN fibers. Samples showed little to no variation in spinning behavior in regards to temperature or processing speeds. The 2 % GA sample was fed through the syringe at a slightly faster rate than the other samples, resulting in a lower as-spun draw ratio. It was noted that the pump used was controlled by a manual dial, often resulting in slight variation between runs. The 1 % GA sample resulted in the highest increase to processibility, increasing the draw ratio at both stages of drawing; the total draw ratio increased by a factor of slightly beyond 1.5× the total draw ratio of the neat PAN control fiber. At the percentages run, the GA samples showed an increase in processibility compared to neat PAN.

Table 3.1. Processing Parameters of Gel-Spun GA/PAN Fibers.

		Neat PAN	1 % GA	2 % GA	3.5 % GA	5 % GA
As-spun	**Temp (°C)**	-4	-6	-3	-6	-5
	Residence Time (ms)	34	35	35	34	34
	DR	7.0	7.0	5.9	6.7	6.7
Stage 1	**Temp (°C)**	135	126	136	134	134
	DR	12.2	13.9	11.8	12.7	13.0
Stage 2	**Temp (°C)**	168	168	166	168	168
	DR	1.5	2	2	1.6	1.0
Total DR		125.7	193.8	139.7	136.8	143.2
Linear Density (dtex)		13.0	4.9	5.4	3.8	4.9
Effective Diameter (μm)		37±	23±2	24±1	20±1	23±1

3.3.2. Effect of Ammonium Glucarate on the Mechanical Properties of PAN Fibers

Cross-sections of each of the fibers were taken, as seen in **Figure 3.2**. These cross-sectional images were then measured and analyzed using software to determine the effective diameters as seen in **Tables 3.1** and **3.2**. These diameters and calculated density of the constituent solids were then used to calculate the linear density of each the samples. The GA/PAN fibers did not appear with easily identifiable contours during laser scanning, so color images were used instead.

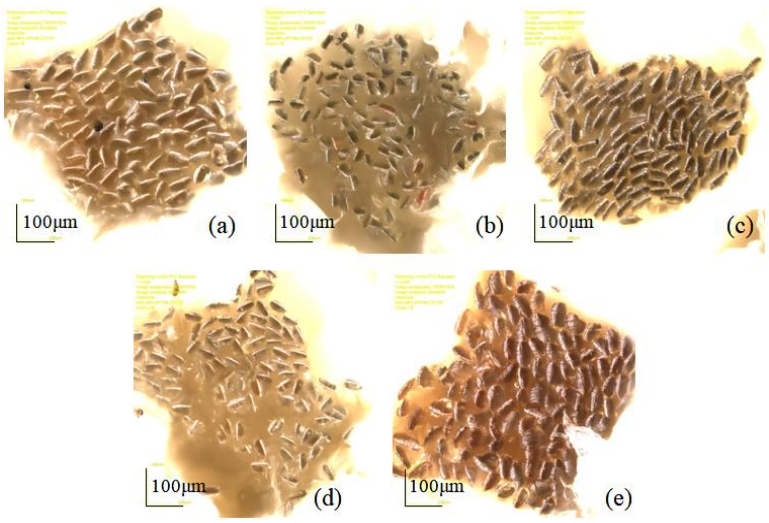

Figure 3.2. Drawn fiber confocal color images of (a) Neat PAN, (b) 1 % GA/PAN, (c) 2 % GA/PAN, (d) 3.5 % GA/PAN, and (e) 5 % GA/PAN.

Mechanical properties of the GA/PAN fibers are shown in **Table 3.2**. The antiplasticizer strengthened the fiber's modulus and tenacity and simultaneously allowed the fiber to be processed through further drawing resulting in lower linear densities and smaller diameters. The sample with the lowest concentration of GA at 1 % even had significantly higher properties than the control sample. The highest performing sample contained 3.5 % GA with a modulus of 193.5 cN/dtex, more than three times higher than the neat PAN control sample at 50.9 cN/dtex. At 5 % GA, the properties, while still higher than the control as well as 1 % and 2 % GA samples, had lower properties than the 3.5 % GA, indicative of the concentration point at which antiplasticizers become less effective. The strain at break values for the GA samples were all less than 6 % strain, implying a greater degree of extension than the neat PAN control.

Table 3.2. Mechanical Properties of Drawn GA/PAN Fibers.

Sample	Neat PAN	1 % GA	2 % GA	3.5 % GA	5 % GA
Modulus (cN/dtex)	50.9±5.1	92.1±7.0	131.6±15.1	193.5±18.0	142.5±8.7
Tenacity (cN/dtex)	3.0±0.3	3.6±0.5	4.0±0.4	5.9±1.1	3.9±0.7
Toughness (J/g)	17.8±2.6	13.7±3.5	12.8±2.7	20.7±4.2	11.9±2.5
Strain at Break (%)	10.5±1.0	5.9±1.1	5.0±0.7	5.3±0.5	4.4±0.6
Linear Density (dtex)	13.0	4.9	5.4	3.8	4.9
Effective Diameter (µm)	37±1	23±2	24±1	20±1	23±1

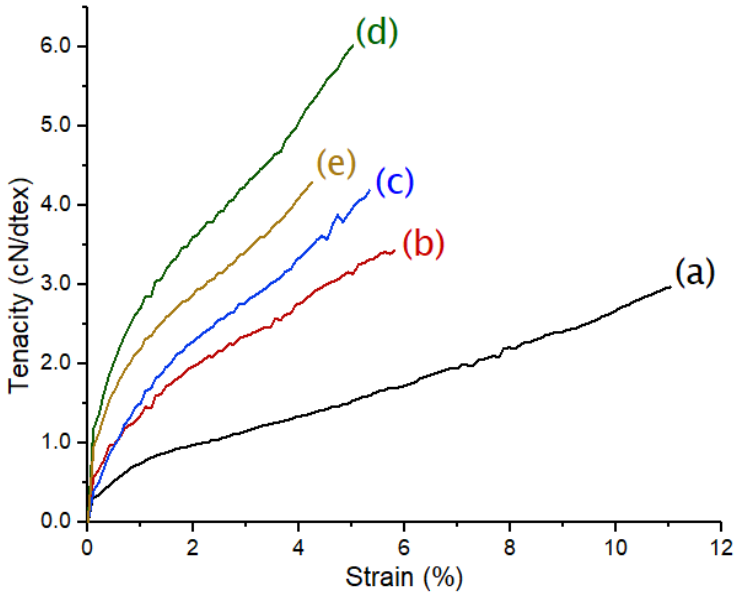

Figure 3.3. Tenacity vs strain curves of (a) Neat PAN, (b) 1 % GA, (c) 2 % GA, (d) 3.5 % GA, and (e) 5 % GA fibers.

From **Figure 3.3**, it can be seen that although the neat PAN sample had the highest strain at break, the modulus and breaking strengths rose with the addition of the antiplasticizer. The increase in mechanical properties was gradual until the concentration of GA reached 5 %, where it then decreased close to the performance of 2 % GA, as shown by **Figures 3.3b** and **3.3c**. This

drop in properties may have been a result of the ratio of the number of small molecule GA to number of polymer chain ends of PAN reached a critical point.

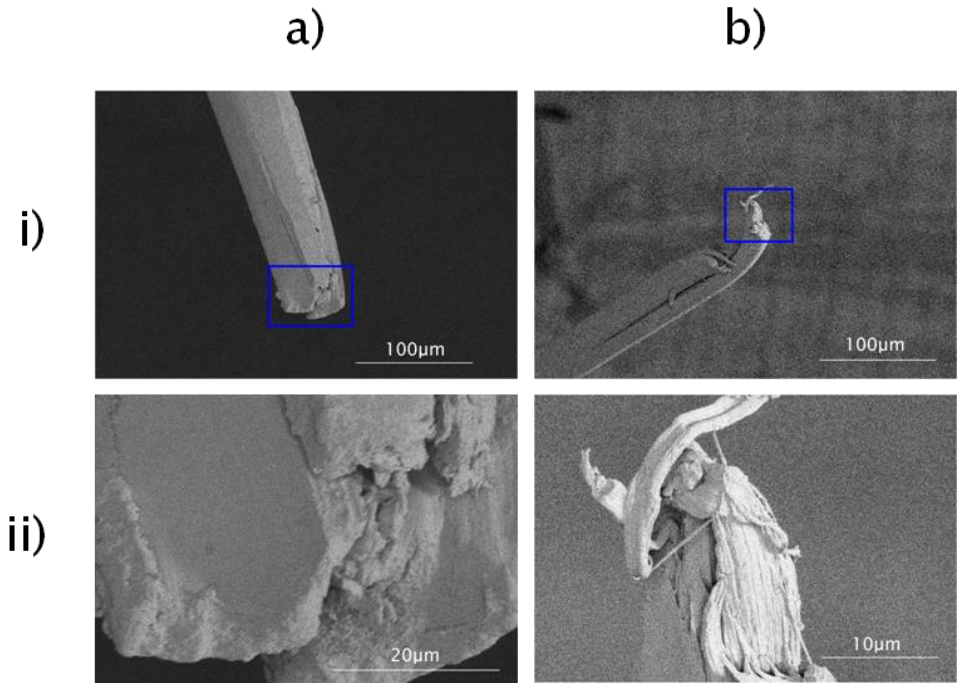

Figure 3.4. SEM micrographs of fracture tips are shown for (a) Neat PAN and (b) 3.5 % GA/PAN fibers at (i) low and (ii) high resolution.

SEM micrographs of the strongest GA/PAN fibers show a high degree of alignment and some nano-scale fibrillation upon fracture (**Figure 3.4**). The fibrils and striations seen in **Figure 3.4b** are not seen in the neat PAN structure, evident of higher energy requirements for breakage than the control. These features also show a highly crystalline structure, indicative that the small molecules of the GA aid in molecular orientation along the fiber axis and do not aggregate.

3.3.3. Structural Analysis of GA/PAN Fibers

WAXD patterns of GA/PAN fibers are shown in **Figure 3.5** along with the respective crystal sizes calculated with the Scherrer Equation. Two evident peaks are located at approximately 17° associated with the (200) and (110) planes and 29° associated with the (310) and (020) planes in the hexagonal form when drawn[12]. The data also show in **Figures 3.5c** and

3.5e that small peaks can be seen forming at approximately 10° to 12°, implying a different crystalline form as a result of the inclusion of GA. The antiplasticizer changed the crystalline size of the PAN, particularly with the 2 % and 3.5 % concentrations. These τ values correspond with the mechanical properties seen in **Table 3.2** and evidenced in the fibrillar structures of the SEM images in **Figure 3.4**.

The crystallinity calculations resulted in a similar pattern as the crystal size and mechanical properties (see **Table 3.3**). An increase in crystallinity, crystal size, and mechanical performance all point to effective antiplasticization behavior in the 3.5 % GA sample, as its crystallinity was 91.6 %, significantly higher than the neat PAN at 85.9 %. However, the 2 % and 5 % GA samples both showed a lower crystallinity than the neat PAN. This is could be due to the development of additional crystal forms that may disrupt the development of typical hexagonal forms, limiting crystallinity.

Table 3.3. Crystalline Properties of GA/PAN Fibers Determined by WAXD.

Sample	Neat PAN	1 % GA	2 % GA	3.5 % GA	5 % GA
Crystal Size (Å)	73.2	75.4	97.0	90.1	68.9
Crystallinity (%)	85.9	89.2	84.0	91.6	84.2

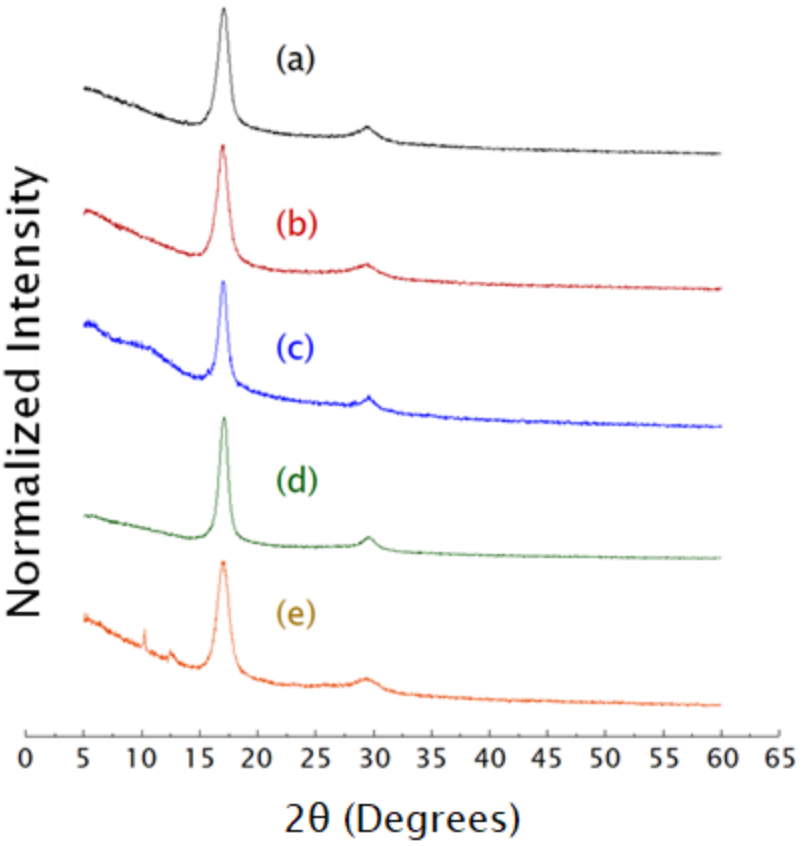

Figure 3.5. WAXD patterns of (a) Neat PAN, (b) 1 % GA, (c) 2 % GA, (d) 3.5 % GA, and (e) 5 % GA fibers.

3.3.4. Effect of Ammonium Glucarate on the Thermal Behavior of PAN Fibers

The TGA and DTGA data of the GA/PAN fibers are shown in **Figure 3.6**. A clear progression of change can be seen with the inclusion of the antiplasticizer. More prominent plateaus between 200 and 300 °C are seen for the samples with GA present, implying that the antiplasticizer helped maintain the mass of the samples at higher temperatures. Of all the samples, 2 % GA had more mass remaining (~92 %) at the 200 to 300 °C plateau, higher than the neat PAN (~60 %), coinciding with the crystal sizes shown in **Figure 3.5**. In general, a larger crystal size requires more energy to reduce the weight of the sample, however the 5 % GA sample did not follow this pattern.

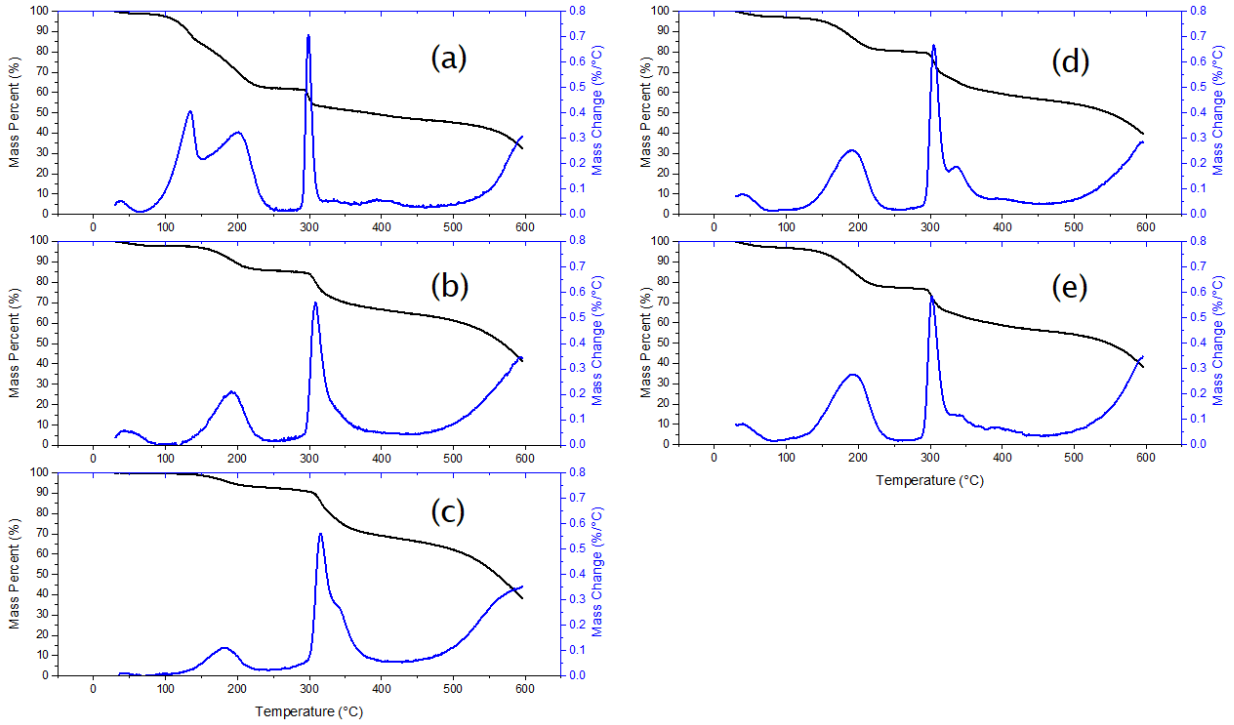

Figure 3.6. TGA and DTGA curves of (a) Neat PAN, (b) 1 % GA, (c) 2 % GA, (d) 3.5 % GA, and (e) 5 % GA fibers.

The DSC curves for the GA/PAN fibers are plotted in **Figure 3.7** and the exotherm peak data are shown in **Table 3.4**. A clear difference can once again be seen that with the inclusion of GA in the fiber increases the temperature and heat flow required for a change to occur, shifting the peaks above 250 °C and tightening the peak distributions, corresponding with the TGA curves in **Figure 3.6**. However, as seen in **Table 3.4**, all of the GA samples required more energy to undergo degradation relative to the neat PAN control. This would corroborate the changes seen in the TGA curves of **Figure 3.6** and WAXD patterns of **Figure 3.5**, implying that a structural change has occurred within the crystalline regions.

Table 3.4. DSC Exotherm Peak Temperatures and Energies of GA/PAN Fibers.

Sample	Exotherm Peak (°C)	Exotherm Energy (J/g)
Neat PAN	228	285
1 % GA	280	380
2 % GA	285	377
3.5 % GA	291	308
5 % GA	291	311

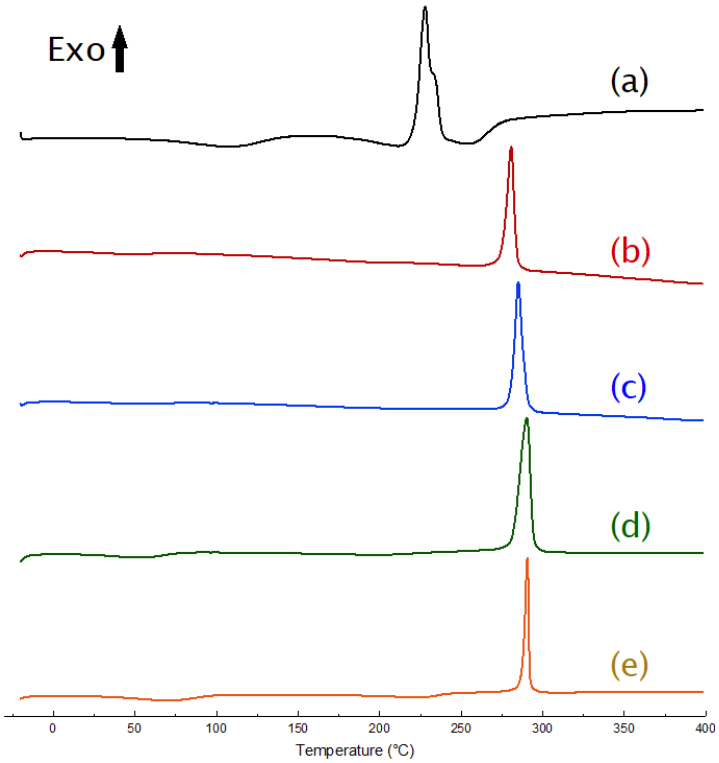

Figure 3.7. DSC curves of (a) Neat PAN, (b) 1 % GA, (c) 2 % GA, (d) 3.5 % GA, and (e) 5 % GA fibers.

3.4. Conclusions

Ammonium glucarate can be used as a feasible, environmentally sustainable, low-quantity, bio-based antiplasticizer in gel-spun PAN fibers. Utilizing the GA additive, mechanical properties of neat PAN fibers can be increased to improve strength while simultaneously improving processibility. Because of its incorporation, GA enhanced processing of PAN fibers

that exceed apparel grade PAN fibers. Using a limited amount increased the Young's modulus of the fiber to 3.8× that of neat PAN fibers. However, too much of the GA can result in less than optimum mechanical performance. Compared to neat PAN, utilizing GA allowed the spinning of fibers with greater overall draw ratios and smaller diameters, resulting in strong, highly fibrillar structures with increased crystallinity and enhanced thermal stability. On the other hand, when considering GA/PAN fibers for stabilization and carbonization, the energy cost undoubtedly increases due to GA's effectiveness as an antiplasticizer.

3.5. References

[1] Adanur, S. *Wellington Sears Handbook of Industrial Textiles;* Technomic Publishing Company, Inc.: Lancaster, PA, 1995;.

[2] Zheng, Z.; Feldman, D. Synthetic fibre-reinforced concrete. *Program of Polymer Science* **1995**, *20*, 185.

[3] Kadla, J. F.; Kubo, S.; Venditti, R. A.; Gilbert, R. D.; Compere, A. L.; Griffith, W. Lignin-based carbon fibers for composite fiber applications. *Carbon* **2002**, *40*, 2913.

[4] Zhidkova, O. V.; Andreeva, I. N.; Radishevskii, M. B.; Serkov, A. T.; Kalashnik, A. T.; Chichinova, N. V. Thermal properties of polyacrylonitrile copolymers having various chemical compositions. *Fibre Chemistry* **1994**, *25*, 368.

[5] Jackson, W. J.; Caldwell, J. R. Antiplasticization. II. Characteristics of antiplasticizers. *Journal of Applied Polymer Science* **1967**, *11*, 211.

[6] Anderson, S. L.; Grulke, E. A.; DeLassus, P. T.; Smith, P. B.; Kocher, C. W.; Landes, B. G. A Model for Antiplasticization in Polystyrene. *Macromolecules* **1995**, *28*, 2944.

[7] Stukalin, E. B.; Douglas, J. F.; Freed, K. F. Plasticization and antiplasticization of polymer melts diluted by low molar mass species. *The Journal of Chemical Physics* **2010**, *132*.

[8] Lu, C.; Ford, E. Antiplasticizing behaviors of glucarate and lignin bio-based derivatives on the properties of gel-spun polyvinyl alcohol fibers. *Macromolecular Materials and Engineering* **2018**, *303*.

[9] Ranade, A.; Wang, H.; Hiltner, A.; Baer, E.; Shirk, J. S.; Lepkowicz, R. S. The solid state structure of polycarbonate blends with lead phthalocyanine. *Polymer* **2007**, *48*, 624.

[10] Polyacrylonitrile, Cat #134. https://scientificpolymer.com/shop/polyacrylonitrile-3/.

[11] Royal Society of Chemistry, Saccharic Acid. http://www.chemspider.com/Chemical-Structure.30577.html.

[12] Liu, H. C.; Chien, A.; Newcomb, B. A.; Liu, Y.; Kumar, S. Processing, Structure, and Properties of Lignin- and CNT- Incorporated Polyacrylonitrile-Based Carbon Fibers. *ACS Sustainable Chemistry & Engineering* **2015**, *3*, 1943.

4. Effect of Lignin-co-Polyacrylonitrile Compatibilizers on the Properties of Gel-Spun Polyacrylonitrile Composite Fibers

4.1. Introduction

High-performance carbon fibers (CFs) are most often derived from PAN-based fibers. These PAN precursor fibers are solution spun; wherein PAN polymer is dissolved in solvent. In the case of acrylics, the PAN polymer can have up to 15 % non-acrylonitrile comonomers[1,2]. In order to fabricate more environmentally responsible and sustainable CF precursors, various research has explored the use of lignin form biomass as a notable candidate for fiber spinning [3-7]. Liu et al. gel-spun lignin/PAN fibers with up to 30 % lignin to polymer in dimethyl acetamide (DMAc). The resulting CF precursors showed decreases in mechanical performance when lignin was added: neat PAN had a modulus of 19.9 GPa versus lignin/PAN with a modulus of 17.2 GPa[3]. In reports to the Department of Energy, Husman pursued the use of lignin and PAN blends, but found significant amounts of lignin had migrated from the fiber. Losses in lignin negatively affect fiber processing and performance fell below expectations[4,5]. Dong et al. blended sulfonated lignin with PAN and wet spun those fibers, but voids were observed among spun fibers[6].

Compatibilizers are incorporated into nanocomposites to improve interfacial adhesion between dissimilar materials, to prevent phase separation, and to improve the homogeneity of the final product. The interphase between constituent materials is made more compatible with additives, which are often copolymers of the blend constituents[7-9]. For example, Martin and Velankar incorporated diblock copolymers of polyisobutylene (PIB) and polydimethylsiloxane (PDMS) at up to 0.1 wt% in 80:20 to 20:80 PIB:PDMS and saw increased viscosity at low stress[7]. Wang et al. grafted lignin to carbon nanotubes (CNTs) and later melt-spun lignin

composite fibers. Tensile strength improved upon adding 0.5 % CNT-grafted lignin; however, higher concentrations of modified CNTs decreased fiber strength. This was perhaps due to the formation of voids within composite fibers [8].

In a study performed in the School of Mechanical and Materials Engineering at Washington State University, Kessler employed modified lignin as a compatibilizer between matrix polymer and lignin[9]. Butyrated lignin was obtained by lignin esterification in butyric anhydride with n-methyl imidizole catalyst. Afterwards, the lignin was blended with polylactic acid (PLA). Carbonized lignin/PLA fibers showed less voids after carbonization when compatibilizer was used [9]. Kessler also copolymerized lignin and PAN in ratios up to 80:20 PAN:lignin. Fibers were spun from blends of PAN-modified lignin and butyrated lignin, but their mechanical properties were not reported[9].

This work explores the use of MODL as compatibilizers for the spinning of homogenous lignin/PAN composite fibers. Kessler showed that MODL is a feasible material on its own[9]. This work employed MODL as additives similar to the concept used by Martin and Velankar[7]. MODL concentrations up to 10 % wt/wt to PAN were added to spinning dopes. The fiber morphology, processing parameters, and mechanical properties of the resulting fibers were studied to compare the efficiency of MODL compatibilizers for lignin/PAN gel-spinning.

4.2. Experimental

4.2.1. Materials

PAN powder of 150 kDa in molecular weight was procured from Scientific Polymer. Kraft lignin powder was provided by Domtar and was used as received. Powders of MODL having 1:4 lignin:PAN was synthesized in the Department of Forest Biomaterials at North

Carolina State University. Solvents included deionized water, dimethyl sulfoxide (DMSO) from Sigma Aldrich, isopropanol (IPA) and methanol (MeOH) from BDH Chemicals.

4.2.2. Spinning Dope Preparation

Spinning dopes of PAN, lignin/PAN, and lignin/MODL/PAN were prepared. 10 g of PAN was dissolved in 50 mL of DMSO under constant stirring at 85 °C for approximately 10 h. For lignin/PAN dopes up to 10 % lignin content (wt/wt), the neat lignin was sonicated in DMSO for up to 18 h, then PAN was dissolved in the lignin/DMSO solution.

For lignin/MODL/PAN dopes at up to 10 % lignin to PAN (wt/wt), neat lignin was sonicated in DMSO up to 18 h, and then PAN and MODL were dissolved in the lignin/DMSO solution. Formulations for spinning dopes are shown in **Table 4.1**. The final concentration of PAN in the spinning dopes was 20 g/dL, and the final concentration of lignin in spinning dopes was 2 g/dL.

Table 4.1. Lignin/MODL/PAN Spinning Dope Recipes.

Sample ID	Added PAN (g)	Added Lignin (g)	Added MODL (g)	Total PAN (g)	Total Lignin (g)
Neat PAN	10.0	0.0	0.0	10.0	1.0
S0V	10.0	1.0	0.0	10.0	1.0
S1V	9.6	0.9	0.5	10.0	1.0
S2V	9.2	0.8	1.0	10.0	1.0

†All samples utilized 50 mL of DMSO

4.2.3. Gel-Spinning

The gel-spinning process in **Figure 4.1** is labeled according to three important steps: dope feed, coagulation, and drawing.

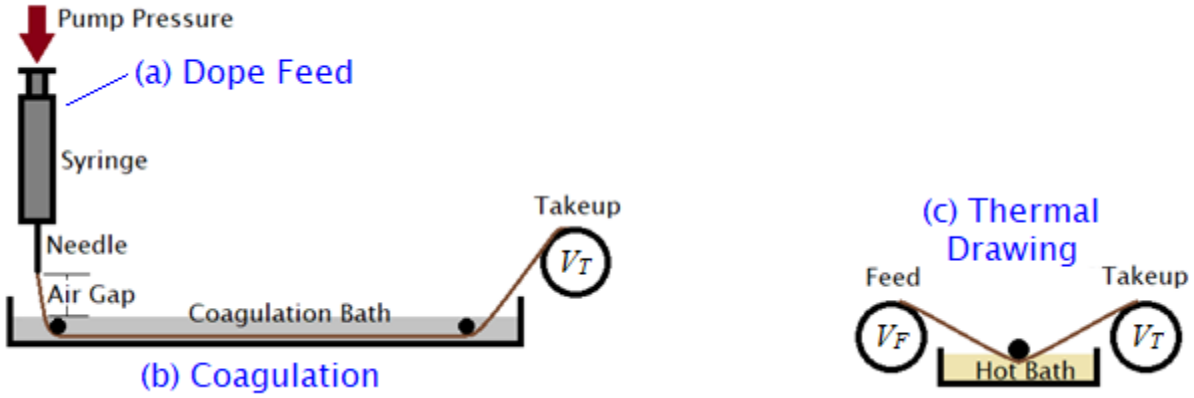

Figure 4.1. Schematic of gel-spinning labels the process as (a) Dope Feed, (b) Coagulation, and (c) Thermal Drawing.

Dope Feed: Spinning dopes were dispensed using a high pressure, stainless steel syringe that was equipped with a 19-gauge needle (0.69 mm inner diameter and 50.8 mm in length). In **Figure 4.1a**, the dope was loaded into the syringe and aged for at least 2 h at ~21 °C. This process of PAN dope aging is known as pre-gelation or the equilibration of dope at room temperature. According to literature, pre-gelation results in a gel-like network; wherein the dope phase separates into domains of polymer-rich PAN and solvent[10-13]. Tan et al. aged PAN dope (of 78 kDa polymer) for up to 10 h. Aging significantly increased the shear modulus (i.e. elasticity) of the dope, while decreasing the number of breaks during fiber spinning[11]. Liu et al. aged 78 kDa PAN dopes for up to 3 h, but dope aged for 1.5 h spun at the highest draw ratio and were the strongest[12].

Coagulation: As seen in **Figure 4.1b**, the dope was fed into the coagulation bath with a vertical dry jet of ~3 cm from the tip of the needle to solvent surface. The coagulation bath

consisted of 50 % v/v MeOH, 25 % v/v water, and 25 % v/v IPA. The resulting fibers were wound onto spools.

Thermal Drawing: As shown in **Figure 4.1c**, as-spun gel fibers were thermally drawn through glycerol in two stages at temperatures ranging from 130 to 170 °C. Fiber draw ratios (*DR*) were calculated according to **Equation 4.1** the ratio of fiber take-up speed (V_T) to feed speed (V_F):

$$DR = \frac{V_T}{V_F} \quad (4.1)$$

4.2.4. Mechanical Testing

The mechanical properties of lignin/PAN fibers were tested using the MTS-Q testing system according to ASTM D3379. Parameters were set to 15 mm/min strain rate, 25.4 mm gauge length, and up to 20 specimen sample sizes. Lignin/PAN fiber density was calculated according to the inverse rule of mixtures (**Equation 4.2**),

$$\rho_{fiber} = \left(\frac{1-w}{\rho_{PAN}} + \frac{w}{\rho_{lignin}}\right)^{-1} \quad (4.2)$$

where *w* is weight fraction, ρ_{fiber} is the density of the lignin/PAN fiber, ρ_{PAN} is the density of PAN at 1.184 g/mL[14], and ρ_{lignin} is the density of lignin at 1.3 g/mL[15].

4.3. Results & Discussion

4.3.1. Effect of Compatibilizer on Lignin/PAN Fiber Spinning

Spinning dopes appeared visually consistent. As spinning dope was feed into the coagulation bath, lignin aggregates were observed within the dry jet as it flowed through the air gap. Variations between spinning parameters for each of the dopes–namely, the controls and the samples with MODL compatibilizer–were observed (see **Table 4.2**). Sample S1V showed similar, but slightly lower overall DR and a significantly larger diameter when compared to the control samples. It was noted during processing of Sample S1V that the sample was more

difficult to handle and had frequent breaks in both spinning and thermal drawing, implying that the fiber was more susceptible to breakage during spinning.

Table 4.2. Processing Parameters of Lignin/MODL/PAN Fibers.

Sample		Neat PAN	S0V	S1V	S2V
As-spun	**DR**	7.0	7.0	7.2	5.6
Stage 1	**Temp (°C)**	135	135	135	135
	DR	12.2	12.1	11.2	7.3
Stage 2	**Temp (°C)**	168	168	162	--
	DR	1.5	1.6	1.4	--
Total DR		125.7	132.7	113.2	41.2
Linear Density (dtex)		13	13	18	--
Effective Diameter (µm)		37±1	37±2	44±2	--

Sample S2V, on the other hand, was not comparable to the rest of the samples due to its poor processibility and obvious defects. The dope sputtered early in the spinning process, but eventually reached laminar flow from the needle after running about 12 % of the dope volume loaded in the syringe. After fiber spinning, thick and thin spots were observed along the fibers. Further, aggregates were observed within the fibers (see **Figure 4.2**). Small particles were seen in the residue of dope that was found in the syringe, as well as partially clogged filters. These visual defects were potential points of mechanical failure during post processing and testing. The apparent heterogeneity of fibers prevented post processing of fibers.

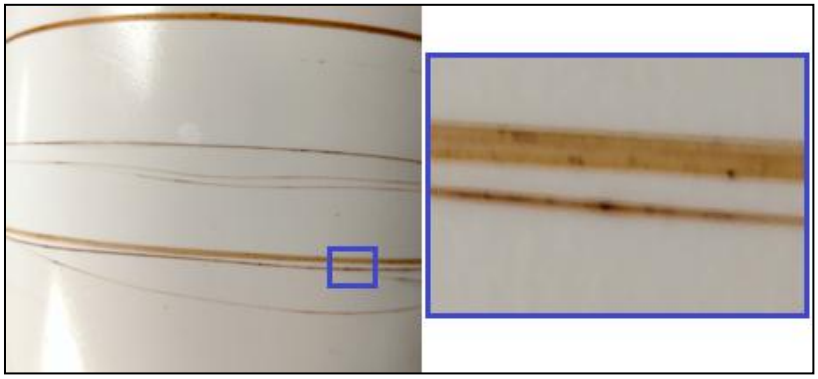

Figure 4.2. Aggregates shown in a spool of Sample S2V.

It is possible that pre-gelation may have had adversely affected the blending of lignin and PAN with MODL. The purpose of pre-gelation was to have low molecular weight PAN spin like high molecular weight PAN. However, MODL may have nucleated heterogeneities that were not beneficial to the blending of PAN and lignin.

4.3.2. Effect of Compatibilizer on Lignin/PAN Mechanical Properties

The mechanical properties of gel-spun fibers are shown in **Table 4.3**. Due to the limitations of processing S2V, data was only shown for the controls and S1V. The two control fibers had mechanical properties that were insignificantly different, but S1V was significantly weaker in terms of performance. The low strength of S1V was likely due to poor interphase adhesion between MODL-compatibilizer/lignin/PAN and the localized aggregation of MODL within fibers.

Table 4.3. Mechanical Properties of Lignin/MODL/PAN Fibers.

Sample	Modulus (cN/dtex)	Tenacity (cN/dtex)	Strain at Break (%)	Toughness (J/g)
Neat PAN	50.9±5.1	3.0±0.3	10.5±1.0	17.8±2.6
S0V	53.8±2.6	2.7±0.4	10.1±1.5	16.0±4.5
S1V	35.2±1.9	0.8±0.1	4.0±0.8	2.2±0.6

4.4. Conclusions

This work has shown that while MODL was capable of dissolution with lignin and PAN, its use as a compatibilizer was not promising. Aggregates were clearly visible in MODL containing fibers. These aggregates ultimately lead to heterogeneities which in turn dramatically decreased fiber modulus, tenacity, and toughness values. Even at just 5 % MODL, fibers were significantly weaker than the controls.

4.5. References

[1] Adanur, S. *Wellington Sears Handbook of Industrial Textiles;* Technomic Publishing Company, Inc.: Lancaster, PA, 1995;.

[2] Zheng, Z.; Feldman, D. Synthetic fibre-reinforced concrete. *Program of Polymer Science* **1995**, *20*, 185.

[3] Liu, H. C.; Chien, A.; Newcomb, B. A.; Liu, Y.; Kumar, S. Processing, Structure, and Properties of Lignin- and CNT- Incorporated Polyacrylonitrile-Based Carbon Fibers. *ACS Sustainable Chemistry & Engineering* **2015**, *3*, 1943.

[4] Husman, G. Development and commercialization of a novel low-cost carbon fiber. **2016**.

[5] Husman, G. Development and commercialization of a novel low-cost carbon fiber. **2014**.

[6] Dong, X.; Lu, C.; Zhou, P.; Zhang, S.; Wang, L.; Li, D. Polyacrylonitrile/lignin sulfonate blend fiber for low-cost carbon fiber. *RSC Advances* **2015**, *5*, 42259.

[7] Martin, J. D.; Velankar, S. S. Effects of compatibilizer on immiscible polymer blends near phase inversion. *Journal of Rheology* **2007**, *51*, 669.

[8] Wang, S.; Zhou, Z.; Xiang, H.; Chen, W.; Yin, E.; Chang, T.; Zhu, M. Reinforcement of lignin-based carbon fibers with functionalized carbon nanotubes. *Composites Science and Technology* **2016**, *128*, 116.

[9] Kessler, M. R. Low cost, bio-renewable carbon fibers from lignin/PLA blends and graft copolymers. **2014**.

[10] Tan, L.; Liu, S.; Song, K.; Chen, H.; Pan, D. Gel-Spun Polyacrylonitrile Fiber From Pregelled Spinning Solution. *Polymer Engineering and Science* **2010**, *50*, 1290.

[11] Liu, S.; Jiang, H.; Du, W.; Pan, D. Spinnability in pre-gelled gel spinning of polyacrylonitrile precursor fibers. *Fibers and Polymers* **2012**, *13*, 846.

[12] Tan, L.; Wan, A.; Pan, D. Pregelled gel spinning of polyacrylonitrile precursor fiber. *Materials Letters* **2011**, *65*, 887.

[13] Liu, S.; Tan, L.; Pan, D.; Chen, Y. Gel spinning of polyacrylonitrile fibers with medium molecular weight. *Polymer International* **2011**, *60*, 453.

[14] Polyacrylonitrile, Cat #134. *https://scientificpolymer.com/shop/polyacrylonitrile-3/*.

[15] Hu, T. Q., Ed.; In *Chemical modification, properties, and usage of lignin;* Springer: Boston, MA, 2002;.

5. CONCLUSIONS & RECOMMENDATIONS

5.1. Conclusions

In this research, lignin/PAN fibers were successfully gel-spun with newly developed coagulation baths previously unseen in literature. The dispersal of lignin into solvent, aging of the spinning dopes, and development of the alternative coagulation baths not only maintained the lignin within the fiber systems, but helped fully incorporate the biomass into the fiber. Major findings are as follows:

- Coagulation baths play a major role in processing, structure, and mechanical properties of the fibers. With weak coagulation of the base polymer, gel-fibers will not fully coagulate and will result in weak fibers with no integrity during the spinning process. With strong coagulation, fibers become too brittle to process, and will break under the slightest tension. By controlling temperature, exposure time, and bath recipes, coagulation baths can be specifically tailored to process high quality as-spun gel-fibers.
- Coagulation baths can be engineered for safety and functionality. Through the Teas Plot, solution spinning processes that once utilized heavily toxic or extremely flammable solvents can be changed to use cleaner, safer solvents without detrimentally affecting the performance of the fiber.
- At very low quantities (≤ 5 %), antiplasticizers can greatly influence the performance of the drawn fiber. The small, rigid molecules can alter how the polymer behaves with respect to the neat polymer by changing its microstructure. This results in higher draw ratios, operator-friendly processibility, altered crystalline structures, increased thermal stability, and enhanced mechanical properties. With an appropriate quantity, the antiplasticizer can enhance the overall performance of the fiber.

5.2. Recommendations

It is recommended to consider the following to expand upon this work:

- Utilize higher molecular weight PAN. High Molecular Weight or Ultra-High Molecular Weight PAN can increase the mechanical performance of the product to exceed apparel grade performance. With increased molecular weight, it is possible to load the system with less PAN and more lignin, increasing the ratio of renewable to non-renewable in the composite fiber.
- Explore other alternative baths. Using the Teas Plot, baths can be engineered with the HSPs of any number of miscible solvents. Baths primarily composed of non-toxic, easily recoverable solvents could provide avenues to more environmentally sustainable and less expensive solution spinning processes. Alternative baths can also be engineered to maintain solids within a fiber system where the fiber would normally suffer from significant migration resulting in voids.
- Antiplasticizers are useful tools. With very little relative concentration in spinning dopes, antiplasticizers can tremendously enhance the mechanical properties and alter the thermal behavior of the fibers, as was seen with the GA/PAN fibers. However, finding an effective amount of antiplasticizer for a composite system, such as lignin/PAN, may provide a challenge.
- This work used as-received kraft lignin, but different types of lignin may provide different properties. It is well known that lignin's structure changes based upon its source and extraction method. Different forms of lignin from the myriad of sources could provide alternative results for incorporation to further reduce or eliminate completely the loss of solids.

APPENDICES

A. APPENDIX A: SONICATION OF LIGNIN/DIMETHYL SULFOXIDE

A.1. Brief

During the preparation of spinning dopes that contained lignin, a sonication technique was utilized in order to disperse the solids into solvent. Excessive sonication has been known to degrade some molecules, such as CNTs. This appendix addresses the effects of sonication on lignin in solution as well as the sonicated solution on the processing parameters of lignin/PAN solutions.

A.2. Experimental

A.2.1. Materials

PAN powder having molecular weight of 150 kDa was procured from Scientific Polymer. Powdered Kraft lignin from Domtar was used as-received. Solvents included water, dimethyl sulfoxide (DMSO) from Sigma Aldrich, and isopropanol (IPA) and methanol (MeOH) from BDH Chemicals.

A.2.2. Sonication

The powdered lignin was added to DMSO such that the concentration was 10 g/dL. The solutions were then sonicated for 3, 9, and 18 h. A control sample of 0 h was prepared by simple stirring on a hot plate at 85 °C for 1 h.

A.2.3. Testing

Each solution sample was then subjected to ASTM D446, Standard Specifications and Operating Instructions for Glass Capillary Kinematic Viscometers utilizing a Size 50 capillary viscometer with a constant of 0.004 mm^2/s^2. In order to measure kinematic viscosity, η in cSt, efflux time, t_e in s, was measured and then multiplied by a given constant unique to the viscometer:

$$\eta = t_e \times 0.004 \qquad (A.1)$$

Each sample was then prepared as a spinning dope and then gel-spun using the same spinning techniques as described in previous chapters.

A.3. Results & Discussion

A.3.1. Effect of Sonication on Lignin/DMSO Viscosity

The resulting kinematic viscosities were very similar, as seen in **Figure A.1**. This implies that sonication beyond 3 hrs has minimal effect on dissolution with this concentration of lignin; however sonication improves the homogeneity of the lignin/DMSO solution. The sample sonicated at 3 hrs was statistically different from the samples sonicated at 9 and 18 hrs, but because the units of cSt are miniscule, minimal realistic difference could be expected for spinning dope preparation or processing.

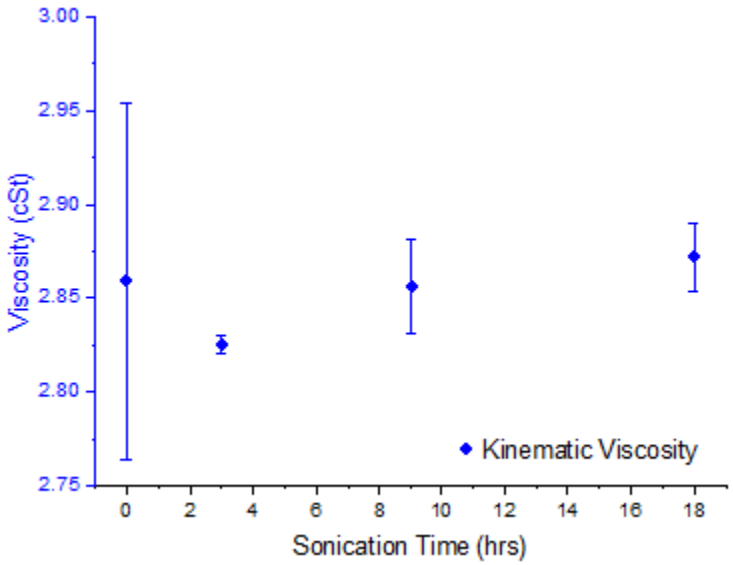

Figure A.1: Kinematic viscosity vs sonication time of Lignin/DMSO.

A.3.2. Dissolution & Gel-Spinning

Dissolution of PAN into the lignin/DMSO was conducted and noted to have little difference between the sonicated samples. On the other hand, the non-sonicated control sample required extra heating, stirring, and time before the dope appeared to be fully homogeneous.

The processing parameters for the sonicated samples are reported in **Table A.1**. Based upon the spinning parameters and draw ratios, there were no significant differences between any of the samples' processing behavior during spinning; however the 18 hrs sample was drawn at the second stage approximately 10 °C cooler than the rest, and this is due to the fact that the samples were fabricated on different days instead of at the same time. Some noticeable diameter inconsistencies appeared on the 0 hrs control sample, implying aggregates formed within the spinning dope and were not easily observable during dissolution.

Table A.1. Processing Parameters of Gel-Spun Lignin/PAN Fibers.

Time Sonicated					
		0 hrs	**3 hrs**	**9 hrs**	**18 hrs**
As-spun	**DR**	7.2	7.2	7.2	7.2
Stage 1	**Temp (°C)**	140	137	140	133
	DR	10.6	10.5	10.7	9.2
Stage 2	**Temp (°C)**	171	171	171	160
	DR	1.5	1.4	1.5	1.6
Total DR		117.4	107.3	114.1	105.8

A.4. Conclusions

Sonication of lignin has shown to be an effective process for aiding in dissolution and consistency in fiber production. Kinematic viscosity does not change significantly between 9 and 18 hrs, but ultimately due to the fact that the difference is miniscule, effective sonication does not require any length of time beyond 3 hrs. No differing effects were seen or noted for samples sonicated beyond 3 hrs.

B. Antiplasticization of Gel-Spun Lignin/Polyacrylonitrile Fibers Utilizing Ammonium Glucarate

B.1. Brief

With the rising demand and development of more sustainable carbon fiber (CF) precursors, other additives have been used in conjunction with PAN to create composite fibers comparable to neat PAN. Biomass additives such as lignin can be used, but often induce further plasticization detrimental to the precursor fiber's mechanical performance and processibility. Liu et al. gel-spun lignin/PAN composite fibers up to 30 % lignin content and saw a reduction in fiber performance and processibility. Their lignin/PAN fibers had a modulus of 17.2 GPa and tensile strength of 742 MPa, lower than the neat PAN fibers with modulus and tensile strength of 19.9 GPa and 879 MPa respectively[1]. However, lignin has shown some promise in improving processibility as lignin has been linked to lower stabilization and cyclization energies. Liu et al. showed Dynamic Scanning Calorimetry thermograms for neat PAN and lignin/PAN, and expressed that widening distributions imply lower stabilization energies which could lead to reduced processing time[1].

In a more recent study, Lu and Ford found that glucaric acid (GA) in small quantities can enhance the mechanical performance and processibility of polyvinyl alcohol (PVA) and lignin/PVA fibers[2]. The mechanical properties of the GA/PVA samples they fabricated exceeded their neat PVA with modulus of 21 GPa and breaking strength of 0.34 GPa. Their strongest fiber with 1.6 % GA concentration achieved a modulus of 49 GPa and breaking strength of 1.1 GPa[2]. Lu and Ford were also able to produce lignin/PVA composite fibers with up to 30 % lignin content and maintain mechanical properties equivalent to neat PVA fibers by means of including only 0.8 % of the antiplasticizer[2]. This appendix addresses the use of GA in

the form of ammonium glucarate within a gel-spun composite fiber of lignin/PAN as an antiplasticizer to enhance the mechanical properties and overall processibility. It has been shown in previous work that it is possible to increase draw ratios throughout processing of gel-spun PAN fibers, thus enhancing the mechanical properties of the resulting acrylic precursor fiber. A Lignin/GA/PAN sample (LGA) was developed and characterized for structural changes as well as tested for mechanical and thermal performance.

B.2. Experimental

B.2.1. Materials

PAN powder having a molecular weight of 150 kDa was procured from Scientific Polymer. GA in the form of ammonium salt crystals was donated by Kalion, Inc. and used as-received. Powdered Kraft lignin from Domtar was used as-received. Solvents included water, dimethyl sulfoxide (DMSO) from Sigma Aldrich, and isopropanol (IPA) and methanol (MeOH) from BDH Chemicals.

B.2.2. Spinning Dope Preparation

A spinning dope of lignin/GA/PAN was prepared. 0.35 g of GA and 5 g lignin were sonicated in 50 mL of DMSO up to 18 h. After sonication, 10 g of PAN was then dissolved in the lignin/GA/DMSO solution at 85 °C under constant stirring for approximately 10 h. The final PAN concentration of the spinning dope was 20 g/dL.

B.2.3. Gel-Spinning

The gel-spinning process in **Figure 1** is labeled according to three important steps: dope feed, coagulation, and thermal drawing.

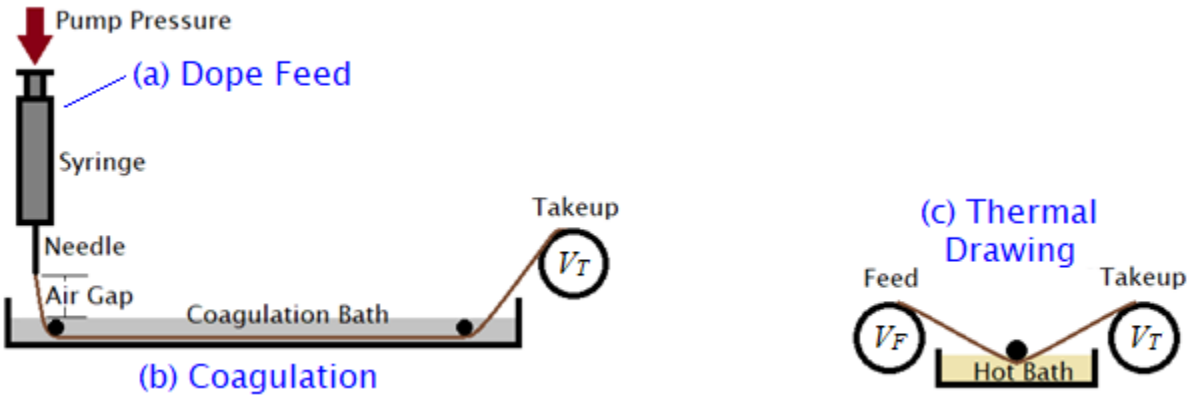

Figure B.1: Schematic of gel-spinning labels the process as (a) Dope, (b) Coagulation, and (c) Thermal Drawing.

Dope: The spinning solutions were spun using a high pressure capable stainless steel syringe equipped with a 50.8 mm (2") 19 ga needle (0.69 mm inner diameter). As depicted in **Figure B.1a**, the dope was loaded into the syringe and aged for at least two hours at ~20 °C. Equilibration to environmental temperature allows a pre-gelation effect to occur, increasing apparent viscosity for spinning and mechanical properties, as well as preventing major temperature variations during spinning.

Coagulation: As seen in **Figure B.1b**, the pre-gelled dope was then spun into a coagulation bath with an air gap of 3 cm from the tip of the needle. The coagulation bath consisted of a mixture of water, IPA, and MeOH. The resulting fibers were then collected onto spools.

Thermal Drawing: As shown in **Figure B.1c**, as-spun gel fibers were thermally drawn through glycerol in two stages at temperatures ranging from 130 to 170 °C. Fiber draw ratios (*DR*) were calculated according to **Equation B.1** the ratio of fiber take-up speed (V_T) to feed speed (V_F):

$$DR = \frac{V_T}{V_F} \qquad (B.1)$$

B.2.4. Mechanical Testing

The mechanical properties of lignin/PAN fibers were tested using the MTS-Q testing system according to ASTM D3379. Parameters were set to 15 mm/min strain rate, 25.4 mm gauge length, and up to 20 specimen sample sizes. Lignin/PAN fiber density was calculated according to the inverse rule of mixtures (**Equation B.2**):

$$\rho_{fiber} = \left(\frac{1-w}{\rho_{PAN}} + \frac{w}{\rho_{GA}}\right)^{-1} \quad (B.2)$$

where w_f is the weight fraction, ρ_{fiber} is the density of the composite fiber, ρ_{PAN} is the density of PAN at 1.184 g/mL[3], and ρ_{GA} is the density of GA at 1.9 g/mL[4].

B.2.5. Imaging

Linear density, $\mathcal{JI}$, reported in dtex, was calculated from measurements of cross-sectional area (*Acs*), which were determined by IMAGEJ analysis. Confocal micrographs were taken on the LEXT OSL4000. With A_{CS} and ρ_{fiber} available, the linear density was calculated according to **Equation B.3**:

$$\mathcal{JI} = A_{CS} \times \rho_{fiber} \quad (B.3)$$

Fiber fracture tips from mechanical testing were imaged by FEI Verios 460L Scanning Electron Microscope (SEM) at 2kV. Prior to imaging, samples were sputter-coated with a 60/40 gold/palladium mixture.

B.2.6. Thermal Characterization

Thermal analysis was conducted through the means of Dynamic Scanning Calorimetry (DSC) and Thermogravimetric Analysis (TGA). The DSC data were retrieved from the DSC Q2000 V24.11 on a range of -20 to 400 °C at a ramp rate of 5 °C/min, with nitrogen carrier gas, and modulating ±5 °C/min. The TGA data were taken with the TGA Q500 V6.7 on a range of 30 to 600 °C at a ramp rate of 10 °C/min with nitrogen carrier gas.

B.2.7. Structural Characterization

1-D equatorial X-Ray Diffraction (WAXD) was also conducted for crystallinity and crystal size, using the Empyrean diffractometer system. The crystal size for each of the samples was calculated through the Scherrer Equation, **Equation B.4**:

$$\tau = \frac{K\lambda}{\beta\cos(\theta)} \qquad (B.4)$$

where τ is the crystal size in Å, K is a shape factor of 0.9, λ is the wavelength for the copper source of 1.54 Å, β is the full width at half max of the crystalline peak in radians, and θ is the Bragg Angle in radians of the crystalline peak.

B.3. Results & Discussion

B.3.1. Effect of Ammonium Glucarate on Lignin/PAN Gel-Spinning

Table B.1 shows the processing parameters of the gel-spun lignin/GA/PAN fibers. Like the GA/PAN samples, processibility increased when utilizing the GA in the lignin/PAN system. While high concentration of lignin has been shown to lower total draw ratio, as seen by the 50 % lignin sample, the lignin/GA/PAN sample showed approximately the same processibility and draw ratio as the neat PAN control fibers, countering the effects of the increase in chain ends in the lignin-saturated system, likely through a structural change and increased interfacial adhesion.

Table B.1. Processing Parameters of Gel-Spun Lignin/GA/PAN Fibers.

		Neat PAN	50 % Lignin	LGA
As-spun	**Temp (°C)**	-4	-7	-8
	Residence Time (ms)	34	34	34
	DR	7.0	7.2	7.1
Stage 1	**Temp (°C)**	135	133	137.8
	DR	12.2	9.2	12.6
Stage 2	**Temp (°C)**	168	160	165
	DR	1.5	1.6	1.4
Total DR		125.7	105.8	126.4
Linear Density (dtex)		13.0	11.5	11.7
Effective Diameter (µm)		37±1	35±1	35±1

B.3.2. Effect of Ammonium Glucarate on the Mechanical Properties of Lignin/PAN Fibers

From **Figure B.2**, it can be seen that no apparent phase separation occurred at the micron level, indicative of homogeneity, however some anomalous dark pits can be observed. These are pits caused by the dulling of the razor blade used to cut the samples, not lignin aggregates, as evidenced by **Figure B.2a**, the neat PAN sample. The samples also showed a ribbon shaped cross-section, which can occur when using high tension and shear during post-processing with flat guides between spools.

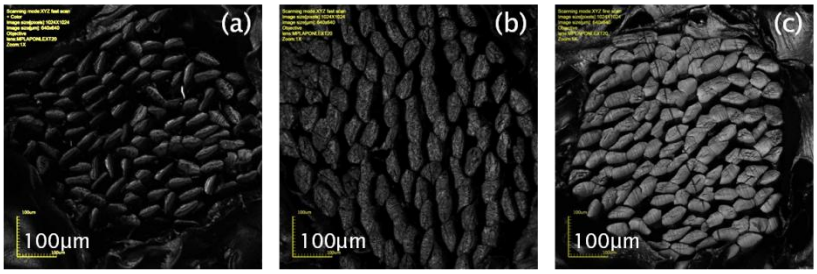

Figure B.2. Drawn fiber laser confocal images of (a) Neat PAN, (b) 50 % Lignin, and (c) LGA.

Table B.2 displays the mechanical properties of lignin/GA/PAN fibers utilizing 3.5 % GA based upon the GA/PAN fiber results and 50 % lignin content. The lignin/PAN sample had

the highest modulus at 85.3 cN/dtex, slightly higher than the modulus of the LGA sample at 78.5 cN/dtex.

Table B.2. Mechanical Properties of Drawn Lignin/GA/PAN Fibers.

Sample	Neat PAN	50 % Lignin	LGA
Modulus (cN/dtex)	50.9±5.1	85.3±6.5	78.5±4.5
Tenacity (cN/dtex)	3.0±0.3	2.4±0.2	2.2±0.2
Toughness (J/g)	17.8±2.6	10.2±2.1	10.7±2.4
Strain at Break (%)	10.5±1.0	6.0±0.8	7.0±1.0
Linear Density (dtex)	13.0	11.5	11.7
Effective Diameter (µm)	37±1	35±1	35±1

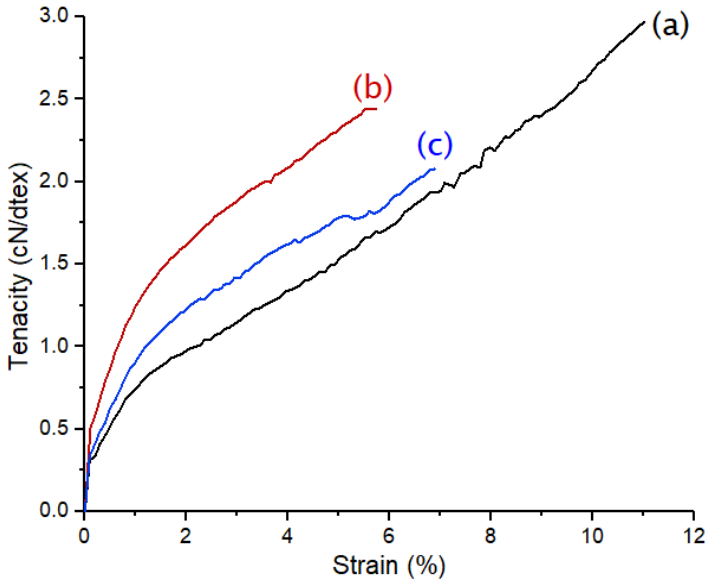

Figure B.3. Tenacity vs strain curves of (a) Neat PAN, (b) 50 % Lignin, and (c) LGA fibers.

The tenacity, toughness, and strain at break of the 50 % lignin fiber did not significantly differ from the LGA sample, but as seen in **Figure B.3**, both showed values lower than that of the neat PAN control, indicative of the increased number of short-chain molecules from the

inclusion of lignin. During processing, the LGA fiber sample resisted breakages and shearing where the 50 % lignin sample would break more readily, implying some degree of antiplasticization. This was also supported by the higher draw ratio of the fibers, as seen in **Table B.1**. However, the amount of solids with more frequent chain ends may have superseded the benefits to the mechanical properties, resulting in a reduced effect.

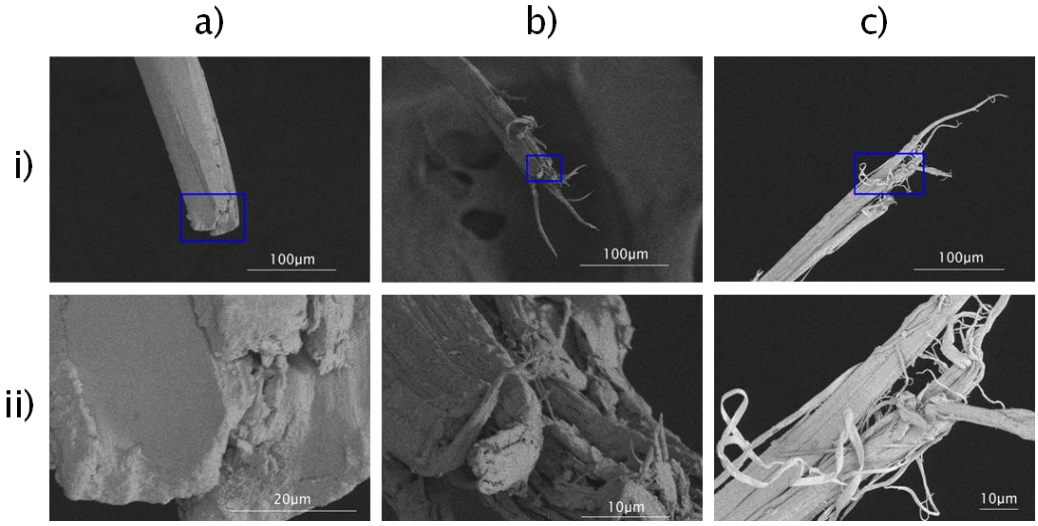

Figure B.4. SEM micrographs of (a) Neat PAN, (b) 50 % Lignin, and (c) LGA at (i) low and (ii) high magnification.

Striations and fibrillation of the lignin/PAN fibers as a result of tensile breakage are shown in **Figure B.4**. The shattering behavior shown in **Figures B.4b** and **B.4c** are characteristic of high-performance fibers that fibrillate instead of breaking cleanly. The PAN fibrils present in both the 50 % lignin and LGA samples are indicative of a greater degree of molecular orientation along the fiber axis than the blunt break seen in the neat PAN. In both cases of the lignin samples, it is unclear where the lignin and PAN actually separate from one another, showing that the solids were well incorporated throughout processing.

B.3.3. Structural Analysis of Lignin/GA/PAN Fibers

WAXD patterns for Lignin/GA/PAN samples are shown in **Figure B.5**. The 50 % Lignin and LGA samples were shown to have the same approximate crystalline peaks at approximately 17° and 29°, maintaining the hexagonal crystalline shape. However, a small but noticeable peak in **Figure B.5b** at approximately 12° can be seen forming, implying another change to the crystalline form. The structure changes coincide with the mechanical properties shown in **Table B.2** and **Figure B.3** and with the apparent bursting fracture behavior and fibrillar morphology shown in the SEM images of **Figure B.4**. The crystallinity and crystal sizes are shown in **Table B.3**. The highest crystallinity was present in the LGA sample that contained the antiplasticizer.

Table B.3. Crystalline Properties of Lignin/GA/PAN Fibers Determined by WAXD.

Sample	Neat PAN	50 % Lignin	LGA
Crystal Size (Å)	73.2	85.9	79.8
Crystallinity (%)	85.9	86.2	88.2

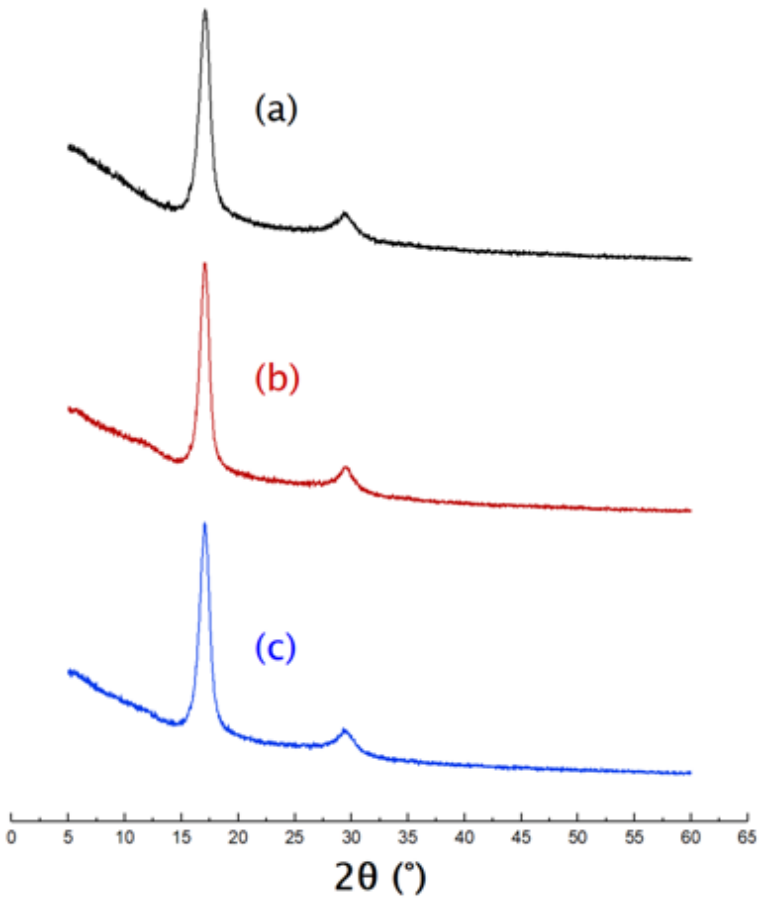

Figure B.5. WAXD patterns of (a) Neat PAN, (b) 50 % Lignin, and (c) LGA fibers

B.3.4. Effect of Ammonium Glucarate on the Thermal Behavior of Lignin/PAN Fibers

The TGA and DTGA data for Lignin/GA/PAN fibers are shown in **Figure B.6**. Like in the GA/PAN samples, a clear change from the neat PAN can be seen. With the addition of lignin, higher plateaus of mass percent between 200 and 300 °C can be seen, fitting the same pattern of crystallinity shown in **Table B.3**. The LGA sample had the highest plateau in this range (**Figure B.6c**) at ~81 % mass retained, higher than the mass retained of the lignin/PAN sample with ~74 % and neat PAN sample at ~60 %.

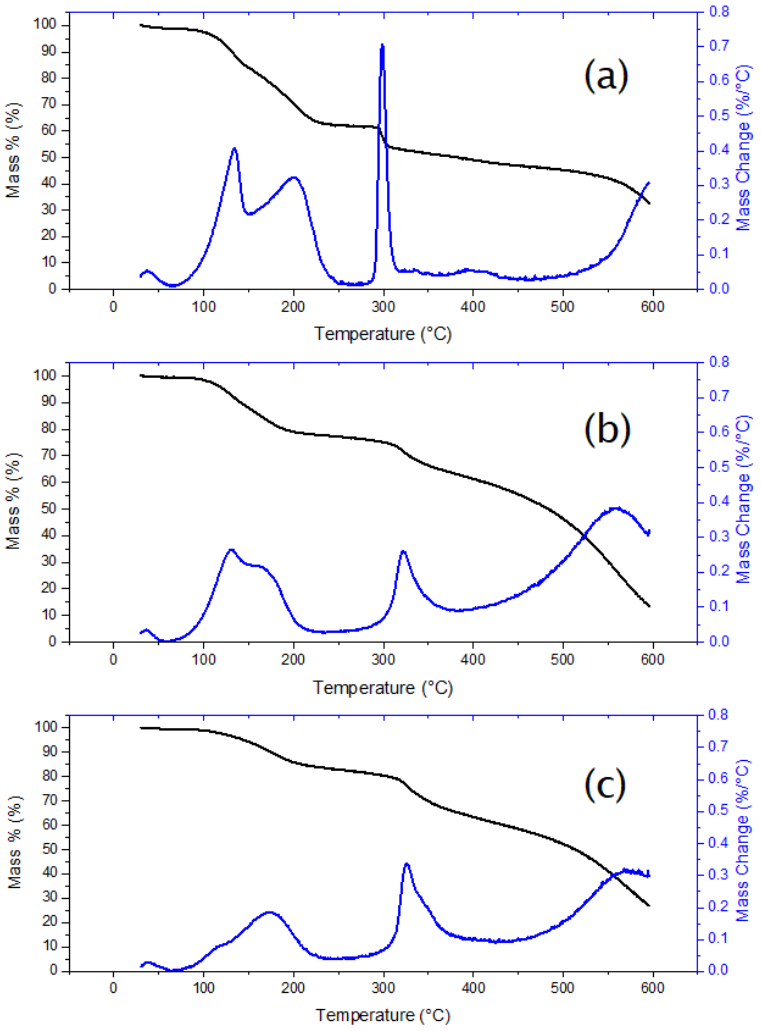

Figure B.6. TGA and DTGA curves of (a) Neat PAN, (b) 50 % Lignin, and (c) LGA fibers

The DSC curves for Lignin/GA/PAN samples are shown in **Figure B.7** and the exotherm peak data are shown in **Table B.4**. Like the TGA curves, the peaks shifted by nearly 80 °C, above 300 °C, and tightened with the addition of lignin and GA. Tightened peaks imply that less energy is required for degradation (and in the case of PAN-based CF precursors, stabilization). In **Table B.4**, the LGA sample requires 189 J/g; about 33% less energy required for the Neat PAN. In **Figure B.7b** and **B.7c**, subtle endothermic depressions can be seen at ~225 °C and ~210 °C respectively.

Table B.4. DSC Exotherm Peak Temperatures and Energies

Sample	Exotherm Peak (°C)	Exotherm Energy (J/g)
Neat PAN	228	285
50 % Lignin	307	224
LGA	310	189

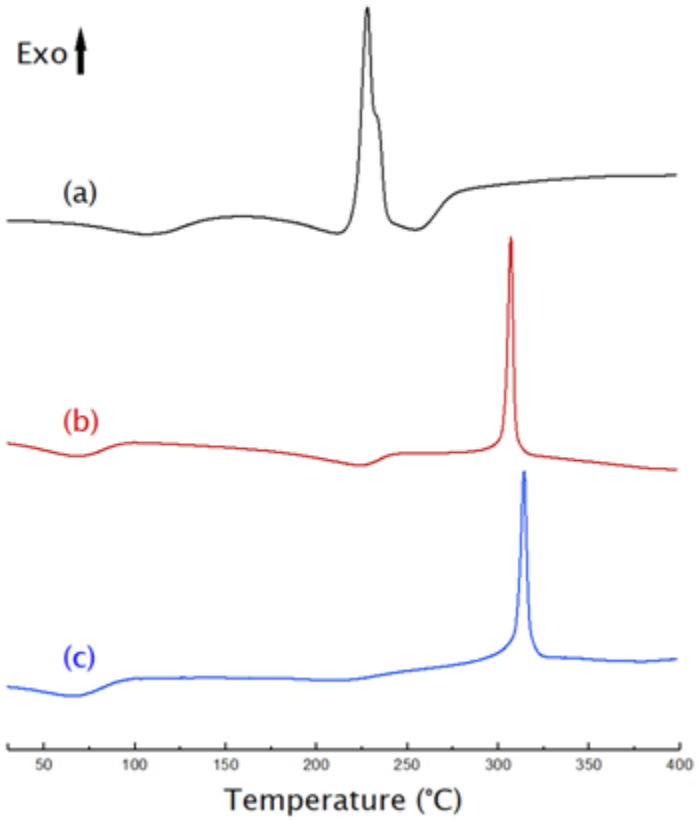

Figure B.7. DSC curves of (a) Neat PAN, (b) 50 % Lignin, and (c) LGA fibers

B.4. Conclusions

Much like the GA/PAN fibers studied in previous work, the addition of lignin into the system also shows the capability of a small amorphous oligomer to improve the processing and thermal performance when incorporated in the fiber. Lignin within the system increased the crystal size, improved ease of handling during processing, and changed the thermal behavior. Tighter exothermic peaks at higher temperatures show a reduced energy requirement for

stabilization for carbon fiber processing. Even though the thermal efficiency was improved with the incorporation of GA, the amount of plasticizer was not optimized for the 50 % Lignin system, as the fibers showed only slight changes to the modulus and crystalline properties, leaving room for further study.

B.5. References

[1] Liu, H. C.; Chien, A.; Newcomb, B. A.; Liu, Y.; Kumar, S. Processing, Structure, and Properties of Lignin- and CNT- Incorporated Polyacrylonitrile-Based Carbon Fibers. *ACS Sustainable Chemistry & Engineering* **2015**, *3*, 1943.

[2] Lu, C.; Ford, E. Antiplasticizing behaviors of glucarate and lignin bio-based derivatives on the properties of gel-spun polyvinyl alcohol fibers. *Macromolecular Materials and Engineering* **2018**, *303*.

[3] Polyacrylonitrile, Cat #134. https://scientificpolymer.com/shop/polyacrylonitrile-3/.

[4] Royal Society of Chemistry, Saccharic Acid. http://www.chemspider.com/Chemical-Structure.30577.html.